1987

Development of the Analytical Methodology for Pyrimethamine and Its Application to Studies of Partitioning and Binding in the Subcompartments of Blood

Anita C. Rudy

School of Basic Health Sciences

Virginia Commonwealth University

This is to certify that the dissertation prepared by Anita C. Rudy entitled "Development of the Analytical Methodology for Pyrimethamine and Its Application to Studies of Partitioning and Binding in the Subcompartments of Blood" has been approved by her committee as satisfactory completion of the dissertation requirement for the degree of Doctor of Philosophy.

[redacted]

Director of Dissertation

[redacted]

Committee Member

[redacted]

Committee Member

[redacted]

Committee Member

[redacted]

Committee Member

[redacted]

Department Chairman/Committee Member

[redacted]

Dean of the School of Pharmacy

[redacted]

Chairman of the Medical College of Virginia
Graduate Council and Dean, Sch of Basic Sciences

18 December 1987

Date

Development of the Analytical Methodolcgy for Pyrimethamine and Its Application to Studies of Partitioning and Binding in the Subcompartments of Blood

A dissertation submitted in partial fulfillment of the requirements for the degree of Doctor of Philosophy at Virginia Commonwealth University

By

Anita C. Rudy
Bachelor of Science in Pharmacy
Auburn University
March 1981

Director: Wesley J. Poynor, Ph.D.
Associate Professor
Department of Pharmacy and Pharmaceutics

Virginia Commonwealth University
Richmond, Virginia
December 1987

Acknowledgements

First, I would like to thank the Department of Pharmacy and Pharmaceutics for letting me share in its exponential growth and for providing financial support.

I would like to express my sincere gratitude to Dr. Wesley J. Poynor for his financial support, for directing my exposure to many areas of research, for making sure I had publications before I graduated, and for his suggestion of a good research project.

Many thanks to Drs. Bill and Phyllis Soine and Dr. Tom Karnes for giving me lessons in analytical chemistry. Thanks are due to Dr. Harold Smith for his straight talk on protein binding and to Dr. Vernon Chinchilli for making statistics relevant and interesting.

Thank you Dr. John Wood for encouraging good science and for explaining the unexplainable plots. To awesome and 50 Dr. Bill Barr, thanks for all those "pearls" (I wish I'd recognized they were pearls earlier). And thanks to both of you for building a good department conducive to graduate research and education.

Thanks to all my professors for pointing out the important material. To Gene Cefali: It was a pleasure having you as a lab mate, and thanks for making grad school tolerable.

Thanks to Dr. Carl Sigel and the Burroughs Wellcome Co. for their gracious gift of pyrimethamine.

Most of all, because I couldn't have done it without him, I give my love and thanks to my husband David, the first Dr. Rudy, but not the last.

Table of Contents

List of tables.....ix

List of figures.....xii

List of abbreviations.....xiv

Abstract.....xvi

1. Introduction.....1

2. Literature Survey.....3

2.1 Physiochemical properties of PYR.....3

2.2 Pyrimethamine pharmacokinetics.....5

2.3 Determination of PYR in biological fluids.....8

2.4 Liquid chromatography.....12

2.4.1 Ion-pair chromatography.....13

2.5 Equations for the expression of binding equilibria.....14

2.6 Statistical considerations in protein binding data fitting.....19

2.7 Nonideal cases of protein binding.....20

2.8 Methods of blood collection.....25

2.8.1 Heparin.....25

2.8.2 Tris(2-butoxyethyl)phosphate (TBEP).....28

2.8.3 Collection tubes.....29

2.8.4 The pH adjustment for protein binding....30

2.8.5 Osmotic volume shifts of fluid.....31

2.8.6 Mass balance considerations.....32

2.9 Red blood cell partitioning.....32

2.9.1 Effects of pH on RBC partitioning.....34

2.9.2 Drug disposition and RBC partitioning....38

2.9.3 RBC partitioning relative to protein binding.....39

2.9.4 Variables from analytical techniques.....40

2.9.4.1 Mass balance considerations.....40

2.9.4.2 Effect of trapped plasma.....42

2.9.4.3 Effect of the medium on RBC levels.....45

3. Definition of the problem.....49

3.1 Background.....49

3.2 Hypothesis.....50

3.2 Objectives.....50

3.3 Proposed methodology.....50

4. Experimental.....51

4.1 Reagents, chemicals, and equipment.....51

4.1.1 Chemicals and reagents.....51

4.1.2 Instrumentation.....55

4.2 Reproduction of Edstein's IPC-HPLC method.....56

4.3 Assay of PYR using original RP-HPLC method.....58

4.3.1 Selection of internal standard.....58

4.3.2 Selection of extraction solvent.....59

4.3.3 Separation of PYR and NAPA.....60

4.3.4 Preparation of the mobile phase.....60

4.3.5 Column, detector, and recorder characteristics.....61

4.3.6 Quantification of PYR in matrices.....62

4.3.6.1 Extraction procedures.....62

4.3.6.2 Calibration curves.....64

4.3.6.3 Recovery and precision studies...65

4.4 Vacutainer™ pH changes.....66

4.4.1 Blood drawing and pH measurement procedures.....66

4.5 Equilibrium dialysis.....66

4.5.1 Membrane preparation.....66

4.5.2 Spectrum equilibrium dialyzer.....67

4.5.3 Protein assay.....68

4.5.4 Adjustment of plasma pH.....69

4.5.5 General ED procedure.....70

4.5.6 Sources of dilution of protein.....70

4.5.6.1 Water content of membranes.....70

4.5.6.2 Volume shifts.....71

4.5.7 Evaluation of binding to ED cells and membranes.....71

4.5.8 Determination of time to equilibrium for dialysis.....71

4.5.9 Influence of plasma pH on protein binding.....72

4.5.9.1 Comparison of pH 7.4 and 8.0 plasma.....72

4.5.9.2 Effects of pH on protein binding.73

4.5.10 Influence of anticoagulants on protein binding.....74

4.5.11 Concentration dependence of protein binding.....74

4.5.12 Binding to pure human serum albumin.....75

4.5.13 Binding to alpha$_1$-acid glycoprotein.....75

4.5.14 Binding to plasma proteins.....76

4.5.15 Binding to hemoglobin.(Hb).....78

4.5.15.1 Stroma-free Hb preparation.....78

4.5.15.2 Measurement of Hb.....78

4.5.15.3 Binding to Hb.....79

4.6 Partitioning of PYR into RBCs.....80

4.6.1 RBC/buffer ratio as a function of buffer pH.....80

4.6.2 Influence of plasma albumin levels on RBC PYR.....82

4.6.3 Determination of RBC/plasma ratio.....83

5. Results.....84

5.1 Reproduction of Edstein's IPC-HPLC assay.....84

5.1.1 Effects of ion pair agent and pH.....86

5.2 RP-HPLC assay results.....88

5.2.1 Effects of pH on retention time.....92

5.2.2 Calibration curves.....93

5.2.3 Recovery, precision and accuracy studies.98

5.3 Vacutainer™ pH as a function of additive and time.....113

5.3.1 Differences in zero-time pH in Vacutainers™.....117

5.4 Effect of pH on cell/medium ratios.....119

5.5 Equilibrium dialysis.....121

5.5.1 Water content of dialysis membranes.....121

5.5.2 Volume shifts.....121

5.5.3 Binding to ED apparatus.....122

5.5.4 Determination of time to equilibrium....123

5.5.5 Influence of pH on protein binding.....126

5.5.5.1 Binding at pH 7.4 vs. 8.0.....126

5.5.5.2 Influence of a range of pH values on binding.....127

5.5.6 Concentration dependence of protein binding in therapeutic range.....128

5.5.7 Summary of influence of albumin on PYR binding.....129

5.5.8 Percent free PYR in different tubes.....131

5.5.9 Binding to pure human serum albumin.....133

5.5.10 Binding to AAG.....133

5.5.11 Analysis of protein binding data from Studies 1, 2, and 3.....134

5.6 RBC partitioning and binding.....151

5.6.1 Binding to hemolysate.....151

5.6.2 RBC/buffer concentration ratio as a function of pH.....153

5.6.3 RBC/plasma PYR ratio.....157

6. Discussion.....164

6.1 Analytical methodology.....164

6.2 Mass balance considerations.....170

6.3 Vacutainer™ pH and cell/medium ratios.....171

6.4 The theoretical effects of pH on RBC partitioning.....173

6.5 Protein binding and ED in general.....174

6.5.1 Influence of pH on protein binding.....175

6.5.2 Influence of PYR concentration on protein binding.....175

6.5.3 Influence of albumin on protein binding.177

6.5.4 Influence of tubes on PYR binding.....177

6.5.5 Binding to pure human serum albumin and AAG.....178

6.5.6 Plasma protein binding.....179

6.6 RBC partitioning and binding.....186

6.6.1 Partitioning from buffer.....186

6.6.2 Influence of protein binding on RBC uptake.....189

7. Conclusions.....192

7.1 Analytical methodology.....192

7.2 Medium pH and theoretical cell/medium ratios..193

7.3 Protein binding of PYR.....195

7.4 RBC partitioning and binding.....199

7.5 Final comments.....200

8. Prospectus.....203

Bibliography.....204

Appendix A. Computer programs.....217

Appendix B. Results of fits to additional models.....230

Vita.....254

List of Tables

1. Physiochemical properties of PYR.....4

2. Pharmacokinetics of PYR.....6

3. Binding of metoprine to plasma proteins.....8

4. Previous methods of quantification of PYR.....11

5. Vacutainer™ systems.....66

6. Summary of Alltech Econosphere™ life.....89

7. Percent recovery from extracted spiked plasma calibration standards.....99

8. Back-calculated concentrations of PYR plasma standards using a linear fit for the low concentrations.....100

9. Back-calculated concentrations of PYR plasma standards using a linear fit for the high concentrations.....101

10. PYR concentrations in spiked control plasma samples.....102

11. Linear regression on peak height ratios (PYR/NAPA) vs. concentration of PYR for plasma curves.....104

12. Percent recovery from extracted spiked RBC standards.....105

13. Back-calculated concentrations of PYR RBC standards using a linear fit of peak heights vs. concentration for the low concentrations.....106

14. Back-calculated concentrations of PYR RBC standards using a linear fit of peak height vs. concentration for the high concentrations....107

15. Linear regression of calibration curves for RBCs peak height vs. concentration.....108

16. Back-calculated concentrations of PYR buffer using a linear fit of peak height vs. concentration for the low concentrations.....109

17. Back-calculated concentrations of PYR buffer using a linear fit of peak height vs concentration for the high concentrations.....110

18. Buffer controls.....111

19. Linear regression on calibration curves for buffer peak height vs. PYR concentrations.....112

20. Measured pH values at various times.....114

21. Change in pH of medium for the first hour.....115

22. ANOVA for zero-time pH in different Vacutainers™.118

23. Cell/medium ratios for weak acids and weak bases.120

24. Albumin changes during dialysis.....122

25. PYR (ng/ml) at the end of dialysis.....122

26. Binding at pH 7.4 vs. pH 8.0.....126

27. Binding at 2 PYR concentrations.....128

28. Linear regression of percent free PYR on albumin concentration.....130

29. Percent free in different tubes.....132

30. Binding to purified human albumin.....133

31. Binding to 3.7 g/L AAG.....134

32. Summary of protein binding Studies 1, 2, and 3...135

33. Estimates of first stoichiometric binding constant K_1.....137

34. Nonlinear fit of data 38 using Klotz equation....142

35. Nonlinear fit of data 41 using Klotz equation....145

36. Nonlinear fit of data 47 using Klotz equation....149

37. Binding to hemolysate.....152

38. RBC/buffer ratio as a function of buffer pH.....155
39. Theoretical RBC/buffer ratio as a function of pH.156

List of Figures

1 . Structure of pyrimethamine (PYR).....4

2. Various protein binding plots.....18

3. Structure of NAPA.....59

4. Chromatogram of PYR and Q in IPC-HPLC assay.....85

5. Effect of SPS concentration on capacity factors...87

6. Plot of the retention times of PYR and Q vs. pH of the mobile phase.....87

7. Effect of pH on retention times of PYR and NAPA...92

8. Chromatogram of PYR and NAPA in a plasma sample...94

9. Chromatogram of PYR and NAPA in RBC sample.....95

10. Chromatogram of PYR and NAPA in buffer sample.....96

11. Typical plasma calibration curve.....97

12. Close-up of the the lower end of the plasma calibration curve.....97

13. Time dependent rise in pH for 2 Vacutainers™.....116

14. Approaches to equilibrium in dialysis experiments.....125

15. Influence of pH on plasma protein binding.....127

16. Influence of albumin on percent free PYR.....129

17. Percent free PYR vs total plasma concentration for data from Studies 1 and 2.....138

18. Scatchard plot of data from Study 1.....139

19. Scatchard plot of data from Study 2.....140

20. Scatchard plot of data from Study 3.....140

21. Klotz plot of data from Study 1 showing observations and predicted points. Line through fitted points.....143

22. Residuals for Klotz fit of above data.....146

23. Klotz plot of data from Study 2 showing observations and predicted points. Line through fitted points.....146

24. Residuals for Klotz fit of above data.....146

25. Klotz plot of data from Study 3 showing observations and predicted points. Line through fitted points.....150

26. Residuals for Klotz fit of data 47.....150

27. Graph of RBC/buffer ratio vs. buffer pH for observed and theoretical data.....154

28. Plot of residuals for fits of observed and theoretical data.....154

29. RBC/plasma ratio vs. plasma albumin concentration for the first experiment.....159

30. RBC/plasma ratio vs. plasma albumin concentration for the combined experiments.....159

31. RBC/plasma ratio vs. plasma PYR concentration for the first experiment.....160

32. RBC/plasma ratio vs. plasma PYR concentration for the combined experiments.....160

33. Plasma vs. whole blood PYR concentration for the first experiment.....162

34. Plasma vs. whole blood PYR concentration for the combined experiments.....162

35. RBC vs. whole blood PYR concentration for the first experiment.....163

36. RBC vs. whole blood PYR concentration for the combined experiments.....163

List of Abbreviations

α	Selectivity
AAG	α_1-acid glycoprotein
ACN	Acetonitrile
ANOVA	Analysis of variance
Cmax	Maximum plasma concentration
CV	Coefficient of variation
D	Molar unbound drug concentration
DF	Degrees of freedom
ED	Equilibrium dialysis
ECF	Extracellular fluid
GLC	Gas liquid chromatography
Hb	Hemoglobin
HPLC	High performance liquid chromatography
IPB	Isotonic phosphate buffer
IPC	Ion pair chromatography
k'	Capacity factor
K	Affinity or association constant
KPB	Potassium phosphate buffer
M	Molar
MeOH	Methanol
MS	Mean square
MSE	Mean square error

n	Number of binding sites
N	Efficiency (HPLC), number
NAPA	N-acetyl procainamide
NaPB	Sodium phosphate buffer
NEFA	Non-esterified free fatty acids
NP	Normal phase
P	Plasma, molar protein
PTFE	Polytetrafluoroethylene
PYR	Pyrimethamine
Q	Quinine
r	Number of moles of drug bound per mole of total protein
R	Resolution, correlation coefficient
R^2	Coefficient of determination
RBC	Red blood cell (erythrocyte)
RP	Reverse phase
Rt	Retention time
SD	Standard deviation
SE	Standard error
SPS	Sodium pentane sulfonate
SS	Sum of squares
t_n	Retention time
TLC	Thin layer chromatography
V	Volume
Vc	Volume of distribution of the central compartment
WB	Whole blood

DEVELOPMENT OF THE ANALYTICAL METHODOLOGY FOR PYRIMETHAMINE AND ITS APPLICATION TO STUDIES OF PARTITIONING AND BINDING IN THE SUBCOMPARTMENTS OF BLOOD

Abstract

A dissertation submitted in partial fulfillment of the requirements for the degree of Doctor of Philosophy at Virginia Commonwealth University

Anita Chaptal Rudy, Ph.D.

Virginia Commonwealth University, 1987

Director: Wesley J. Poynor, Ph.D.

An original HPLC assay was developed for pyrimethamine (PYR) in plasma, RBCs, and buffer for the purpose of studying its plasma protein binding and RBC partitioning.

Equilibrium dialysis (ED) was used to study protein binding. Isotonic phosphate buffer used in ED did not prevent small volume shifts. The pH of the plasma affected the protein binding of PYR although it was not significant for the comparison of binding at pH 7.4 vs. 8.0. PYR at 1000 ng/ml averaged 93.1% bound to plasma proteins. Binding to pure human albumin was 86.5% at lower levels of albumin and PYR (350 ng/ml). There was a significant difference ($p<.03$) in the plasma binding at two levels in the therapeutic range, with more free at higher levels. There was also concentration dependent binding at higher concentrations; the drug did not follow to law of mass action when binding increased at

higher concentrations. This is a solubility phenomenon. Linear regression of the effect of albumin concentration on plasma binding yielded the equation percent free = -0.467(albumin g/L) + 23.5. The binding to pure albumin was only slightly above that predicted by this equation (83.1%). The first and second stoichiometric binding constants are K_1 = 2.83 X 10^4 and K_2 = 1.74 X 10^4 M^{-1} from nonlinear regression of data. There was no binding to normal levels of α_1-acid glycoprotein.

PYR is preferentially bound to plasma proteins in comparison to RBCs. The mean RBC/plasma ratio was 0.42 (10.2% CV, n=5). When plasma was removed and pH 7.4 isotonic buffer substituted, mean RBC/buffer ratio was 5.2 (11.8% CV, n=2). Mean percent bound to hemolysate was 42.5% (19% CV, n=10). Binding to hemoglobin did not account for all the RBC uptake. Therefore, PYR binds to RBC membranes.

Chapter 1

Introduction

Pyrimethamine (PYR) has been used as an antimalarial since its introduction in the 1950s (45). More recently, it has gained recognition in fighting plasmodia resistent to other antimalarial drugs (96,109). In combination with a sulfonamide, it is the only agent for use in toxoplasmosis (128). It is also used for pneumonia caused by Pneumocystis carinii in acquired immunodeficiency syndrome (96). In addition, PYR has had some success in neoplastic diseases of the central nervous system such as meningeal leukemia (19).

Yet, for a drug that has been on the market for so long and is used throughout the world for malaria (96), relatively little is known about its pharmacokinetics (1, 2, 70, 109, 112, 113, 125). Surprisingly, studies examining its protein binding (2, 19) and red cell uptake are almost nonexistent (1).

The lack of analytical methodology in the early years of its marketing is partly responsible for the scarcity of pharmacokinetic studies. Recently, as described in Chapter 2, there have been several assays published.

In general, studies of the uptake of drugs by erythrocytes or red blood cells (RBCs) have also been infrequent in the pharmaceutics literature. These studies are so infrequent that standard procedures have not been established. Analytical artifacts which will be discussed in Chapter 2 are frequently found in RBC studies.

In the same way, conventional methods for determining protein binding are limited. Several authors have questioned the validity of the majority of published protein binding studies (14, 16, 25, 76, 119).

Therefore, several important factors involved in measuring RBC uptake were selected for study. The same factors were also evaluated relative to plasma protein binding because RBC uptake and protein binding are so closely related. PYR was chosen as a model drug because it is a lipophilic weak base that is likely to have significant RBC uptake and the protein binding of this drug has not been studied extensively. RBC uptake is essential for antimalarial activity. This is an uncommon chance to study a very accessible tissue compartment (the RBC) in which the malarial parasite and, therefore, the site of action is located. Information about the relationship between plasma and RBC levels would be enlightening for pharmacodynamic studies.

Chapter 2

Literature Survey

In this chapter, a review is presented of the physicochemical properties and pharmacokinetics of PYR, liquid chromatography, the analysis of protein binding data, ideal and nonideal cases of protein binding, some of the artifacts associated with the collection of protein binding data, and the concepts of red blood cell (RBC) partitioning and binding as they apply in this work.

2.1 Physicochemical properties of PYR

The physicochemical properties of PYR (2,4-diamino-5-(5-chlorphenyl)-6-ethylpyrimidine) from Cavallito et al. (19) are given in Table 1. It is a strongly lipophilic weak base. The structure is given below Table 1.

Table 1. Physicochemical properties of PYR

Molecular weight	248.71 g/mole
Aqueous solubility:	practically insoluble (<1 in 10,000 parts)
Log P (partition coefficient, octanol/water)	2.69
pKa	7.34
pKa (Ref. 2)	7.13
pKa (Ref. 90)	7.0

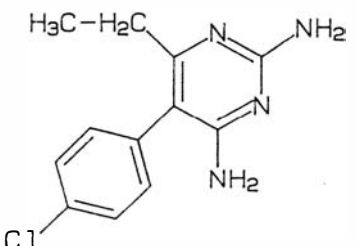

PYR

Figure 1. Structure of pyrimethamine (PYR).

2.2 Pyrimethamine pharmacokinetics

PYR is an antimalarial that was one of a series of compounds synthesized by Falco (45) in the late 1940's. It proved to be better than proguanil as an antimalarial agent. Its pharmacokinetics were not examined until recently due to lack of analytical knowledge. The basic pharmacokinetics of PYR are listed in Table 2. Complete absorption of the dose of PYR was assumed in each study in Table 2. Smith and Ihrig (113) determined the bioavailability to be 1.0 in monkeys. Human bioavailability has not been reported in the literature.

TABLE 2. PHARMACOKINETICS OF PYR

Ref.	No. of subjects	Analytical method	Dose (mg)	Cmax (ng/ml)	Elimination half-life (h)	Vd	Clearance (ml/h/kg)	Model
(1)	7	TLC	25	234 ± 21	83 ± 14	2.93 ± 0.52 L/kg	24.8 ± 3.8	1 compartment
(2)	6	TLC	25		81 ± 14			2 compartment
(19)	4	TLC	100	600-1000	85 (79-93)			linear
(70)	11	HPLC	12.5		80 (35-175)			linear
(109)	6	HPLC	25	314 ± 90.	123 ± 27	2.46 ±0.6 L/kg	14. ±2.5	2 compartment
(125)	14	Micro	25	214 (127-398)	96 (46-150)	75.9 ± 28.6 L	20.5 ± 7.2	2 compartment

Mean ± standard deviation or ranges of values are given.
Vd = volume of distribution of central compartment.
Cmax = maximum plasma concentration
Analytical methods are discussed in Section 2.3

The study of the protein binding of PYR yields information about its disposition. Ahmad and Rogers (2) reported the plasma protein binding of PYR as 82.3 +/- 2.6% (n=8) *in vitro* and 84.9 +/- 2.5% (n=9) *ex vivo*. Cavallito and others (19) reported the plasma protein binding of PYR as 87 +/- 1% (n=3). Percent binding information about PYR is of limited value. More explicit information regarding the protein binding of PYR is necessary for later reference in this work (Section 6.5.6), thus a more detailed description of the protein binding of a similar compound is provided here.

The study by Cavallito et al. (19) included metoprine, 2,4-diamino-5-(3,4-dichlorophenyl)-6-methylpyrimidine, which is a mammalian dihydrofolate reductase inhibitor and a structural analog of PYR. Metoprine binding was studied in greater detail than PYR binding and because their structures differ by only one chlorine, the two drugs may have similar binding characteristics. Plasma and serum samples were spiked with radiolabelled metoprine. After equilibration with protein fractions in the samples, the protein fractions were separated by electrophoresis, and radioactivity was associated with the albumin band. However, in equilibrium dialysis experiments where pure protein fractions were dissolved in phosphate buffer at concentrations found in human plasma, it was discovered that metoprine

bound to other plasma proteins as well.

Table 3. Binding of metoprine to plasma proteins (19)

Protein	Concentration g/100 ml	Binding % (SD)	K X 10^3
Albumin	1.8	58. (1.0)	5.96
β-globulin	0.2	8.2 (3.9)	10.3
γ-globulin	0.5	3.4 (3.0)	2.25
β-lipoprotein	0.1	5.6 (1.2)	311.0
fibrinogen	0.2	0.9 (1.0)	5.7

K = affinity constant

In fact, the affinity constant, K, for binding to β-lipoprotein fraction was 50 times that for albumin. Table 3 gives a summary of metoprine binding at 1 μg/ml which may be similar to PYR binding in pure fractions of protein.

In the only mention of RBC levels in the literature, Ahmad and Rogers (1), as an aside, stated that the plasma and RBC concentrations for PYR were similar. In their study, PYR competitively displaced dapsone from plasma binding sites.

More recent papers on PYR concern its kinetics in animals (22, 23, 24) rather than in humans.

2.3 Determination of PYR in Biological Fluids

It has been stated (21) that the pharmacokinetics of PYR are not well understood due to the lack of sensi-

tivity of previous analytical methods. On examination of the minimum detectable limits in Table 4, the level of detection is well below the trough on multiple dosing (20 ng/ml) and the pharmacokinetics of PYR should be able to be studied. However, these analytical methods were not utilized extensively to discern the basic pharmacokinetics in humans. The more sensitive methods have been used to study the pharmacokinetics of PYR in animals (22, 23, 24).

Previous methods of quantification included those listed in Table 4. The earliest senstive assay was developed by DeAngelis et al. (30) in 1975. DeAngelis et al. (30) quantitated PYR on TLC (thin-layer chromatography) plates with a UV absorbance scanning method. A method using HP-TLC (high performance-TLC) by Ahmad et al. (1) had high coefficients of variation. Normal phase high pressure liquid chromatography (NP-HPLC) methods were developed by two groups. Jones et al. (70) used ultraviolet (UV) detection and nonlinear standard curves while Timm et al. (118) used fluorescence detection and had linear calibration curves. In both cases the disadvantages were the volatile mobile phases of normal phase chromatography. Jones et al. (71) developed a sensitive gas liquid chromatographic method (GLC) with a range of 5-400 ng/ml. Weidekamm et al. (125), to their advantage, used the antimicrobial activity of PYR

in their microbiological assay. Three reverse phase ion pair chromatographic (RP-IPC) procedures were developed. Coleman et al. (21) had a micro-analytical technique requiring only 20μl of sample in a study of the pharmacokinetics of PYR in mice. Edstein (38, 39) was able to quantitate PYR with metabolites and other drugs usually given in combination products. The main difference in these assays was that one used acid extraction and the other used base extraction. Optimizations of the extractions in these assays were for the other drugs of interest, not PYR. Midskov (89) has reviewed the other assays. He developed the most sensitive analytical method with a 1 ng/ml detection limit; but it is complicated, and his Spherisorb columns only lasted 600 injections.

Table 4 lists the assays discussed above. The detection limits are listed as determined by the authors even though authors used different definitions of minimum detection limit. The minimum detection limits have been standardized for detection in 1.0 ml of plasma.

Table 4. Previous methods of quantification of PYR

Method	Author	Min Det Lim (ng/ml)	
TLC UV	DeAngelis et al. (30)	10	(15)
NP-HPLC	Jones et al. (70)	10	(15)
HP-TLC	Ahmad et al. (1)	25	(25)
GLC	Jones et al. (71)	5	(5)
NP-HPLC	Timm et al. (118)	10	(5)
Microbio	Weidekamm et al. (125)	13	(26)
RP-IPC	Coleman et al. (21)	330	(6.6)
RP-IPC	Edstein (38)	5	(5)
RP-IPC	Edstein (39)	5	(5)
RP-HPLC	Midskov (89)	1	(1)

Min Det Lim = Minimum detection limit (standardized detection limit in 1.0 ml of plasma)

2.4 Liquid chromatography

In order to develop an HPLC assay for PYR, knowledge of the basic principles of liquid chromatography are necessary.

Separation by HPLC depends on the distribution of sample molecules between the mobile phase and stationary phase. Different molecular species are thus retained to different degrees. From components in the original sample that are introduced into the mobile phase, bands form in the column. Ideally bands should emerge completely separated. Bands tend to broaden the longer they stay on the column (55).

In liquid chromatography, resolution, R, is defined as the distance between the centers of adjacent peaks divided by the average base width of peaks. R is a measure of separation. R can also be defined as the product of efficiency (N), capacity (k'), and selectivity (α).

Efficiency, N, is the number of theoretical plates demonstrated by a column and is a measure of column quality. High values of N demonstrate a superior column and better separation ability.

$$N = 5.54 \, (V/w_{1/2})^2 \qquad (1)$$

where $w_{1/2}$ is the width at half the peak height and V is the retention volume. Efficiency can be expressed as plates per meter in order to compare columns of differ-

ent length. N can be influenced by the manner in which a column is packed, size and distribution of particle sizes, type of support structure, and quality of packing material.

Capacity, k', is a parameter describing the retention of molecular species. It is the ratio of the moles of solute in the stationary phase divided by the moles in the mobile phase.

$$k' = \frac{V_1 - V_o}{V_o} = \frac{t_1 - t_o}{t_o} \qquad (2)$$

where V_1 and V_o are the retention volume of the retained solute (analyte) and void volume respectively and t_1 and t_o are the retention times of the analyte and unretained solute respectively.

Selectivity, α, is a ratio of capacities and a comparison of the relative retention of two components. It relates their peak to peak separation.

$$\alpha = \frac{k_2}{k_1} = \frac{V_2 - V_o}{V_1 - V_o} \qquad (3)$$

Larger α values mean greater separation (55).

2.4.1 Ion pair chromatography

Ion pair chromatography (IPC) is one kind of HPLC.

It can be used for ionic or ionizable compounds. IPC especially has advantages for basic compounds that are ionized at the pH in which silica based columns are stable. The theory of IPC, factors controlling retention, typical counterions and applications of RP-IPC have been reviewed (58)

2.5 Equations for the expression of binding equilibria

The topic of PYR protein binding was introduced in Section 2.2. The following is a discussion of the theoretical concepts of protein binding.

In the study of protein binding, equations have been developed to express the interaction between drug and protein molecules. Briefly, the binding of drugs to proteins in the ideal case follows the law of mass action where:

$$[P] + [D] = [PD] \quad (4)$$

$$K = \frac{[PD]}{[P]\,[D]} \quad (5)$$

$$r = \frac{[PD]}{[P]} \quad (6)$$

where r = number of moles of drug bound [PD] per mole of total protein, [P], and [D] = the molar unbound drug concentration, and K is the affinity or association constant. [PD] is the concentration of the protein-drug complex. The basic assumptions for this model are that binding sites on the protein are identical and affinity

does not change as occupancy increases (independent sites) (76). The relationship for r below is identical to the Langmuir isotherm, an expression for adsorption (78). Eq. (7) is a more useful equation for expressing protein binding data (106) where m is the number of classes of binding sites.

$$r = \sum_{i=1}^{m} \frac{n_i K_i [D]}{1 + K_i [D]} \qquad (7)$$

Eq. (7) was linearized by Wolff in 1929 and since then other names have been attached to these equations (Eq. 8 and 9) and graphical representations of them (27, 76).

$$\frac{1}{r} = \frac{1}{nK[D]} + \frac{1}{n} \qquad (8)$$

$$\frac{r}{[D]} = nK - rK \qquad (9)$$

Two linear plots are represented by Eq. (8), which is known as the double-reciprocal plot, and Eq. (9), which is known as the Scatchard plot (106). The linear equations and their plots as depicted in Fig. 2 assume that all sites are identical and their affinities do not change with increasing occupancy. This is called the site approach. Eq. (7) is often referred to as the Scatchard model (47) also.

The alternative to the site approach is the ther-

modynamic or stoichiometric model as described by Klotz with Eq. (10). The binding constants reflect the nature of interactions between sites with increasing occupancy. A semilogarithmic plot of r versus log free drug concentrations is not linear, but is S-shaped (Fig. 2) (74).

$$r = \frac{K_1[D] + 2K_1K_2[D]^2 + \ldots + N(K_1 \ldots K_N)[D]^N}{1 + K_1[D] + K_1K_2[D]^2 + \ldots + (K_1 \ldots K_N)[D]^N} \quad (10)$$

The Scatchard approach assumes the independence of sites and that they all exist initially. The stoichiometric approach is valid whether or not sites are present and irrespective of cooperativity or anticooperativity of binding. At low ligand concentration if $[D_b]$ is small compared to [albumin], Eq. (10) simplifies to $r = [D]K_1$ and therefore $K_1 = ([D_b]/[D])/[albumin]$. This equation is very useful when the only information is percent bound. In contrast, the Scatchard model does not simplify (63).

Klotz (75, 77) has also questioned the use of nonlinear Scatchard plots to yield definite intercepts as binding parameter estimates. The parameter estimates are meaningless unless sufficient data have been collected such that plotting in a Klotz plot surpasses an inflexion point on an S-shaped curve. Simply put, there is usually a need for higher ligand concentrations than most authors use, and the r versus log [D] plot provides

the best graph for ascertaining the saturation levels (75, 76). The site approach completely collapses when there is more than one binding constant for each site (when site affinities change with the extent of occupancy) even though the equation is widely used in such situations (77).

Nevertheless, the shape of the Scatchard plot reveals useful information about the from of the binding model one should choose for fitting the data. For instance, a positive slope indicates that as ligands bind, the probability of more ligand binding increases. Positive cooperativity is the term for the enhancement of tendency to bind, an allosteric effect in the binding process. A negative slope or negative cooperativity signifies a decrease in the probability of more binding as each ligand binds. Scatchard plots should have an continuously negative slope if the data satisfy the assumption of independent and pre-existence of sites. Even though apparent K_i's obtained from data may not provide direct information about the nature of the binding site, Scatchard plots provide adequate initial estimates for nonlinear iterative search methods in which the search procedure has constraints so that meaningless values are not found (46).

In Fig. 2, the parameter estimates that can be obtained from these graphs are given.

PERCENT FREE VS. TOTAL DRUG CONC.

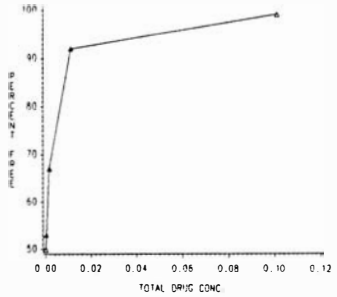

% BOUND VS. TOTAL DRUG CONC.

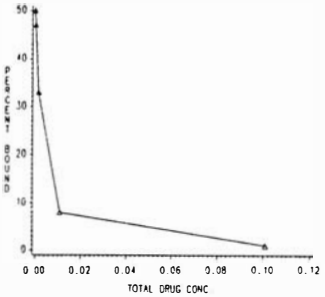

KLOTZ PLOT
R AT INFLECTION POINT IS 1/2 N
LOG D AT INFLECTION POINT IS -LOG K

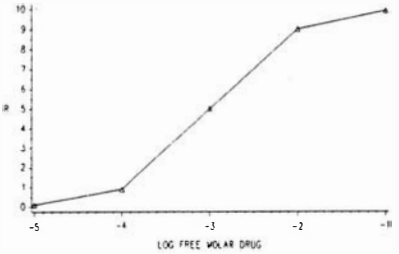

DIRECT HYPERBOLIC PLOT
R = n AT ASYMPTOTE
AT R = n/2, Df = 1/K

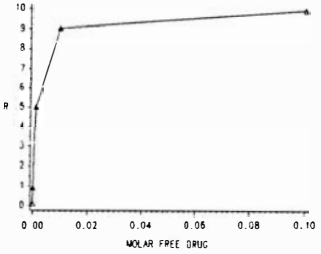

DOUBLE RECIPROCAL PLOT
SLOPE 1/nK, Y-INTERCEPT 1/n

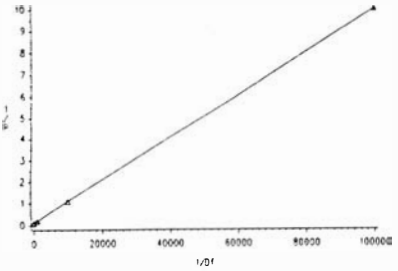

SCATCHARD PLOT
SLOPE -K, X-INTERCEPT n
Y-INTERCEPT nK

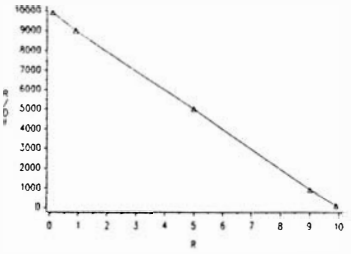

Figure 2. Various protein binding plots.

2.6 Statistical considerations of protein binding data fitting

As discussed in the previous section, the Scatchard plot has been the method of choice for plotting data. Curvature indicates the existence of more than one type of binding site (86). When the Scatchard plot gives a curved line, extrapolations to the intersections of the axes do not give reasonably accurate estimates of binding parameters and should not be used (63). Klotz and Hunston (77) stated that assignment of the binding constants in these circumstances is incorrect. As stated above, the Scatchard model can be fit to data for which the parameters estimates from fits to the Scatchard model cannot be interpreted as binding constants (47). Others claim that the non-integer n determined by statistical analyses is physically meaningless and it indicates a more complicated model. They believe that one needs to know total saturation. Error is greater in both the low and high concentration range, but the Scatchard plot has low error. Dowd and Riggs (35) have found both linear plots to be objectional and that the double reciprocal plot is the worst because it heavily weights experimental points at low concentrations of free drug [D]. The Scatchard model does not suffer from this disadvantage and at that time, 1965, it was the method of choice for plotting data according to *Dowd*

and Riggs.

To give the high concentrations more nearly equal weighting when evaluating by the method of least squares, it has been suggested that each point be weighted in proportion to the concentration of free drug present (78). In that way, weighting accounts for the nonuniformity of the dependent variable (91).

Another criticism of the Scatchard plot is that fitting it with linear regression defies one of the main assumptions of least squares, namely, that error exists in one variable only (36, 99). Luecke and Wosilait (84) have described a general procedure to find a maximum likelihood estimate when both the independent and dependent variables are subject to error. Riggs et al. (99) used geometric regression to solve this problem.

2.7 Nonideal cases of protein binding

In most reviews of protein binding, methods for the analysis of ideal data are presented, as I have discussed above. However, some authors have reported nonideal systems (9, 15, 76), and this review of protein binding will be completed with examples of nonideal binding situations.

Brodersen et al. (15) have called serum albumin a nonsaturable carrier. They reported that the binding of ligands to serum albumin showed no signs of saturation for the 15 ligands studied. Saturation would have been

supported by the occurence of an inflexion point in the binding isotherm where the ratio of bound ligand to albumin is plotted against log free ligand concentration (Fig. 2). The adaptability of the tertiary structure of albumin may account for the failure to observe saturation.

They also state that it is generally not meaningful to distinguish specific from nonnspecific binding because bound drug molecules are merely transported by albumin. The effect of the drug is not related to binding to a specific or nonspecific site on the albumin as it would be in the case of a drug binding to a receptor that produces an action. In the latter case, only, the term specific binding applies. Also, the term high versus low affinity is not justified (15).

The fact that binding classes of diverse affinity have been found supports the idea that binding to albumin is heterogeneous. In cases of heterogeneous sites, one cannot assume independence of sites (77), and thus the Scatchard model should not be used to fit the data. Some of the numerous binding phenomena that exist are adsorption to the protein surface, dissolution of the ligand in the interior of the carrier molecule, and binding to heterogeneous sites. They would all give Scatchard curves as seen with albumin binding and could possibly be fit by the Scatchard equation (Eq. (9)), but

the conclusion of the presence of sites with certain affinities is unjustified unless supported by additional evidence. The stoichiometric approach has the advantage of avoiding dubious claims of the existence of sites (63).

There are at least two sources of curvature in the linear plots: (1) the presence of more than one class of binding sites and (2) electrostatic effects. Curvature in the double-reciprocal plot may occur when the binding of drug molecules to a protein exert additional electrostatic repulsion toward oncoming drug molecules (74). That is, the affinity of one site may be altered as other molecules are bound at other sites (77).

The Scatchard equation produces a straight line only when one class of binding sites is present. In cases where m classes of sites exist, each class i having n_i sites and association constants K_i, curvature exists (86). Curvature may be an indication of interactions between initially identical sites where assignments of site constants are incorrect (77).

Binding may fall below the ideal, as in the case of attenuated affinites, and a curve would appear below the line in the Scatchard plot (Fig. 2). In the Klotz plot decreasing affinities or fixed different affinities make it look like there is no inflexion point, and the line occurs below the ideal S-shaped curve. This lack

of inflexion point in the binding isotherm suggests a lack of saturation. When the binding curve falls below the ideal, the affinities may be fixed but be from different classes of sites or the sites may be initially identical but some affinity decreases with increasing occupancy (negative cooperativity). These two situations cannot be differentiated (76).

Sager et al. (104) investigated the binding of propranolol to albumin, lipoproteins, and $alpha_1$-acid glycoprotein (AAG). Scatchard plots of the binding of propranolol to albumin and AAG at the same time showed curvature. Binding to lipoproteins produced Scatchard plots where the slope of the curve was not significantly different from zero and the y-intercept was 0.75. Their conclusion was that the drug was not bound but distributed to lipoproteins independent of propranolol concentration. Binding was variable between subjects and correlated with AAG concentration.

The case of multiple classes of sites has been reviewed by Blanchard et al. (9). Due to the considerable variation in the determination of both free and bound drug concentration, it may not be possible to determine more than the first classical association constant. Their equation accounts for a class of binding sites that possess an infinite (nonsaturable) binding capacity with zero affinity. That class of sites pro-

duces a horizontal asymptote on a Scatchard plot. Km becomes very small indicating "zero" affinity.

$$r = \sum_{i=1}^{m-1} \frac{n_i K_i[D]}{1 + K_i[D]} + n_m K_m[D] \qquad (11)$$

When m = 2 in Eq. (7) (the case of two classes of sites), binding data plotted as in a Scatchard plot is nonlinear. However, many parameter fitting programs fail to converge when K_2 approaches 0 and n_2 approaches infinity. Accordingly, they suggest the use of this equation:

$$r = \frac{n_1 K_1[D]}{1 + K_1[D]} + n_2 K_2[D] \qquad (12)$$

where the $n_2K_2[D]$ term describes the horizontal asymptote and Eq. (12) becomes a three parameter model where $n_2K_2[D]$ is fit as C in the following rearrangement.

$$\frac{r}{[D]} = \frac{n_1 K_1}{1 + K_1[D]} + C \qquad (13)$$

At low r values, ligands associate with high affinity-low capacity sites. At saturation, molecules partition into a class of high capacity-low affinity sites.

In another recent attempt to simplify the analysis of binding data, Larsen et al. (82) have promulgated a two-constant equation for multiple albumin binding

isotherms. Their equation is not a saturation function but accounts for declining affinities as ligand concentration increases.

$$R(C) = \frac{K_1}{2[K_1-2K_2]} \ln[2(K_1 - 2K_2)C + 1] \qquad (14)$$

where R(C) = r and C = free ligand concentration and K_1 and K_2 are the first and second stoichiometric binding constants. The disadvantage of this equation is that it cannot be applied to situations involving cooperativity.

2.8 Methods of blood collection

Analysis of data can only produce results as good as the data themselves (75). There has been a great deal of interest in the possible alteration of drug protein binding by the method of blood collection (18, 25, 73, 111, 115, 130). In fact, there are many artifactual changes associated with protein binding measurements (130). These changes have especially been associated with basic drugs (51).

In the following pages, several of these sources of error will be discussed.

2.8.1 Heparin

Flushing the cannulas with heparin raises the level of non-esterified free fatty acids (NEFA) by increasing lipoprotein lipase activity (49). One study in dogs (111) reported that intravenous plasma concentration-time curves for propranolol before and after

heparin administration were superimposible even though NEFA concentrations slightly increased after heparin.

Wood et al. (130) examined the binding of propranolol after the alternating cycle of heparinized saline administration and blood sampling. This cycle was repeated every 8 min for 6 doses. They measured propranolol and NEFA levels and constructed a cumulative dose-response curve for heparin (50 to 1200 IU). The protein binding was measured. The free fraction increased from 9.9% to 12.4% after only 50 IU of heparin had been administered. There was a significant ($p<0.001$, $r=0.988$) correlation between the change in free fraction and the log cumulative dose of heparin. There was also a correlation between the log cumulative heparin dose and change in NEFA ($p<0.001$, $r=0.996$). Most significantly, there was a correlation between change in NEFA levels and change in free fraction of propranolol ($p<0.001$, $r=0.988$). They also reported that heparin *in vitro* does not alter the binding of propranolol. There was a significant difference between free fractions of propranolol in samples drawn through a Butterfly® cannula and direct venipuncture while, at the same time, there was no difference in NEFA levels. The elevation in the free fraction may affect drug disposition acutely by making more drug available for distribution out of the plasma space and into the red blood cells and tis-

sues. As a result, volume of distribution may increase and plasma levels may fall. The overall effect on drug metabolism will also depend on whether or not the clearance is affected (restrictive or nonrestrictive elimination).

Guentert and Oie (60) found that the effect of injected heparin was dose dependent and that its effect on "protein binding could be prevented merely by reducing its concentration." Only 5 U of heparin/ml is sufficient to prevent coagulation *in vitro*. In certain cases, altered protein binding can have a profound effect on pharmacokinetic parameters such as clearance and apparent volume of distribution as well as the interpretation of such data (83).

Brown et al. (18) examined the effects of several potential lipoprotein lipase inhibitors to find a suitable one to suppress heparin-induced changes. EDTA and pyrophosphate were ineffective. Paraoxon (diethyl p-nitrophenyl phosphate), mepacrine, and DFP (diisopropyl fluorophosphate) decreased lidocaine binding. Only protamine reduced the effects of heparin without altering plasma binding. They suggested an EDTA/protamine mixture. The reversal of the heparin effect by protamine/EDTA supported the hypothesis that heparin's effect involves the release of lipoprotein lipase and hepatic triglyceride lipase. These lipases continue to release

NEFA during equilibrium dialysis. There were apparent shortcomings in the selection of an inhibitor. Protamine/EDTA affected propranolol binding but not diazepam or lidocaine binding; thus selection of the appropriate inhibitor would depend on the particular ligand.

Heparin induced a decrease in quinidine protein binding more *in vivo* than *in vitro* (73).

2.8.2 Tris(2-butoxyethyl)phosphate (TBEP)

Cotham and Shand (25) were the first to postulate that there was a chemical in Vacutainer™ (Becton Dickinson and Co., Rutherford, NJ) stoppers that reduced the plasma binding of propranolol and that the increased free drug could re-partition into RBCs. Kessler and others (73) reported a decrease in quinidine binding in blood in Vacutainers™. Contact with the rubber stopper produced highly variable (0 to 3.5 fold) elevations in free quinidine fraction. Later isolated from Vacutainers™ was tris(2-butoxyethyl)phosphate (TBEP) which has been shown to inhibit protein binding of alprenolol and imipramine to alpha$_1$-acid glycoprotein (10). Fremstad (51) also showed reduced binding of quinidine and its redistribution into RBCs. He mentioned this effect occurred with other basic drugs.

Stargel et al. (115) found that lidocaine binding in in plasma fell significantly from 56% to 28% when Vacutainer™ tubes were used in blood collection.

Lidocaine concentration in serum fell significantly from 6.5 to 4.9 μg/ml. The effect was seen only when whole blood was introduced into the tubes. This indicated that RBCs were involved. The relative affinity of TBEP is greater than the affinity of lidocaine for binding sites in the plasma.

The plasticizer TBEP is not used anymore (93). Recently, it was shown that the new red-top Vacutainer™ tubes and the anticoagulant sodium citrate did not affect the protein binding of lidocaine in blood (114). However, there is the possibility that other chemicals, perhaps a replacement for TBEP, affect protein binding.

2.8.3 Collection tubes

After the removal of TBEP from most stoppers by Becton Dickinson and Co., Nyberg and Martensson (93) tested eight types of blood collection tubes and two types of plasma separators on the stability of three tricyclic antidepressants and their monodemethylated metabolites. Tubes with serum separator gel or filters were unsuitable and were responsible for losses of greater than 40%. These losses were due to contact between the contents and the caps of the tubes, not re-distribution between red cells and plasma. The losses may have been from drug binding to the stoppers. EDTA-containing Venoject™ lavender and Vacutainer™ lavender tubes gave the most stable plasma samples but

only by a small margin. Royal blue tubes were also unsuitable. They found minimal effects on serum or plasma concentrations from freezing and thawing or storage at -20°.

Potter and Self (97) attributed variability in cyclosporin A whole blood levels collected in heparin tubes to the microaggregations of RBCs and small fibrin clots seen under microsopic examination. The clots would not disintegrate with gentle mixing. Commercial tubes containing EDTA produced homogenous suspensions of RBCs and variability was much less than that from heparin-containing tubes. Freezing the samples collected in heparin tubes and thawing before assay reduced variablity.

2.8.4 The pH adjustment for protein binding

In the effort to reproduce physiologic conditions, plasma pH has been adjusted to 7.4 in protein binding studies. The pH adjustment has been carried out by adding small vclumes (5-10 μl) of phosphoric acid (61) or by titration with HCl (17) immediately before equilibrium dialysis.

More correctly (this practice is more physiologic), others (52, 104) gassed plasma with 5% CO_2 before dialysis. However, pH is often not mentioned in protein binding experiments. Brors and Jacobsen (16, 17) reviewed the many drugs that have been found to have

pH-dependent serum binding. Due to the loss of CO_2 (98), pH of serum left open to the atmosphere or frozen and thawed is pH 8 or higher. The pH of thawed serum after storage at -20° was 7.7 - 7.6 at 3 h. Using Perspex™ cells sealed with tape, when serum was adjusted with HCl to 7.4 and then dialyzed at 22° against sodium phosphate buffers, the serum pH increased to 7.55 - 7.6 at 3 h. When serum was dialyzed against ungassed Krebs Ringer bicarbonate buffer, the serum pH increased to 7.74 after 1 h and 8.37 after 3 h. At 37° the increases were greater than at 22°. Dialysis against all buffers produced mean pH 7.8 for serum after 3 h. Even when serum was adjusted to pH 7.4 (with HCl) prior to dialysis against Krebs Ringer bicarbonate buffer, the serum pH rose to 7.85 after 1 h and 8.45 after 3 h (17).

The unstable serum pH is caused by loss of CO_2 during dialysis resulting in a decrease in hydrogen ion and bicarbonate concentrations in serum. The pH increase was greater at lower buffer molarity and at higher temperatures. The authors believe that a large part of published data on drug binding in serum contains such errors in pH and exceed acceptable limits for analytical errors (17).

2.8.5 Osmotic volume shifts of fluid

In equilibrium dialysis, it is important to measure shifts in water across the membrane (56, 64, 119).

Dialysis cells consist of a membrane separating a cell into two cell-halves. Dieterle et al. (34) and Giacomini et al. (56) measured the protein concentration in each cell-half before and after dialysis to determine the volume shift. Authors (56, 64, 119) have presented equations for correcting for volume shifts. Hu and Curry (64) have stated that the use of isotonic buffers in ED reduces the magnitude of volume shifts.

2.8.6 Mass balance considerations

From the experimental viewpoint, the determination of protein binding by equilibrium dialysis has many inherent artifactual errors. The lack of controls concerning mass balance is the major cause of these variations (14). Often, the conservation of mass is probably assumed but is not addressed in reports in the literature (64). Two details frequently left out of most reports are corrections for binding to dialysis membranes and apparatus and drug decomposition (14, 64). A method (14) and an equation (64) that correct for loss of drug during dialysis have been presented.

2.9 Red blood cell partitioning

Binding to plasma proteins has been discussed above. However, drugs bind to other blood constituents as well. Early work in pharmacology revealed that many drugs had an unusual affinity for RBCs. Maren et al. (85) observed that a number of aromatic N^4-substituted

sulfonamides which were carbonic anhydrase inhibitors showed a high RBC/plasma concentration ratio. Their comparison of different categories of sulfonamides enabled them to describe a "diffusible component" and bound components. Compounds fit into three patterns of distribution in the blood: (1) drugs like acetazolamide with strong binding to red cells (probably to carbonic anhydrase) and a diffusible component that followed a concentration gradient and was dependent on ionization and plasma protein binding; (2) compounds that accumulated in RBCs but were not firmly bound; and (3) compounds with no affinity for RBCs. The diffusible component was the drug that diffused freely into the RBC, was not bound, and could be easily washed out by rinsing the RBCs with an isotonic buffer. N^1-substituted drugs were not bound to RBCs, whereas unsubstituted ones were bound. They dismissed the role of lipid solubility after finding inconsistencies, placed ionization at a moderate importance, and decided that plasma binding was the major determinant of diffusion. They also examined binding to hemoglobin.

In contrast to Maren et al., the classic studies of Schanker et al. (108) found that lipid solubility and degree of ionization were the major properties of bases that determined their rate of passage into RBCs and that the unbound, unionized molecules were distributed

according to a Donnan equilibrium. They also looked at binding to nondiffusible cell components such as hemoglobin (107).

Schanker et al. (107) found that organic anions entered the cell more rapidly than organic cations of similar low lipid solubility and suggested a possible explanation. They proposed that anions entered through both the lipoid regions and the positively charged aqueous pores.

Korten and Miller (80) found that the anion form of barbiturates doesn't significantly partition into biological membranes using the RBC membrane model. The potency and pharmacodynamics of barbiturate anesthetics depend on their ability to diffuse through membranes.

Many basic drugs have been found to have higher concentrations in RBCs. Ahtee and Paasonen (3) noted that the uptake of three phenothiazines by RBCs was related to their tranquilizing activity. The binding of chlorpromazine and imipramine to RBC membranes has been studied by Bickel (8).

2.9.1 Effects of pH on RBC Partitioning

More often than not, researchers refer to any drug in the blood that is not in the plasma as being "bound" by RBCs. In a sense, this is true because the drug is not free in the blood. To be more correct, however, they should distinguish between the bound and diffusible

components as Maren et al. did in 1960 (85).

Using the RBC as a model, Schanker et al. (108), determined that two properties, lipid solubility and degree of ionization, of basic drugs were very important in determining their rate of distribution into cells. In general, weak electrolytes diffuse according to the lipid solubility of the unionized species which depends on the ionization of the molecule at the pH of the extracellular medium. The degree of ionization of the compounds is important because it defines the proportion of drug in the lipid soluble (unionized) form according to the Henderson-Hasselbach equation.

There is normally a pH gradient across the cells in the human body, with more acidity (higher partial pressure of CO_2) intracellularly. The range inside RBCs is normally pH 7.13-7.29 (59). The pH gradient is greater in cirrhosis and after nephrectomy. In anoxia, acidosis is more marked in the extracellular fluid compared to the intracellular fluid (122).

If the pH of the cell and medium differ, basic molecules will favor the acidic side of the membrane (94) and the total concentration of drug will not be the same on different sides of the membrane. The concentration of unbound drug may be somewhat higher on the inside compared to the outside of cells (117). It is also possible that the unionized forms of weak acids and

bases will have different concentrations on different sides of the membrane if the membrane is permeable to the ionized conjugate partners (101).

The pH dependent distribution of any drug should not be influenced by the concentration of that drug (52). According to Schanker et al. (108), what is not accounted for by the pH differential is due to binding. Measuring the cell/medium concentration ratio enables us to discriminate between diffusible and bound components. With certain restrictions, the concentration ratio of unbound diffusible anion is 0.7. For cations, the ratio is 1.38 as discussed more thoroughly below. A common practice is to assume that if the ratio is greater than 1.0, binding is occurring (41), but one must consider that bases have a higher free concentration in cells due to ion-trapping and that partitioning depends on pKa.

The following equation, first derived by Jacobs (68), describes the distribution of a weak base between two solutions separated by a cell membrane permeable only to the unionized molecule:

$$\frac{C_{cell}}{C_{medium}} = \frac{1 + 10^{(pKa-pH_{cell})}}{1 + 10^{(pKa-pH_{medium})}} \qquad (15)$$

By substituting into the equation the intracellular and extracellular pH values, one obtains ratios which are identical to those calculated for the Donnan distribution of the hydrogen ion because strong bases

are mainly in the cationic form at these pH values. The higher the extracellular pH, the greater the cell/medium ratio for the hydrogen ion and strong bases. When experimentally determined pH values for the medium are 6.7, 7.4, and 8.0, the intracellular pH values for the RBC are 6.67, 7.26, and 7.69, and the cell/medium ratios for PYR for these pairs of pH values would be 1.05, 1.13, and 1.12. So, for PYR, with pKa 7.13 that is near physiologic pH, the theoretical cell/medium concentration ratio does not parallel the ratios of the hydrogen ion (1.07, 1.38, 2.04).

The importance of maintaining physiologic pH in the medium of blood cell suspensions cannot be understated when doing in vitro determination of RBC binding and partitioning.

Considering lipophilicity, Korten and Miller (80) have shown that partition coefficients determined with RBCs correlate more closely with physiological permeability constants than do those determined with organic solvents. The solvents failed to reflect partitioning into biomembranes adequately. The pH partition hypothesis described above was confirmed by Korten and Miller.

Taylor and Turner (116) also confirmed that partition coefficients overestimated differences in in vivo membrane permeability. They found similar RBC/free plasma drug concentration ratios for three adrenergic

blockers which had greatly differing lipophilicity according to their organic solvent partition coefficients. They also noted that for lipophilic drugs, partitioning into the membrane is of greater importance than the accumulation of weak bases due to the lower intracellular pH.

Bickel (8) has noted a common trend for lipophilic drugs capable of hydrophobic interactions. They tend to interact with RBC, microsomal, and mitochondrial membranes as well as lipoproteins, alpha and beta globulins, white blood cells, and platelets.

2.9.2 Drug disposition and RBC partitioning

In 1973, Garrett and Lambert (53) expressed the need for the determination of protein binding and RBC partitioning to provide a realistic physicochemical and physiological pharmacokinetic description of drug disposition in the body. Others observed the need for the investigation of RBC uptake of drugs because of similarities to plasma protein binding (43, 44, 52, 53, 81, 87). Drug binding in the blood can affect drug distribution, activity, and elimination (43, 44, 72). The importance of their work is the recognition that only the unbound fraction of drug is able to elicit pharmacological actions. As a result, efforts to elucidate the relationship between plasma protein binding, tissue distribution, and RBC uptake have been undertaken by

many scientists.

In 1973, binding to and partitioning into RBCs was shown to alter the delivery of drug to its site of elimination by Evans and Shand (44). One way to catagorize drugs is by their metabolism. In this case, classification of drug metabolism can be based on hepatic clearance. Hepatic clearance is either restricted to the free drug in the circulation (restrictive clearance) or includes both free and protein bound drug (nonrestrictive clearance). In their opinion, this classification should also include reference to the reservoir of drug in the RBCs. Drug in the RBCs may be removed during passage through eliminating organs as in the cases of propranolol (43), quinidine (52), cyclophosphamide (123), and chlorothiazide (110). The clearance of chlorothiazide from the blood was found to differ between intravenous and oral administration due to the influence of the time-dependent distribution to the RBCs.

2.9.3 RBC partitioning relative to protein binding

The unbound diffusible concentrations of drugs in the plasma are determined by protein binding. The idea that drug distribution into the tissues is dependent on the unbound concentration in the plasma led to the examination of the interaction between plasma protein binding and RBC partitioning (11, 43, 44, 69, 81).

Several authors noted a linear relationship between the RBC/P drug concentration ratio and free drug in the plasma (43, 54, 62, 65, 69, 81, 116). Evans and Shand (44) and Taylor and Turner (116) also reported a linear relationship between WB/P ratios and free drug concentration. With this information, the degree of protein binding in plasma drug could be determined given a RBC/P concentration ratio.

In contrast, Derendorf et al. (31) found a lack of correlation between protein binding and RBC partitioning for morphine, naloxone, and naltrexone.

2.9.4 Variables from analytical techniques

2.9.4.1 Mass balance considerations

Binding to serum albumin has been studied extensively. The phenomena of RBC partitioning and binding are much more complex and the measurement of these processes is ultimately more complicated. The entry and rate of entry of molecules is governed by physiocochemical properties of the molecules and the RBC membrane. Drugs may be bound by the RBC membrane or intracellular components such as hemoglobin or carbonic anhydrase, and may exist in the intracellular fluid or cytoplasm in a freely diffusible, unbound form (95).

Many investigators use the rough estimate that if the whole blood/plasma (WB/P) drug concentration ratio is greater than (1-hematocrit) (41) or if the WB/P ratio

exceeds 1.0 (88), the drug is distributed to the RBCs. However, there is a difference in the ratios depending on whether the drug is a weak acid or a weak base. Schanker et al. (108) calculated the RBC/P concentration ratio of unbound diffusible anion at pH 7.4 and found it to be 0.7. For cations such as weak bases, the ratio is near 1.4. The ratios given by Schanker et al. are near the actual ratios for anions and cations. However, for more precise estimates of the RBC/P ratios, one must consider the pKa values of individual weak acids and bases. The theoretical RBC/P ratios will be more thoroughly discussed in Sections 5.4 and 6.4.

It is a common practice in studying RBC partitioning to calculate the RBC level based on the assays of the plasma (or supernatant in buffer suspensions or serum) and the whole blood knowing the hematocrit and assuming mass balance in the blood; the amount in the plasma is subtracted from the whole blood content and the remainder is assumed to be in the RBCs. Often this is done without even assaying the whole blood by assuming it to contain the spiked blood concentration (12, 43, 53, 62, 65, 66). This is done due to the ease of assaying plasma compared to assaying whole blood or RBCs.

However, this procedure does not account for the *in vitro* artifacts such as drug degradation or

metabolism, binding to glass, or partitioning into white blood cells or platelets. Erythromycin proprionate hydrolyzes to erythromycin during storage at room temperature and in the frozen state. Thus erythromycin levels are increased (121). Hemoglobin catalyzes the formation of the sulfoxide of chlorpromazine and may lead to a trapping effect and discrepancies in binding experiments (8). Drayer et al. (37) found that procainamide, para-aminosalicylic acid, and dapsone were acetylated by whole blood, and the de-acetylated metabolite of dapsone was also metabolized back to dapsone. For these reasons, it is necessary to confirm whole blood levels by assay at the same time as one measures levels in the fractions of blood.

2.9.4.2 Effect of trapped plasma

Some authors have measured the RBC and plasma levels after separating them by centrifugation (6, 48, 62, 81). For this method, it is necessary to account for trapped plasma or the volume of extracellular fluid in the packed cell mass (41, 50, 79, 108). These researchers assumed constant packing of cells. However, plasma trapped in the red cell column in a centrifuge tube is highly variable. It varies with centrifugal force which depends on the radius of the centrifuge, the distance from the center of the head to the middle of the packed cell column, and the speed of the centrifuge

as well as the viscosity of the medium. Packing also depends on the time centrifuged and fluctuations in the acceleration and deceleration. As the packed cell volume increases the percentage of plasma trapped in the RBC column increases due to the reduction in effective radius of centrifugation. It is better to spin samples for a longer period of time, 55 minutes, to reduce variations (20).

In the case of measuring concentrations in the centrifugally separated RBC fraction of blood, great errors can result from not accounting for trapped plasma. This source of error increases as the plasma protein binding increases, the trapped plasma increases, and in low percentage RBC partitioning, creating falsely elevated RBC levels. It is possible the fractional amounts in the RBCs and plasma could add up to greater than the true whole blood concentration.

Researchers have attempted to correct for plasma trapping. Kornguth and Kunin (79) determined the trapped extracellular antibiotics in the RBC fraction by measuring the hematocrit of the RBC fraction as did Roos and Hinderling (102). Parsons and Vallner (95) erroneously assumed a constant 9% trapped extracellular fluid (ECF) in the RBCs and subtracted it from the percent hematocrit to get the true cell volume. This was a preventable source of error. They borrowed the

value 9% +/-0.5 s.d. (n=31) from Schanker et al. (108) who determined it under different conditions than in the Parsons and Vallner lab. Schanker et al. determined the volume of ECF by re-centrifuging the packed RBCs in capillary tubes at 12,000 X g. This data cannot be extrapolated to other labs or instruments contrary to the belief of Parsons and Vallner.

A more sophisticated measurement of trapped plasma is by the addition of Evans blue dye (20), tritiated inulin (52), or tritiated cobalt blue (50) which can then be measured in the fraction of separated RBCs. Fremstad (52) reported that plasma space was more accurately determined by labelled inulin rather than by hematocrit centrifugation and that the hematocrit overestimated the RBC volume due to plasma trapping. One study corrected the hematocrit value by a factor of 0.98 to account for plasma trapped in the packed cells (62). However, according to Rustad (103), the hematocrit should be corrected by a factor of 0.97 to allow for trapped plasma in the RBC column in micro-hematocrit techniques.

For practical purposes, preliminary experiments may reduce the need for measuring trapped plasma in every sample by providing consistency. For instance, the variation of the centrifugal force on venous blood samples was shown to affect the concentration of chloro-

quine in the plasma. However, there was little variation in plasma levels when samples were centrifuged above 1000 g forces (7).

2.9.4.3 Effect of the medium on RBC levels

The medium in which RBCs are suspended has been shown to affect the RBC levels of drugs. For chloroquine and its metabolite, desethyl-chloroquine, serum levels were 2 and 4 times higher than plasma levels. Bergqvist et al. (7) speculated that the higher concentrations were due to release of drug from leucocytes and thrombocytes during the clotting process. Another antimalarial agent, quinidine, was shown to have higher concentrations in serum (29)

Binding data has often been obtained using washed cells or cell membranes (ghosts) in buffer. Washing cells has been shown to alter binding properties either by removing lipids or adsorbed proteins from membranes or by "removing the influence of plasma water" to increase or decrease binding (52). Kornguth and Kunin (79) found that using plasma as the medium rather than buffer enhanced the egress of antibiotics.

Ehrnebo et al. (40) found that for the basic drug pentazocine the blood cell/plasma water ratio in whole blood was higher than the blood cell/buffer ratio. In their study blood cells included leucocytes and platelets as well as RBCs. Washed RBCs had a greater binding

ability than unwashed RBCs in whole blood. In another study (41), pentobarbital and phenytoin were bound to washed blood cells more than cells in whole blood and the change was not due to pH differences. The blood cell/water ratio also decreased in washed cells when human serum albumin (4 g/100ml) was present, suggesting an alteration of RBC membrane binding properties due to an interaction with the albumin.

Others speculated that plasma binding sites still attached to RBCs after washing were probably responsible for a small deviation from the theoretical linear relationship between the hematocrit and the RBC/buffer ratio for phenytoin. The influence of plasma water was greater at higher hematocrits (81). Williams (126) has shown that bovine albumin is adsorbed by a finite number of sites on the surface of the human RBC, and it competes with other endogenous and possibly exogenous molecules and that the albumin is not easliy removed by washing with saline. In fact, they are not displaced by the human albumin fraction (Cohn fraction 5) proteins.

Cruze and Meyer (26) found that bovine albumin was an inadequate substitute for human serum albumin.

Another source of error is the effect of pH of the medium on the cell to medium ratio. As discussed earlier, the pH gradient across the membrane affects the concentration gradient for weak acids and bases. Plasma

becomes more alkaline upon sitting uncovered due to the escape of CO_2 and the re-equilibration of CO_2 in the plasma with it in the atmosphere (100). The CO_2 from RBCs is replaced by the intracellular movement of chloride ions known as the "chloride shift". The basic buffer anions in the whole blood are bicarbonate, hemoglobin, and plasma proteinate (33). In fact, 95% of the excess or deficit of carbonic acid is buffered intracellularly (101).

Given whole blood having 100% (0.0385 gEq/L/pH unit) of the buffer capacity of the blood, these are the percentages contributed to buffer capacity by each constituent: cells 79, plasma 21, plasma bicarbonate 6.1, plasma protein 13.6, plasma phosphate 1.5. Hemoglobin contributes about half of the total cellular buffer capacity (42). For this reason, plasma pH rises rapidly, while RBCs have the buffer reserve to maintain normal pH.

Investigators have several ways of adjusting the pH of blood samples. The most common method is by performing centrifugation and equilibrium dialysis in a 5% (v/v) CO_2 atmosphere (52). It is possible to bubble carbon dioxide in air or nitrogen through samples to adjust their pH (67). Citric acid was added to samples to study the effect of pH on the partition coefficient of fentanyl between RBCs and plasma (12).

The pH can be confirmed by measuring the pH of samples at the beginning and end of experiments (62, 102). Trung et al. (120) recommended that tubes of blood or plasma samples be covered with PTFE (polytetrafluoroethylene) tape during all procedures because drug binding could be affected.

Disease states may affect the pH of the blood. Anuria lowers plasma pH. The quinidine blood cells/plasma ratio was lower in anuric rats and unbound quinidine concentrations in plasma were lower as determined by equilibrium dialysis. Anuria reduced the distribution to blood cells (52).

Care has to be taken to prevent hemolysis. Even a stir bar can produce significant hemolysis (26). Plasma from blood banks has been shown to bind quinidine less than fresh serum or plasma probably due to preseratives or anticoagulants (129).

Chapter 3

Definition of the Problem

3.1 Background

RBC partitioning is closely related to protein binding. Due to the infrequent measurement of drugs in RBCs in studies reported in the biopharmaceutics literature, methods to study them have not become routine. Many analytical variables affect these studies in addition to the ones that affect protein binding studies. Recently, sources of error in protein binding studies have been mentioned more and more frequently, even though plasma protein binding has been widely studied for many years.

It is important to characterize the protein binding and RBC partitioning of a drug for the understanding of the drug's disposition. This is especially true for drugs like PYR because RBC uptake is important for antimalarial activity and because it is a weak base and weak bases tend to have significant RBC levels. Even though PYR has been used for many years, studies of its binding and partitioning are lacking in the literature. For these reasons, PYR was chosen as a model drug.

3.2 Hypothesis

Several factors such as the pH of the media, the additives in evacuated collection tubes, and albumin levels may significantly affect the protein binding and RBC partitioning of PYR.

3.3 Objectives

(1) To reproduce an HPLC assay for PYR in plasma, RBCs, and buffer.

(2) To investigate variables such as pH, types of evacuated collection tubes, and albumin levels on RBC partitioning and plasma protein binding.

(3) To determine binding of PYR in plasma and to plasma albumin, AAG, and Hb.

3.4 Proposed methodology

(1) Edstein's IPC-HPLC assay will be reproduced. If this method is not sufficient, an original HPLC method will be developed.

(2) Plasma and RBCs will be spiked with PYR. All studies will be *in vitro*.

(3) Statistical data analysis will be done using the SAS System version 5 (105) on the VAX-11/780 CPU at Virginia Commonwealth University.

Chapter 4

Experimental

4.1 Reagents, chemicals, and equipment

4.1.1 Chemicals and reagents

Methanol, acetonitrile, methylene chloride, n-butyl chloride, and hexane were all HPLC grade and purchased from Fisher Scientific Co., Fair Lawn, NJ.

Water: Deionized/organic-free water was distilled in a model One Liter MP-1 apparatus (Corning Glass Works, Corning, NY). This water was used to make all buffers and mobile phases.

PYR: Purified PYR (5-(4-chlorophenyl)-2,4-diamino-6-ethylpyrimidine) was a gift of Dr. Carl Sigel and the Burroughs Wellcome Co. (Research Triangle Park, NC). Precisely 50.00 mg of PYR was weighed out and placed in a 100 ml volumetric flask. HPLC grade methanol was added to the 100 ml mark to make a stock solution of 500 μg/ml PYR in methanol. It was kept refrigerated at 4° in silanized (0.2-0.35% AquaSil™, Pierce Chemical Co., Rockford, IL) light resistant, low actinic Pyrex glassware (Corning Glass Works, Corning, NY). Solutions in methanol containing 0.10, 0.12, 0.15,

0.2, 0.3, 0.5, 0.7, 1.0, 2.0, 3.0, and 5.0 μg/ml PYR were made by dilution of (using volumetric pipets and volumetric flasks) this stock solution. For the IPC-HPLC method, stock solutions from 0.125 to 10.0 μg/ml were made.

Plasma controls were made by using a volumetric pipet to place 6 ml of PYR in methanol (6 μg/ml) in a 50 ml volumetric flask, evaporating it under nitrogen until almost dry, and reconstituting with expired blood bank plasma. After thorough mixing, using a syringe, volumes of the spiked plasma were placed in 50 ml volumetric flasks and plasma was added to the 50 ml marks. From these spiked controls, other controls were made by similar dilutions with plasma to make 720, 420, 330, 150, 128, 68, 35, and 32 ng/ml controls. Each control was divided into 3 plastic vials. Two vials were frozen for later use and one vial was kept in the refrigerator.

Buffer controls were made by evaporating PYR from a standard methanol solution in a volumetric flask and adding filtered phosphate buffer to the mark. Other solutions were made by making dilutions of this solution to make 40, 100, 140, 280, 480, and 700 ng/ml controls. Each control was divided into 3 plastic vials which were kept in the dark.

All methanol solutions of PYR were kept in silanized glassware in the dark except for solutions used for

spiking biological samples. They were kept in silanized culture tubes which were kept in the dark except during use.

Quinine HCl (Q): Quinine HCl, the internal standard for the IPC-HPLC assay was from an unknown manufacturer. Individual stock solutions of Q were prepared in methanol at concentrations of 1.0 to 5.0 μg/ml and stored at 4° in low actinic glass that had been silanized with AquaSil™.

N-acetylprocainamide (NAPA) HCL: Precisely 50.0 mg of the internal standard NAPA HCl, 99% pure, purchased from Aldrich Chemical Co. (Milwaukee, WI), was placed in a 50 ml volumetric flask. Methanol was added to the 50 ml mark to make a solution of 1.0 mg/ml NAPA HCl. Dilutions of this stock solution were made to make a 0.8 μg/ml solution with which to spike plasma samples.

Sodium salt of 1-pentanesulfonic acid (SPS): SPS was purchased from Sigma Chemical Co., St. Louis, MO.

Potassium hydroxide (KOH): A solution of 4.0 M KOH was prepared by placing 22.4 g of pellets (Baker Analyzed Reagent grade, J. T. Baker Chemical Co., Phillipsburg, NJ) in a 100 ml volumetric flask and adding water to the 100 ml mark. This solution was later diluted by adding 52 ml of 4 M KOH to 210 ml of water to make a total volume of 262 ml of 0.8 M KOH.

Sodium carbonate: A solution of sodium carbonate

was made by adding 10.6 g of Na_2CO_3 (Baker Analyzed Reagent grade) to a volumetric flask and adding water to the 50 ml mark to make 2 M sodium carbonate. Later, this was diluted to 0.5 M by adding 3 volumes of water.

Buffers: Solutions of 0.03 M monobasic potassium phosphate (KH_2PO_4) were prepared by placing 4.08 g of HPLC grade KH_2PO_4 (Fisher Scientific Co., Fair Lawn, NJ) in a volumetric flask and adding water to the 100 ml mark. Solutions of 0.03 M dibasic potassium phosphate (K_2HPO_4) were prepared by placing 5.22 g of K_2HPO_4 (Baker Analyzed Reagent grade) in a 1000 ml volumetric flask and adding enough water to make 1000 ml. These 2 solutions were added together to get the desired pH of 6.95 for the mobile phase.

Isotonic phosphate buffer (IPB): IPB was prepared by making 2 isotonic buffer solutions and adding them together to get the desired pH. The amounts of 9.465 g of dibasic sodium phosphate (ACS grade, Fisher Scientific Co.) and 3.983 g of sodium chloride (ACS grade, Fisher Scientific Co.) were weighed out and placed in a 1000 ml volumetric flask. To this flask was added enough water to make a 1000 ml isotonic solution (pH 9.0). The amounts 9.073 g of monobasic potassium phosphate (ACS grade, Fisher Scientific Co.) and 5.005 g sodium chloride were weighed out and placed in a 1000 ml volumetric flask. To this flask was added enough water

to make a second 1000 ml isotonic solution (pH 4.4). The approximate volume:volume ratio of the 2 buffer solutions for pH 7.4 IPB was 85:15.

Phosphoric acid (85% w/w) was made by Mallinckrodt (St. Louis, MO) and purchased through Scientific Products (McGaw Park, IL).

4.1.2 Instrumentation

This is a list of the chromatographic instruments:

(1) Model 110 A Altex pump (Beckman Instruments, Inc., Berkeley, CA)

(2) Model 440 single wavelength UV detector at 254 nm and using a 280 nm slit at a sensitivity of 0.005 or 0.01 a.u.f.s. (Waters Associates, Inc., Milford, MA)

(3) Syringe-loading injector 7125 with a 100 μl loop (Rheodyne, Berkeley, CA)

(4) A 2 cm X 2 mm I.D. Uptight precolumn packed with Perisorb RP-18 30-40 micron pellicular packing (Upchurch Scientific, Oak Harbor, WA)

(5) 10 mv Recordall Series 5000 OmniScribe (Fisher Scientific, Fair Lawn, NJ) chart recorder

(6) Series 700 100μl syringe (Hamilton Co., Reno, NV)

Other equipment:

(7) Horizontal shaker (Eberbach Corp., Ann Arbor, MI).

(8) Centrifuge, IEC model UV or desk top model HN-S (International Equipment Co., Needham MA).

(9) Evaporator with water bath, Meyer N-Evap model 111

(Organomation Assoc., Northborough, MA).

(10) Water bath, model MW-1130A-1 (Blue M Electric Co., Blue Island, IL).

(11) Hemato-Kit for converting the IEC model HN-S centrifuge into a micro-hematocrit machine (VWR Scientific, San Francisco, CA).

(12) Spectrophotometer, Model DB-GT, (Beckman Instruments, Fullerton, CA).

(13) Sorvall RC-58 refrigerated superspeed centrifuge (DuPont Co. Instrument Products, Newtown, CN). 4.2

(14) Accumet model 630 pH meter with a pencil thin gel filled polymer body combination electrode (Fisher Scientrific Co., Pittsburgh, PA).

4.2 Reproduction of Edstein's IPC-HPLC method

Because this exact method (39) was not used for the analysis of samples except in the initial search for an extraction solvent, the slightly modified assay procedure will be presented in an abbreviated form.

A 30 X 3.9 mm I.D. 10 μm particle size, μBondapak™ C_{18} (Waters Assoc.) reverse-phase column was used. It had about 20,000 plates/meter and had been stored for at least 5 years in 50% methanol after an unknown history of use. The mobile phase consisted of methanol-acetonitrile-water (25:15:60 v/v) containing 0.001 M sodium pentane sulfonate (SPS) adjusted to pH 3.0 with 6-8 drops of phosphoric acid. The mobile phase was

filtered prior to use with an Alpha-450 metricel membrane (47 mm, 0.45 μm, Gelman Sciences, Ann Arbor, MI) and then ultrasonicated under vacuum for an additional 10 min. The flow rate was 1.7 ml/min at ambient temperatures. The volume injected was 100 μl. The internal standard was quinine.

Extraction procedure for IPC-HPLC:

(1) 100 μl each of PYR standards (1-50 μg/ml) was added to 16 X 125 mm glass culture tubes with PTFE lined screw caps (Kimble, Corning, NY).
(2) Blank RBCs, plasma, or buffer 0.5 ml was added.
(3) 100 μl of Q 4.0 μg/ml was added.
(4) For RBCs only, 1.0 ml of water was added, briefly vortexed.
(5) 150 μl of 4 M sodium hydroxide was added.
(6) 15 ml of hexane/methylene chloride (2:1) was added.
(7) Tubes were shaken 30 min at 220 cycles/min.
(8) Samples were centrifuged for 20 min in IEC UV centrifuge at 2100 rpm.
(9) Tubes were placed in acetone bath in -70° freezer for 15 min or until frozen.
(10) Organic phase was decanted into another tube and evaporated to dryness in 38° water bath under a gentle stream of nitrogen.
(11) The residue was reconstituted with 500 μl of

methanol and 100 μl was injected.

The concentration of the counter-ion SPS was varied to see its effect on retention times and capacity factors for PYR and Q. The pH of the mobile phase was also varied. The extraction recoveries of PYR and Q were also studied.

4.3 Assay of PYR using original RP-HPLC method

4.3.1 Selection of internal standard

Internal standards used in the published assays could not be obtained. Prospective compounds with structures similar to PYR and other antimalarials were reviewed for their UV absorbance and other properties. Chlorpheniramine, ranitidine, quinine, procainamide, N-acetylprocainamide (NAPA), dapsone, phenytoin, and trimethoprim were some of the compounds examined. All but one of them were ruled out for one of these reasons: (1) binding to glass, (2) being commonly found in expired blood bank plasma, (3) known chromatographic difficulties, or (4) different extraction properties.

NAPA was chosen because of its appropriate UV absorbance, basic functional group, known stability, and most importantly, because a test injection on the preliminary system used to analyze PYR revealed a retention time very similar to PYR's.

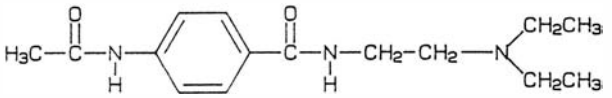

NAPA

Figure 3. Structure of N-acetylprocainamide (NAPA)

4.3.2 Selection of extraction solvent

A review of the literature revealed that PYR was extractable into nonpolar solvents such as ethylene chloride at an alkaline pH. However, they did not have the same internal standard. Experiments were performed to determine the extraction recovery of 11 μg/ml PYR and NAPA HCL from hexane, 2-propanol, ether, ethyl acetate, ethylene chloride, and methylene chloride using expired blood bank plasma that had been alkalinized with 0.2 ml of 4M KOH. Note: Later, the molarity of the KOH was decreased to 0.8M and the same volume was used. This was because the strong alkalinity of the 4M KOH removed the silanes from silanized glass and allowed PYR to bind to the glass. The 0.8M KOH produced less silane removal

but adequately alkalinized plasma samples for extraction purposes.

4.3.3 Separation of PYR and NAPA

The chromatographic separation of PYR and NAPA was evaluated using phosphate buffer with acetonitrile and methanol as the organic modifiers. The percentage of each constituent was varied, the pH of the aqueous phase was varied, and the best chromatography determined by evaluating peak symmetry, retention times, peak resolution, and peak heights. Different molarities and salts of phosphate buffer were evaluated.

4.3.4 Preparation of the mobile phase

The mobile phase consisted of acetonitrile and methanol as organic modifiers and a phosphate buffer adjusted to a pH of 6.95. The phosphate buffer was prepared by making 0.03 M solutions of KH_2PO_4 (4.08 g/L) and K_2HPO_4 (5.22 g/L) in water. The pH of the buffer was adjusted to 6.95 by the addition of KH_2PO_4 to the K_2HPO_4 solution while stirring with a PTFE stir bar and monitoring the pH of the solution with a Fisher Accumet model 630 pH meter. Volumes of 400 ml of potassium phosphate buffer, 450 ml of methanol (Fisher HPLC grade), and 150 ml of acetonitrile (Fisher HPLC grade) were mixed together. They were filtered through an Alpha-450 0.45 μm metricel membrane filter (Gelman Sciences, Inc., Ann Arbor, MI) and then ultrasonicated

for 7 additional minutes. The phosphate buffer was near its limit of solubility in the organic-aqueous mixture because often the filter membrane would have to be changed before filtration was complete due to precipitation clogging up the filter before 1000 ml could be filtered.

4.3.5 Column, detector and recorder characteristics

Separation was conducted on a 150 mm X 4.6 mm I.D. Econosphere™ column packed with 5 micron RP-18 spherical particles (Alltech Associates, Inc./Applied Science Labs, Deerfield, IL). There was an additional precolumn between the pump and the injector. It was a saturator column, a 25 cm X 3.9 mm I.D. column packed with 50 micron high capacity silica (Alltech/Applied Science Labs, Deerfield, IL). This saturator column protects the analytical column from the neutral pH of the mobile phase by saturating the mobile phase with dissolved silica (5, 122). The mobile phase consisted of 45:15:40 methanol:acetonitrile:pH 6.95, 0.03 M potassium phosphate buffer at a flow rate of 1.6 ml/min with a column inlet pressure of 1500-2500 psi. The separations were performed at ambient temperature at a detection wavelength of 254 nm and a nonstandard 280 nm slit in the detector. The sensitivity setting was 0.005 a.u.f.s. (absorbance units full scale) for the lower concentrations and 0.01 a.u.f.s. for above 500 *ng/ml*

for the plasma and RBC curves. The sensitivity was 0.005 a.u.f.s. for the buffer curve injectons. The recorder speed was 0.25 cm/min. Peak heights were measured by hand with a single ruler to the nearest 1 mm.

4.3.6 Quantification of PYR in matrices

4.3.6.1 Extraction procedures

Plasma Extraction Procedure

(1) Add 100 µl each of PYR standards (0.1 to 5.0 µg PYR/ml in methanol) to silanized 16 X 125 mm glass culture tubes with PTFE lined screw caps for standard curve. For unknown samples and controls, methanol was added instead.

(2) Add 100 µl of NAPA HCl (0.8 µg/ml in methanol).

(3) Add 0.5 ml plasma (control, sample, or blank).

(4) Add 200 µl of 0.8 M potassium hydroxide.

(5) Add 7 ml of methylene chloride, briefly vortex.

(6) Shake 10 min in Eberbach shaker (220 shakes/min).

(7) Centrifuge 10 min in model UV centrifuge at 2100 rpm.

(8) Aspirate to waste the aqueous layer.

(9) Decant organic phase into another tube and evaporate to dryness in 38° water bath under a gentle stream of nitrogen.

(10) Reconstitute residue with 200 µl of pH 6.95 potassium phosphate buffer and inject 100 µl.

RBCS Extraction Procedure

(1) Add 100 μl each of PYR standards (0.12 to 5.0 μg PYR/ml methanol) to 16 X 125 mm glass culture tubes with PTFE lined screw caps. For samples methanol was added instead.

(2) Add 0.5 ml of RBCs (unknown samples or blank RBCs for standard curve) with a 1 ml syringe.

(3) Add 0.5 ml of 0.5 M Na_2CO_3 solution, vortex 15 sec.

(4) Add 12 ml of 1:3 mixture of methylene chloride and n-butyl chloride, vortex 20 sec.

(5) Rotate on wheel while processing others.

(6) Shake on Eberbach shaker 20 min.

(7) Centrifuge at 2100 rpm for 15 min.

(8) Quantitatively remove using a graduated cylinder 12 ml of the organic layer and place it in another tube.

(9) Evaporate the organic phase in each tube to dryness, vortex each tube every 5 min as evaporation proceeds.

(10) Reconstitute residue with 200 μl of potassium phosphate buffer and inject 100 μl.

Buffer Samples

Buffer samples and controls were injected directly. Buffer standards were prepared by evaporating 100 μl of each standard in plastic tubes and reconstituting with 500 μl of phosphate buffer.

4.3.6.2 Calibration curves

Calibration curves in blank plasma were prepared by plotting peak height ratios of PYR to internal standard as a function of theoretical PYR concentration. Concentrations were then back-calculated from these curves using a linear regression program. One control was run for every 10 samples. The acceptable limit of error for controls was 10% of the spiked concentration. Blank plasma on each day was the same as that used in the experiment of that day.

Calibration curves in blank RBCs and buffer were made by plotting peak heights (after 100 μl injections) of PYR as a function of theoretical PYR concentrations. Concentrations were then back-calculated from these curves. A hand-held calculator (TI-59 III, Texas Instruments, Inc., Lubbock, TX) was used for these calculations. Buffer controls were run for every 10 samples. There were no controls for RBCs.

Concentrations of PYR in plasma, RBCs or buffer unknown samples and controls were determined by applying peak height ratios or peak heights to the appropriate

calibration curves.

4.3.6.3 Recovery and precision studies

Recoveries of PYR and the internal standard were determined by triplicate analysis of plasma and RBC standards at many different concentrations. Peak heights obtained from extracted standards were compared to peak heights obtained following direct injections of unextracted standards (evaporated spiked solutions that were reconstituted with the same volume of phosphate buffer as the extracted samples).

The reproducibility of the extraction procedure and HPLC analysis was determined by extracting and analyzing 10 replicates of 4 controls in plasma on a single day.

4.4 Vacutainer™ pH changes

4.4.1 Blood drawing and pH measurement procedures

A normal subject's blood was drawn from a forearm vein using a Vacutainer™ needle and holder (through the stoppers) into replicate Vacutainer™ tubes. These Becton-Dickinson Vacutainer™ Systems (Rutherford, NJ) were used:

Table 5. Vacutainer™ Systems

Vacutainer™	Additive	Blood Volume
B-D No. 6451 (lavender tops)	10.5 mg Na_2EDTA	7. ml
B-D No. 6480 (green tops)	143 USP Units Na Heparin	10. ml
B-D No. 6419 (blue tops)	18 mg Na Citrate and 2.4 mg Citric Acid	4.5 ml

The tubes were centrifuged while still sealed. The zero time pH was taken as the pH immediately upon removing the stoppers while the plasma rested over the RBCs. Then the plasma was transferred by pasteur pipet to culture tubes and the remaining pH values obtained using the Accumet pH meter.

4.5 Equilibrium dialysis (ED)

4.5.1 Membrane preparation

Spectrapor® 1 membrane tubing (Spectrum Medical

Industries Inc., Los Angeles, CA) made of cellulose with a molecular weight cutoff 6000-8000 was used in the dialysis experiments. At no time was tubing touched except with metal surgical instruments. A piece of tubing was removed from the box and washed in running lukewarm tap water for at least 2 h to remove glycerol (humectant and plasticizer). The tubing was rinsed 5 times with distilled water and then rinsed 3-5 times with isotonic phosphate buffer (IPB). The tubing was cut into small circles that fit the ED cells. The cut membranes were stored in the refrigerator and before use were rinsed 5 times with fresh IPB.

4.5.2 Spectrum equilibrium dialyzer

The Spectrum equilibrium dialyzer was assembled according to the instructions that came with it. Briefly, using tweezers, membranes were blotted on tissues, placed on the PTFE semi-micro cell half with the sealing ridge, and the matching cell-half was placed on top, sandwiching the membrane between the two halves. The cells, in sets of 5 cells, were placed between spacers in the cell carriers. After placing the assembled unit in the filling clamp on a ring stand, they were filled using a Pipetman® (Gilson International, Middletown, WI) and a Rainin C-200 microliter pipette tip (Rainin Instrument Co., Inc., Brighton, MA). These tips snugly fit the holes in the cells. The 5 cell units

were placed in the drive unit which was placed in the 37° water bath. The speed of rotation was 12 - 20 rpm depending on the experiment.

Removal of cell contents was performed by blowing the contents out with a pipettor and catching the liquid in a plastic tube (12 X 75 mm polystyrene culture tubes with snap caps, Elkay Products, Inc., Shrewsbury, MA). When a volume of 1 ml was placed in the cell-half at the beginning of the dialysis, about 0.7 ml was recovered.

4.5.3 Protein assay

In every ED experiment involving albumin, the albumin content of each of the cells at the end of dialysis was measured using an assay specific for albumin. Samples (< 1.0 ml) from ED were collected in plastic tubes as described above. For the assay of albumin, the following standard procedure as described in the pamphlet that came with the BCG Reagent was followed:

(1) Pipet 5.0 ml of BCG [bromcresol green] Albumin Reagent (Stanbio Laboratory, Inc., San Antonio, TX) into each PET vial (20 ml polyethylene terephthalate scintillation vial, Wheaton Scientific, Millville, NJ).

(2) Pipet 20.0 μl using an SMI micro/pettor (Scientific Manufacturing Industries, Berkeley, CA) of each

sample into the BCG reagent and rinsed the tip of the siliconized glass pipet in the BCG.

(3) Wait 5 mins, gently swirl the sample and then pour an aliquot into the polystyrene cuvets (Fisher Scientific, Fairlawn, NJ) and read the UV absorbance at 550 nm.

(4) The albumin concentration of the unknown was not calculated from the following equation given in the instructions,

$$\frac{\text{Abs unk}}{\text{Abs std}} \times \text{Conc. std} = \text{g/dl unknown} \qquad (16)$$

but from a 3 point linear regression calibration curve using albumin standards in normal saline (Sigma Diagnostics™, St. Louis, MO) 2 g/dl and 4 g/dl as well as a zero point for albumin determination.

The results were usually identical because the absorbance for the 2 g/dl standard was the same as half the absorbance for the 4 g/dl standard.

4.5.4 Adjustment of plasma pH

Plasma pH was adjusted immediately before dialysis by blowing 5% CO_2 in oxygen over the plasma in a plastic scintillation vial (Wheaton Scientific, Millville, NJ). Approximately 30 min were required to bring the pH from 7.8 to 7.35. Usually pH was adjusted to 7.3 because the pH rose about 0.1 unit during dialysis; and this phe-

nomenon varied with the amount of buffer added to the plasma to dilute the proteins (e.g. the more buffer added, the less the pH rose during dialysis).

4.5.5 General ED procedure

PYR was added to the buffer solutions in concentrations given for the specific experiments. The concentration of PYR in the buffer and protein containing solutions after ED was measured by HPLC. Separate calibration curves were made for each matrix using the same plasma or buffer solutions as in the ED for the blank solution. Changes in volumes of each cell-half during dialysis were determined from the changes in protein concentration measured by the BCG dye binding procedure. Plasma and protein solutions were diluted only 5% by volume shifts. Buffer concentrations were considered the free concentrations of PYR. Plasma or other protein containing solutions contained the total PYR concentrations. Bound PYR was the difference or total - free = bound. Fraction free was calculated as free PYR divided by the total PYR.

4.5.6 Sources of dilution of protein

4.5.6.1 Water content of membranes

Two membranes that had been prepared in the usual manner were weighed, allowed to dry, and weighed again. The difference in the weight was taken as the water content.

4.5.6.2 Volume shifts

During dialysis, free water from the buffer side of the membrane often passes through the membrane to the protein containing side. This dilution is called a volume shift. To measure volume shifts, the albumin concentration for each cell was measured after dialysis. The original solution of protein (plasma or albumin in buffer) was measured and taken as the original albumin level.

4.5.7 Evaluation of binding to ED cells and membranes

Binding to the ED apparatus was evaluated by adding 1 ml of pH 7.4 IPB to one cell-half in the carrier and 1 ml of 85 ng/ml PYR in IPB to the other cell-half. This was done with 5 cells. The cells were dialyzed for 4 h at 15 rpm in the 37° water bath. At the end of 4 h, samples were removed from each of the cells and analyzed for PYR. The amount of PYR placed in the cells at the beginning of dialysis was compared to the amount removed after dialysis to determine the recovery of PYR from the system.

4.5.8 Determination of time to equilibrium for dialysis

The following 2 paragraphs describe the 2 experiments done to determine the time to equilibrium for dialysis.

Isotonic solutions of PYR 400 ng/ml (pH 7.4) were dialyzed against equal volumes (1 ml) of expired blood

bank plasma (pH 8.01) at 12 rpm in a 37° water bath. Samples of cells were taken from 2 min to 240 min. Albumin concentration measured at the end of dialysis was 25.9 g/L. Using the buffer side data, noncompartmental analysis was performed to find the time to equilibrium. The area under the curve (AUC) and area under the moment curve (AUMC) were calculated using the trapezoidal rule (57) and a hand calculator.

The pH of some of the above expired blood bank plasma was adjusted by gassing with 5% CO_2 in oxygen. It was dialyzed against an equal volume (1 ml) of IPB spiked with 400 ng/ml of PYR. The cells were rotated at 12 rpm in a 37° water bath. The cells were emptied from 3 to 280 min. The AUC and AUMC for the buffer PYR were calculated as described above. Due to column failure the plasma cell concentrations were lost. The albumin concentration at the end of dialysis was 30.4 g/L.

4.5.9 Influence of plasma pH on protein binding

4.5.9.1 Comparison of pH 7.35 and pH 8.0 plasma

A drug free male (DR) volunteer's blood was collected into Vacutainers™ containing heparin. After separating the plasma from the cells, the plasma pH was adjusted by gassing with 5% CO_2 in oxygen immediately prior to ED. Cells were rotated in the Spectrum apparatus at 17 rpm in a 37° water bath for 5 h. The average total PYR in plasma (n=6) at the end of dialysis was 362

ng/ml (4.7% CV, range 336.05-379.67 ng/ml). At the end of dialysis the average albumin level (n=6) in plasma was 51.3 g/L or 7.4 X 10^{-4} M (6.4% CV). The unbound fraction in plasma was determined by dividing the PYR concentration in the buffer compartment (free drug) by the PYR concentration in the plasma compartment (total drug). This assumed that no protein was found in the buffer compartment. Each dialysis cell was treated individually.

4.5.9.2. Effects of pH on protein binding

Solutions of isotonic phosphate buffer at various pHs were made by mixing isotonic (NaCl added) solutions of Na_2HPO_4 and KH_2PO_4 to make pH 6.7 7.0, 7.4, 7.7, and 8.0. These solutions were used to reconstitute evaporated PYR in volumetric flasks to make solutions of PYR at 400 ng/ml. A drug-free individual's (EC) heparinized plasma was used. It was adjusted to the pH as near as possible (minimum 7.3) to the buffer pH before dialysis. The pH values reported are for the plasma at the end of the 5 h dialysis. These PYR-containing buffer solutions were dialyzed against plasma in triplicate. Cells were rotated at 17 rpm in 37° water bath. Albumin concentration of the plasma side at the end of dialysis was 43.7 g/L (3.92% CV).

A second experiment was performed in triplicate as above except that due to equipment failure the Spectrum

cells had to be rotated by hand and dialysis time was increased to 6 h 20 min. Solutions of PYR were made at pH 6.3, 6.5, 6.7, 6.9, and 7.1 at 400 ng/ml. Albumin concentration at the end of dialysis was 45.6 g/L (6.49% CV).

4.5.10 Influence of anticoagulants on protein binding

The day before the ED, blood from a drug-free volunteer (AR) was collected into 3 kinds of Vacutainers™: Vacutainers™ containing EDTA or heparin for plasma and red-top Vacutainers™ containing no anti-coagulant for serum. IPB solutions of PYR at 1200 ng/ml were made by reconstituting evaporated PYR in volumetric flasks. Spiked IPB solutions were dialyzed against plasma or serum in triplicate. Albumin in the samples measured at the end time averaged 41.8 g/L (6.06×10^{-4} M) and the ending pH was 7.4. ANOVA was performed using SAS PROC GLM.

4.5.11 Concentration dependence of protein binding

Two solutions of PYR were made by reconstituting evaporated PYR in volumetric flasks. A drug-free volunteer's (DR) heparinized plasma was dialyzed against spiked solutions of PYR at 118 ng/ml and 363 ng/ml IPB. Before dialysis the plasma pH was adjusted to pH 7.4 with 5% CO_2 in oxygen. Samples were removed after 5 h in a 37° water bath rotating at 18 rpm. At the end of the dialysis the albumin was 45.56 g/L (6.6×10^{-4} M)

and the pH of the plasma was 7.5. A *t* test was performed on the data using SAS PROC T TEST.

4.5.12 Binding to purified human serum albumin

To 47 mg of purified human serum albumin (HSA) (Pierce no. 30445 affinity purified HSA, Pierce Chemical Co., Rockford, IL) was added approximately 2 ml of pH 7.35 IPB. One milliliter of this protein solution was dialyzed against an equal volume (1 ml) of IPB spiked with PYR 350 ng/ml in duplicate. Cells were rotated in the Spectrum dialyzer apparatus at 18 rpm for 5 h in a 37° water bath. Albumin was 14.18 g/l or 2.06×10^{-4} M at the end of dialysis.

4.5.13 Binding to α_1-acid glycoprotein (AAG)

About 2 ml of IPB pH 7.35 was added to approximately 7.4 mg of AAG (Prod. No. G-9885, human α_1-acid glycoprotein, Sigma Chemical Co., St. Louis, MO). This AAG solution was dialyzed in duplicate against an equal volume (0.9 ml) of IPB spiked with PYR 350 ng/ml as described in Section 4.5.12. The AAG concentration was calculated to be 3.7 g/L at the beginning of the experiment without corrections for water content. PYR content was assayed using 0.5 ml of each sample. The solutions recovered from this experiment that were not used in the assay of the drug were combined with what was left of the original AAG solution to make about 0.73 ml. Added to this volume was 4 ml of pH 7.35 IPB. Thus,

the AAG was calculated to be less than 0.571 g/L at the beginning of the second AAG experiment. This AAG solution was dialyzed against 0.9 ml of pH 7.35 IPB containing 350 ng PYR/ml for 5.5 h. At the end of dialysis, the pH was 7.4.

4.5.14 Binding to plasma proteins

Three studies (Studies 1, 2, and 3) were performed to determine affinity constants for PYR to albumin in plasma.

This paragraph is a description of Study 1. Plasma was obtained from a drug-free volunteer (EC). Isotonic pH 7.4 phosphate buffer (IPB) spiked with PYR concentrations 140, 280, 480, 720, 1440, 4100 ng/ml (maximum 1.6 X 10^{-5} M) was dialyzed against plasma that was adjusted to pH 7.23 with 5% CO_2 in oxygen prior to dialysis. The cells were filled in duplicate with regards to PYR concentration. The cells were rotated in the Spectrum dialyzer at 20 rpm for 5 h in a 37° water bath. The albumin concentration at the end of the dialysis was 23.5 g/L or 3.41 X 10^{-4} M (3.9% CV).

This paragraph is a description of Study 2. The pooled drug-free heparinized plasma that was used came from three volunteers (EC, DR, AR) and it was diluted to one-fifth plasma with pH 7.35 IPB. The plasma-IPB mixture was dialyzed against IPB containing PYR at 140, 250, 400, 600, 780, 1200, 2200, 4100 ng/ml in duplicate.

The cells were rotated in the Spectrum dialyzer at 18 rpm for 5 h in a 37° water bath. The albumin concentration of the plasma at the end was 8.13 g/L or 1.18 X 10^{-4} M (4.1% CV).

This paragraph is a description Study 3. Heparinized plasma from a drug-free female (AR) was diluted with IPB pH 7.3 and dialyzed against solutions of PYR at concentrations of 720, 3700, 9100, 18000, and 45000 ng/ml IPB. The cells were rotated in the Spectrum dialyzer at 18 rpm for 6 h in a 37° water bath. The pH at the end of the dialysis was 7.3 and the albumin concentration of the plasma side was 0.66 g/L or 9.59 X 10^{-6} M (7.2% CV).

The data collected in Studies 1, 2, and 3 were fit to the Klotz, Scatchard, Blanchard, and Larsen equations assuming one or two binding sites and using 1/buffer concentration, 1/squared buffer concentration, 1/plasma concentration and 1/squared plasma concentration as the weighting functions. The fits were evaluated on the basis of correlation coefficients, R^2 values, sums of squares, weighted sums of squares, residuals, correlation matrix of the parameters, plots of the data, plots of the residuals, and reasonability of the parameter estimates.

4.5.15 Binding to hemoglobin (Hb)

4.5.15.1 Stroma-free hemoglobin preparation

Blood was obtained from a human subject (AR) and transferred by syringe into 4 heparin Vacutainers™. These were centrifuged for 15 min in a desk-top IEC centrifuge. The plasma and buffy coat were removed. Approximately 2 volumes of IPB pH 7.4 were added as a washing solution. The mixture was rocked for 5 min, a sufficient time to redistribute the RBCs. Then the cell mixture was spun for 5 min. The washing procedure was repeated 3 times with care to remove any remaining buffy coat. After removing the residual IPB, an equal volume of distilled deionized water was added to the packed cells. The tubes were vortexed 1 - 2 min and complete hemolysis was assumed. The hemolysate was transferred to 2 plastic centrifuge tubes and the tubes were centrifuged in a Sorvall RC-58 Superspeed centrifuge at 27,000 X G for 30 min at room temperature. The Hb-containing hemolysate was decanted for further analysis and the pellet (RBC stroma) was discarded.

4.5.15.2 Measurement of Hb

The following is the procedure used to measure Hb in whole blood and in plasma to check for hemolysis.

Hb was measured using the Sigma Diagnostics™ Total HB kit (Proc. No. 525, Sigma Chemical Co., St. Louis, MO). Drabkin's solution was prepared by reconstituting

Drabkin's reagent with 1000 ml of water and adding 0.5 ml of 30% Brij-35 solution (30 g/dl). The Hb standard containing lyophilized human methemoglobim was reconstituted with 50.0 ml of Drabkin's solution to make a cyanmethemoglobin standard solution. Hb has a MW 64,458. The millimolar absorptivity of cyanmethemoglobin is 44.0 at 540 nm. Diluted working standards equivalent to blood Hb levels of 0.0, 6.0, 12.0, and 18.0 g/dl were prepared. The absorbance of these diluted standards read at 540 nm on the Beckman DB-GT spectrophotometer were used to make a calibration curve of absorbance values versus blood Hb. The curve was linear and passed through the origin.

Procedure to measure blood Hb:

(1) Add 5.0 ml of Drabkin's solution to each tube.
(2) To each tube add 20.0 μl (with an SMI pipettor) of whole blood and rinse the pipet with reagent. Mix well.
(3) Allow to stand at least 15 min at room temperature.
(4) Read absorbance of each tube versus blank (0.0 g/dl standard) as reference.
(5) Determine total Hb concentration of each sample from calibration curve.

4.5.15.3 Binding to Hb

The binding of 4 levels of PYR (65, 300, 400, and 940 ng/ml) to hemoglobin was investigated by dialysis

against pH 7.4 IPB at 37° for 5 h.

4.6 Partitioning of PYR into RBCs

A few experiments were done to determine the partitioning of PYR into RBCs. Preliminary studies showed that equilibrium between medium and RBCs in RBC suspensions in buffer was reached very quickly. The same levels were achieved by less than 5 min as in 20 or 30 min rocking time. The 20 min rocking times were chosen to assure good mixture of PYR and cells.

4.6.1 RBC/buffer ratio as a function of buffer pH

The volume of 30 ml of blood was drawn from a male volunteer (DR) through a Butterfly® infusion set (21G X 3/4 X 12", Abbott Hospitals, Inc., North Chicago, IL) into a syringe and transferred into 5 heparin containing tubes (No. 6483, Becton Dickinson, Rutherford, NJ). The blood was centrifuged, the plasma was removed and the cells were washed 3 times with pH 7.33 IPB. The washing consisted of adding 2 or 3 volumes of IPB, rocking 5 min, spinning 10 min at 2100 rpm, removing the buffer as well as the buffy coat, and repeating this procedure. The cells were washed in Kimax® culture tubes (16 X 125 mm, Kimble, Corning, NY) rather than in the original Vacutainers™. PYR (2 μg in methanol) was evaporated in six 50 ml volumetric flasks. The methanol was evaporated and the residue was reconstituted with pH 6.7, 7.1, 7.4, 7.7, 7.9, or 8.0 IPB to make 6 400 ng/ml solutions.

The volumes of 1.5 ml of packed cells and 2.5 ml of IPB containing PYR were placed in plastic vials. They were rocked for 20 min. The HCT was taken in microcapillary tubes. The tubes containing the cells suspended in buffer were centrifuged. Nearly all of the buffer was removed, and the cells gently resuspended in the remaining buffer before a second HCT was taken on the packed cells. PYR was assayed in the packed cells and in the buffer.

The RBC concentration was corrected by this equation using the HCT for the cell suspension:

$$RBC_{corrected} = \frac{WB - P(1-HCT)}{HCT} \qquad (17)$$

which can be derived from:

$$WB = RBC*HCT + P*(1-HCT) \qquad (18)$$

where WB is the whole blood PYR concentration (in this case the RBC suspension concentration); P is the plasma, buffer, or buffer-plasma mixture concentration; and HCT is the hematocrit of the cell suspension. The true WB concentration, after measuring the RBC and plasma concentrations and making corrections, was calculated from Eq. (18).

Regression analyses of this data and theoretical data calculated from equations in Chapter 2 were performed using SAS PROC REG.

4.6.2 Influence of plasma albumin levels on RBC PYR

This paragraph is a description of Study R1. The volume of 30 ml of blood was drawn from a male volunteer (DR) through a Butterfly® infusion set (Abbott Hospitals, Inc., North Chicago, IL) into a syringe and transferred into 5 heparin containing tubes (No. 6483 Vacutainers™, Becton Dickinson, Rutherford, NJ). The whole blood hematocrit (HCT) was measured. The blood was centrifuged, the plasma was removed and the cells were washed with pH 7.4 IPB. PYR (1 μg) was evaporated in 4 tubes.

To these silanized culture tubes were added pH 7.33 IPB, plasma, and RBCs in the following manner:

(1) To each tube was added buffer first, then 1.75 ml RBCs with a syringe, then plasma.
(2) To the first tube was added RBCs then 4 X 0.8 ml plasma.
(3) To the second tube was added 1 X 0.8 ml IPB, RBCs, and 3 X 0.8 ml plasma.
(4) To the third tube was added 2 X 0.8 ml IPB, RBCs, and 2 X 0.8 ml plasma.
(5) To the fourth tube was added 3 X 0.8 ml IPB, RBCs, and 1 X 0.8 ml plasma.

Study R1 was performed to determine the dependence of the partitioning of PYR into RBCs upon albumin levels in plasma in a manner originated by Garrett (54). The

albumin was measured in 20 μl of the plasma or plasma-buffer mixture. Hb was measured in the plasma after its separation from the cells to detect significant hemolysis. An Hb level greater than 0.0 was determined to be unacceptable hemolysis and the sample was discarded.

These 4 tubes were gently rocked 20 min. The HCT was taken on each tube. They were spun 20 mins. Nearly all of the plasma-buffer was removed, and the packed cells were gently resuspended in the plasma remaining in the tube. A HCT was taken on the RBC suspension (packed cells). The cell suspension was used to determine the RBC level. The RBC level was corrected for trapped plasma using Eq. (17).

4.6.3 Determination of RBC/plasma ratio

This paragraph is a description of Study R2. Blood was collected as described in Section 4.6.2. Approximately 2 or 3 μg of PYR was evaporated in 5 tubes. Three ml of whole blood was added to each tube and they were rocked for 20 min. The HCT was taken on the whole blood; the tubes were spun 20 min; the plasma was removed; and the cells were mixed gently before a HCT was taken on the packed cells. Albumin was measured in the plasma. PYR concentrations were determined in the packed cells and in the plasma. RBC levels were corrected for trapped plasma as described above.

Chapter 5

Results

5.1 Reproduction of Edsteins's IPC-HPLC assay

Fig. 4 shows chromatograms of the resolution of PYR and Q. Due to the age and previous use of the μBondapak™ column and the deleterious effects of the counter-ion sodium pentane sulfonate (SPS) on the column, the column's performance declined rapidly from 19,000 to less than 6000 plates/meter. In fact, split peaks and inadequate resolution developed in the chromatograms after only 12 liters of mobile phase. Examples of a peak with a shoulder (PYR peak) and lack of resolution of PYR and Q can be seen in the last injection in Fig. 4. At its best, this IPC-HPLC procedure had a limit of detection for PYR of 200 ng/ml of plasma or RBCs.

Only minor alterations of Edstein's (39) assay were necessary for peak resolution. The column was identical. The mobile phase used by Edstein created too much back pressure and long retention times in this author's system. Therefore, it was changed from 0.005 M SPS pH 3.4 to 0.001 M SPS pH 3.0. The flow rate was decreased from 1.7 to 1.5 ml/min.

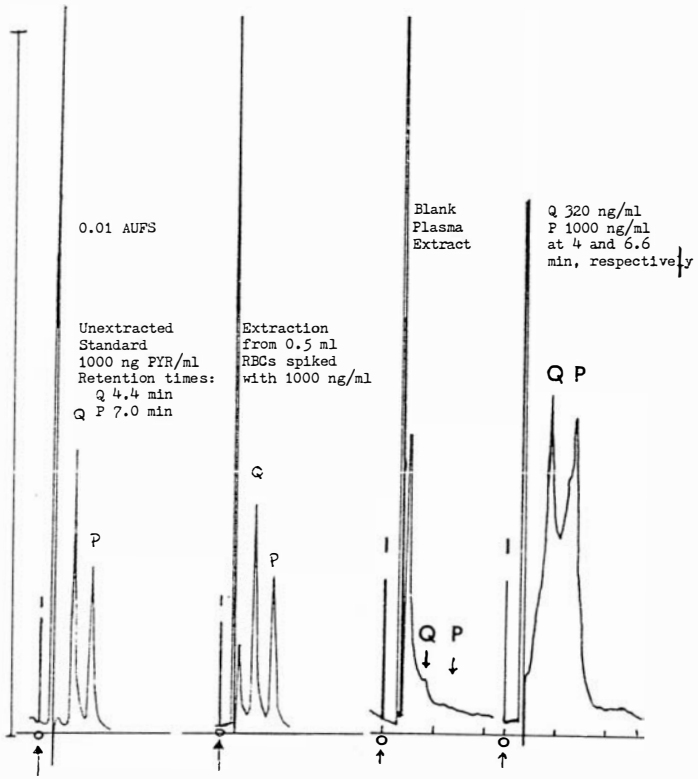

Figure 4. Chromatograms of PYR and Q in IPC-HPLC assay.

5.1.1 Effects of ion pair agent and pH

The effects of varying the concentration of the ion pair agent and pH were evaluated while optimizing Edstein's assay on my system.

The effects of the concentration of the ion pair agent SPS can be seen in the plot of capacity factor versus concentration of SPS (Fig. 5). As the counter-ion concentration increased, peaks became asymmetric, split, and were not resolved. The retention times also increased with SPS concentration. Chromatographic conditions for Figure 5 were mobile phase 25:15:60 v/v methanol:acetonitrile:0.001 M SPS pH 3.14 at a flow rate of 1.6 ml/min using a Waters μBondapak™ 10 μm particle size 30 cm X 3.9 mm ID column.

The effects of pH on retention times (Rt) of PYR and Q are shown in plots of Rt versus pH of the mobile phase at 5.0 mM SPS and a flow rate of 1.5 ml/min (Fig. 6).

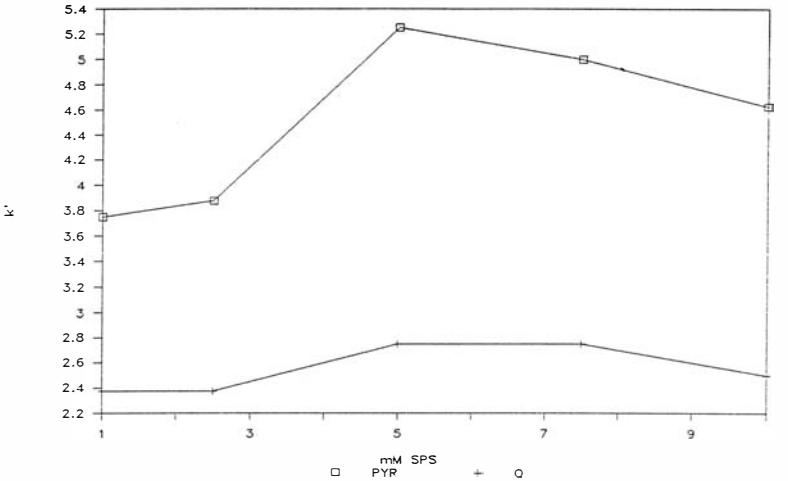

Fig. 5. Effect of SPS concentration on capacity factors.

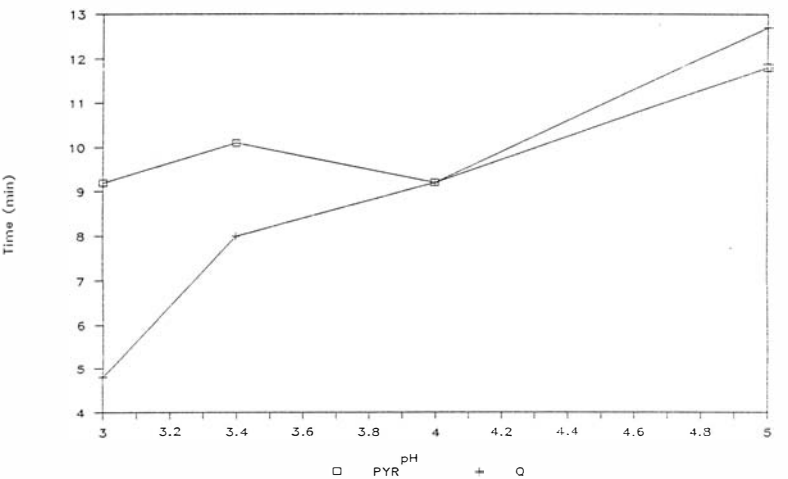

Fig. 6. Plot of the retention times of PYR and Q versus pH of the mobile phase.

5.2 RP-HPLC assay results

More than 15% v/v acetonitrile caused decreasing peak height and tailing. More than 60% v/v total organic caused PYR and NAPA to have the same retention times or to run into the plasma unwanted constituents. Retention times were 4.5 and 5.35 min for NAPA and PYR respectively.

By far the most difficult obstacle to overcome in the development of this assay was the deleterious effects of the neutral pH of the mobile phase on the analytical column. The pH of the mobile phase was responsible for the dissolution of the column packing material that led to column failure. When column failure developed, the samples run that day had to be discarded. Typically, the standards, controls, and samples would be prepared for injection (extracted, etc.). Then, at some time during their injection, the column would deteriorate to the point that it was noticable. Sometimes, column failure would not be noticed until the regression of the calibration curves at the end of the day, and all of the samples would be lost for that day.

The rapid dissolution and development of voids in the column packing led to the failure of the Econosphere™ columns. The lifetime in liters of mobile phase is presented in Table 6 for before and after the use of the saturator column. When new, the columns tested by

the Alltech procedure had 60-90,000 plates/meter. When they failed they had less than 40,000 plates/meter. After 2 columns had failed, the saturator column developed high back pressure. A 6.5 cm (22% of the column length) void had developed in the saturator column. This particle size reduction had caused the pressure problem. At that time, the saturator column was repacked.

Tested by the Alltech procedure, the new Econosphere™ columns typically had 60,000-100,000 plates/meter at the retention time of PYR. After failure, the same columns would have around 40,000 plates/meter.

Table 6. Summary of Alltech Econosphere™ life

Mobile phase	Liters until lost
47:15:38 v/v MeOH:ACN:0.015 M NaPB, KPB pH 6.9	8.5
45:15:40 MeOH:ACN:0.03 M KPB, pH 6.95	15.5
same mobile phase as above, with saturator column	32.
same mobile phase as above, with saturator column	20.

KPB=potassium phosphate buffer, NaPB=sodium phosphate buffer, MeOH=methanol, ACN=acetonitrile, v=volume

The saturator column increased the lifetime of the Econosphere™ columns. It would have been better to use a column with a higher carbon load because they are known to resist the effects of pH better (124).

Changing from the sodium salt to the potassium salt of phosphate also improved the lifetime of the columns and reduced the back pressure of the system. The sodium salt was not as soluble in the mobile phase and precipitates clogged the column as well as the mobile phase filtering apparatus. Use of the potassium salt allowed the increasing of the molarity of the phosphate buffer and achievement of better peak shape.

Some of the symptoms of column failure observed were peak changes and standard curve changes. Peak changes included irregular peak height and area; peak broadening, tailing, and fronting; split peaks; base of peaks higher on one side; and disappearance of peaks. The most common peak change was splitting of peaks. These split peaks could not be used to make a calibration curve. Standard curve changes included variability in slope and peak height from day to day and loss of sensitivity. Overall, column failure led to baseline drift and decreases in column efficiency.

Another problem was the binding of the PYR and internal standard to glass. Even though all of the glassware was silanized, the buffer used for reconstitution dissolved the silanes off the glass when allowed enough time. Because the reconstitution volume was small, only one injection (sometimes two for the higher concentrations) was possible for each sample for the

plasma and RBC extracts. Storage of the samples which were in glass tubes was also not possible because the buffer stripped the silanes off the glass and allowed the drug to bind to it. Storage was possible in plastic tubes.

The time involved in the extraction of the plasma and RBC samples was also critical. For the plasma extraction procedure, more than a 10 min shake resulted in great variability in the NAPA recovery due to its binding to glass stripped by the potassium hydroxide added to alkalinize the sample. The reason that the molarity of the potassium hydroxide was decreased from 4 to 0.8 M was that there was less stripping of the silanes at the lower buffer concentration. Variability in the peak heights of the NAPA made calibration curves very difficult.

When exposed to organic solvents, RBCs become hard clumps from which drug is impossible to extract, even after vortexing. Tubes had to be rotated between addition of the organic solvent and the 20 min shaking time to prevent settling of the RBCs into a hard mass. For the RBC extraction procedure, shaking had to be increased to 20 minutes because PYR extraction was poor at less shaking time due to the clumping of the RBCs. However, that gave the NAPA time to bind to glass and get trapped in the RBC clumps which introduced too much

variability in its recovery. For this reason, an internal standard was not used and quantitative removal of the organic phase was introduced.

5.2.1 Effect of pH on retention times

The effect of the changes in pH of the phosphate buffer in the mobile phase can be seen in Figure 7. The chromatographic conditions for this were: 35% 0.02 M Na and K phosphate buffer, 15% acetonitrile, and 50% methanol at flow rate 1.6 ml/min.

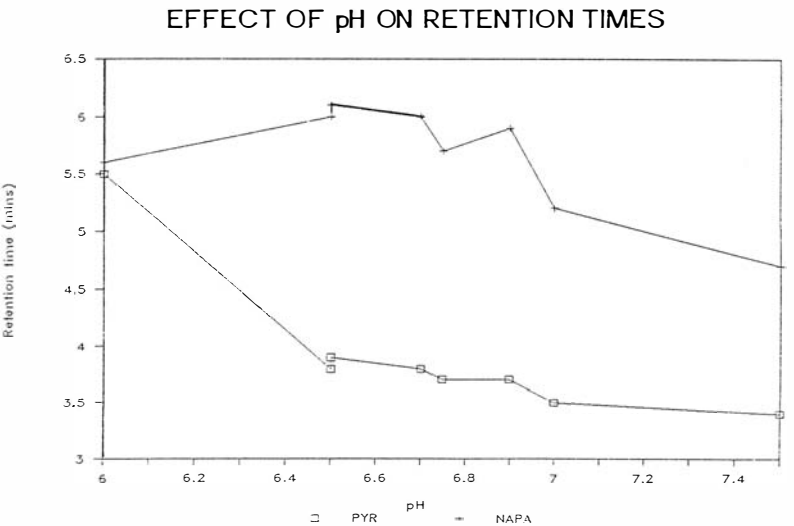

Fig. 7. Effects of pH on retention times for PYR and NAPA.

5.2.2 Calibration curves

A chromatogram for the plasma samples appears in Figure 8, for the RBCs in Figure 9, for the buffer in Figure 10. Examples of calibration curves appear in Figures 11 and 12.

Two calibration curves were necessary for each matrix for 24-140 ng/ml and 140-1000 ng/ml. A close-up of the lower end of the high calibration curve (Figure 12) shows the change in slope at 140 ng/ml.

Although the slopes do not appear to be that different for the two calibration curves for each matrix, the concentration predicted for the 100 ng/ml sample using the high curve (range 140 - 1000 ng/ml) was off by 20 - 25%.

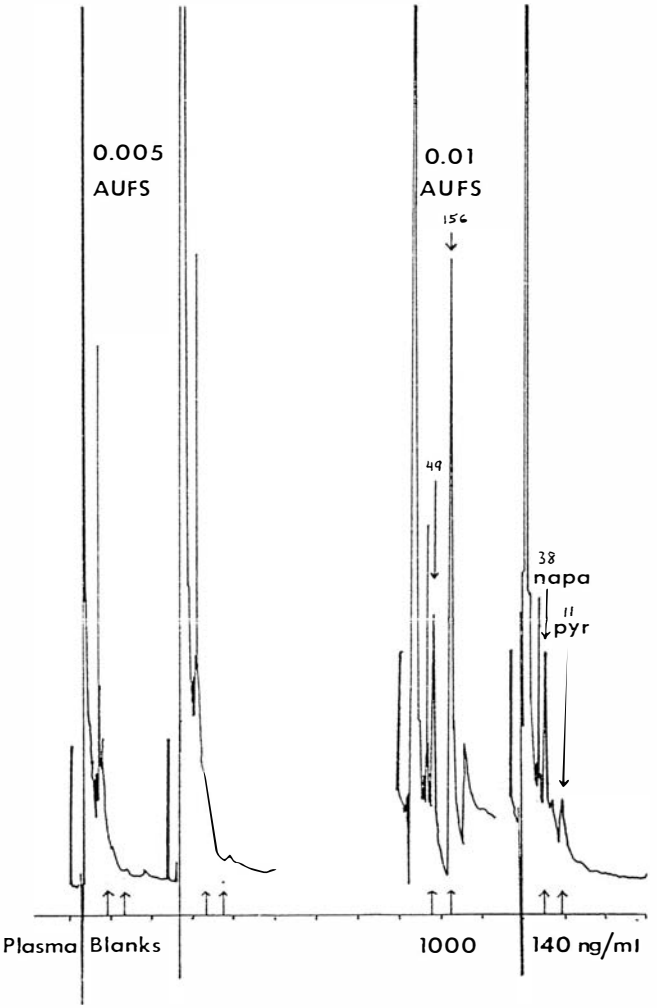

Figure 8. Chromatogram of PYR and NAPA in plasma sample.

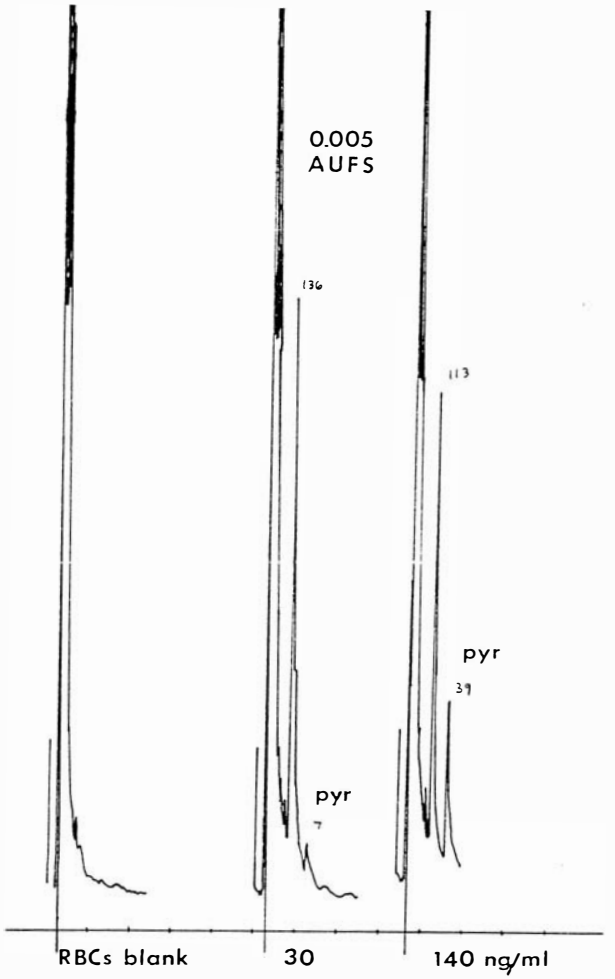

Figure 9. Chromatogram of PYR in RBC sample.

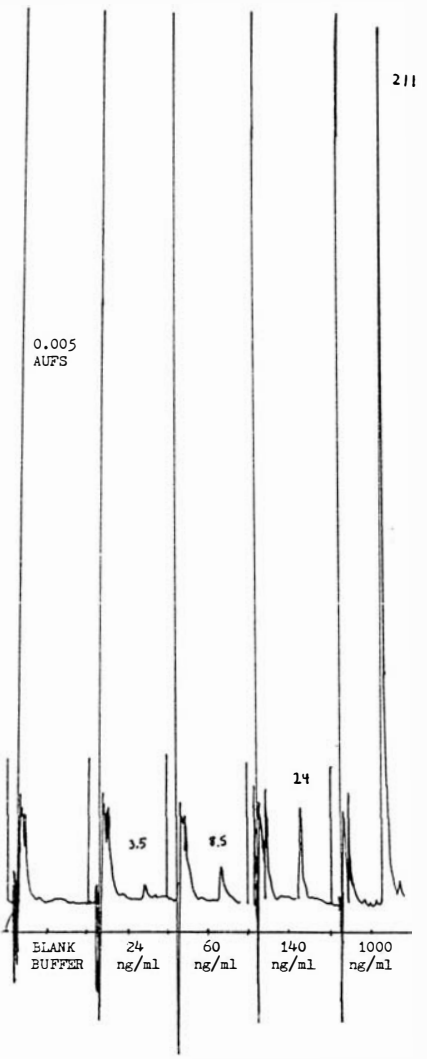

Figure 10. Chromatogram of PYR in buffer sample.

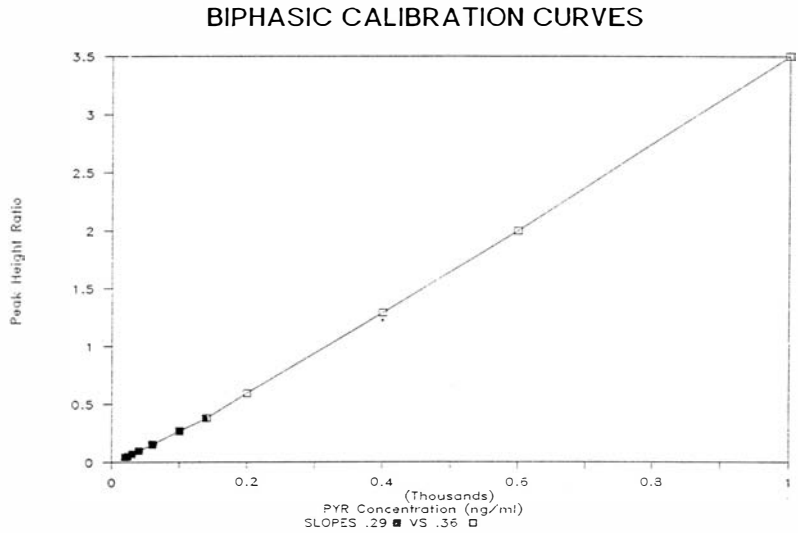

Figure 11. Typical plasma calibration curves.

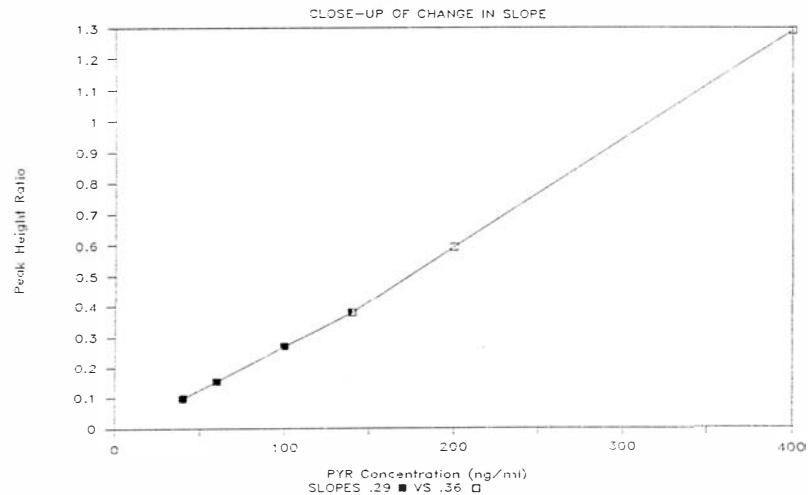

Figure 12. Close-up of the lower end of the plasma calibration curves.

5.2.3 Recovery, precision and accuracy studies

Results of the precision, accuracy and recovery studies for the RP-HPLC method are in Tables 7-11 for the plasma, Tables 12-15 for the RBCs and Tables 16-19 for the buffer.

At least one control was run for every 10 samples and it was not acceptable to have greater than 10% error from the spiked concentration of the control. Controls were varied from day to day because the choice of the controls was dependent on the expected concentrations in the samples. In other words, in an ED experiment where the expected plasma concentration at the end of dialysis was 360 ng/ml, the control used in that day's run was around 350 ng/ml.

The percent recovery values in Table 7 were determined by comparing the peak heights from extracted samples to the peak heights of unextracted samples (evaporated standard solutions that had been reconstituted the same way).

In Table 8, on Day 1, the calibration curve included a 20 ng/ml standard. On later days, the limit of detection was found to be higher, and the 20 ng/ml standard was replaced with a 30 ng/ml standard in order to retain a 6 point calibration curve.

In Tables 16 and 17, 7 standards are missing because they were lost or went off scale.

Table 7. Percent recovery from extracted spiked plasma calibration standards

Low Calibration Curve

PYR Concentration

(ng/ml)	N	Mean Recovery	% CV .
24	4	78.6	10.5
40	4	85.1	10.8
140	4	86.6	5.2
Overall	12	81.9	8.7
	(Range 71.4 - 95.2 %)		
NAPA	32	82.6	10.2
	(Range 69.7 -106%)		

High Calibration Curve

PYR Concentration

(ng/ml)	N	Mean Recovery	% CV .
140	3	90.4	3.7
200	3	78.2	3.8
400	3	81.4	1.2
600	3	79.7	5.7
1000	3	91.7	7.6
Overall	15	85.4	7.9
	(Range 75.4 - 99.3)		
NAPA	15	80.9	7.7

TABLE 8. BACK-CALCULATED CONCENTRATIONS OF PYR PLASMA STANDARDS USING A LINEAR FIT FOR THE LOW CONCENTRATIONS

	Calibration Standards (ng/ml)						
Day	20	24	30	40	60	100	140
1	19.95	24.20		37.81	60.94	106.79	142.14
	18.97	25.10		42.76	57.82	93.12	136.64
	19.75	23.51		36.41	60.15	105.08	138.60
	18.23						
5		23.06	31.77	42.40	57.25	96.94	142.37
7		24.72	lost	38.74	60.53	lost	140.01
10		23.95	29.65	41.92	60.41	95.50	142.57
N	4	6	2	6	6	5	6
Mean	19.2	24.1	30.8	40.0	59.5	99.5	140.
% CV	4.09	3.13	4.87	6.74	2.63	6.10	1.72
% Error	-3.9	0.38	2.57	0.02	-0.80	-0.51	0.28

TABLE 9. BACK-CALCULATED CONCENTRATIONS OF PYR PLASMA STANDARDS

USING A LINEAR FIT FOR THE HIGH CONCENTRATIONS

	Calibration Standards (ng/ml)				
Day	140	200	400	600	1000
1	146.39	194.46	405.22	616.46	1066.02
	143.47	210.78	362.21	567.24	939.99
	143.27	198.74	435.46	575.74	1014.52
2	150.00	214.50	361.76	566.46	1028.49
3	149.61	183.60	408.00	612.14	994.65
4	149.80	195.50	396.92	592.56	1005.23
6	151.35	208.94	365.87	590.32	1014.87
7	148.26	202.21	391.72	590.24	1007.57
8	142.39	188.23	402.80	614.18	992.39
9	140.00	200.23	408.21	596.69	999.60
11	143.12	201.38	398.15	593.31	1004.04
N	11	11	11	11	11
Mean	146.	200.	394.	593.	1010.
% CV	2.63	4.67	5.78	2.95	2.98
% Error	4.39	0.06	-1.45	-1.24	0.61

Table 10. PYR concentrations in spiked control plasma samples

	Control Concentrations (ng/ml)					
Day	35	68	150	330	420	720
1	37.65	67.56	149.73	320.80		727.10
	40.17	68.46	145.87	355.67		684.14
	33.10	65.38	143.57	319.2		692.42
	35.35	68.70	153.86	335.66		737.16
	38.34	65.55	151.74	345.30		734.68
	37.47	63.73	138.88	327.88		735.58
	37.50	73.99	152.49	366.84		707.52
	34.84	70.04	153.40	320.18		730.61
	38.53	68.70	148.20	325.52		682.02
	35.41	67.93	151.50	321.75		772.99
	32.16		151.58			
2			149.71	333.12		698.42
			146.39			
			144.42			
			153.26			
			151.44			
			140.38			
			152.08			
			152.87			
			148.40			
			151.23			

(continued on next page)

Table 10 continued:

			151.30			
3				326.76		
4						717.29
5	34.97					
6			160.00			
7	32.71			317.36		
8			135.53			
9					412.27	700.07
10	41.51		133.95			
11					437.10	737.74
N	14	10	25	13	2	14
Mean	36.4	68.0	148.	332.	424.	718.
% CV	7.68	4.17	4.13	4.60	4.13	3.56
%Error	1.14	2.84	-1.02	0.61	1.16	-0.22

TABLE 11. LINEAR REGRESSION ON PEAK HEIGHT RATIO (PYR/NAPA) VERSUS CONCENTRATION OF PYR FOR PLASMA CURVES

	Low Curve			High Curve		
Day	Slope	R	Y-intercept	Slope	R	Y-Intercept
1	0.00306	0.997	0.053	0.00356	0.996	-0.022
2				0.00429	0.996	-0.188
3				0.00284	0.999	-0.039
4				0.00250	0.999	0.009
5	0.00262	0.998	-0.009			
6				0.00364	0.998	-0.142
7	0.00255	0.999	-0.005	0.00274	0.999	-0.055
8				0.00310	0.999	-0.004
9				0.00064	0.999	-0.016
10	0.00273	0.999	-0.010			
11				0.00298	0.999	-0.034

Table 12. Percent recovery from extracted spiked RBC calibration standards

Low Calibration Curve

PYR Concentration

(ng/ml)	N	Mean Recovery	% CV
24	3	82.0	5.42
30	3	82.4	0.00
40	3	87.9	5.97
60	3	86.7	1.91
100	3	80.6	0.00
140	3	87.1	1.51
Overall	18	84.4	4.53

(Range 76.9 - 90.9 %)

High Calibration Curve

PYR Concentration

(ng/ml)	N	Mean Recovery	% CV
140	3	71.7	11.6
200	3	82.6	1.63
400	3	93.8	5.01
600	3	85.9	1.68
1000	3	88.0	7.28
Overall	15	84.4	10.4

(Range 62.5 - 98.1)

Table 13. Back-calculated concentrations of PYR RBC standards using a linear fit of peak height versus concentration for the low concentrations

Calibration Standards (ng/ml)

Day	24	30	40	60	100	140
1	24.54		41.99	62.92	94.31	139.66
	24.54		36.75	62.92	94.31	146.64
	24.54		38.50	62.92	96.06	141.41
2	25.09	28.65	35.78	60.72	96.35	142.66
	26.87	28.65	39.34	64.28	96.35	144.44
	25.09	32.22	39.34	60.72	96.35	139.10
3	25.33	30.71	41.47	59.39	95.24	141.85
	25.33	30.71	41.47	59.39	95.24	145.43
	23.54	30.71	37.88	61.19	95.24	141.85
N	9	6	9	9	9	9
Mean	25.0	30.3	39.2	61.6	95.5	143.
% CV	3.61	4.58	5.57	2.81	0.87	3.91
%Error	4.12	0.93	-2.08	2.68	-4.51	2.34

Percent CV = (standard deviation/mean) X 100

Table 14. Back-calculated concentrations of PYR RBC standards using a linear fit of peak height versus concentration for the high concentrations

	Calibration Standards (ng/ml)				
Day	140	200	400	600	1000
4	155.43	208.25	400.16	565.65	1009.33
	132.55	211.77	414.24	583.26	945.94
	148.39	206.49	379.03	572.70	1086.79
5	131.29	187.49	412.27	625.35	983.60
N	4	4	4	4	4
Mean	141.	203.	401.	586.	1010.
% CV	8.39	5.35	4.03	4.56	5.92
% Error	1.37	1.75	0.36	-2.21	0.64

Percent CV = (standard deviation/mean) X 100

Table 15. Linear regression of calibration curves for RBCs peak height versus concentrations

Low Concentrations

Day	Slope	R	Y-intercept
1	0.00287	0.997	-0.020
2	0.00281	0.998	-0.020
3	0.00279	0.998	-0.016

High Concentrations

4	0.00284	0.995	-0.126
5	0.427	0.999	-7.07

TABLE 16. BACK-CALCULATED CONCENTRATONS OF PYR BUFFER STANDARDS USING A LINEAR FIT OF PEAK HEIGHT VERSUS CONCENTRATION FOR THE LOW CONCENTRATIONS

	Calibration Standards (ng/ml)					
Day	24	30	40	60	100	140
1	23.90	27.91		61.98	102.07	138.14
4	26.20	29.36	37.25	60.93	100.40	139.98
5	25.24		37.28	58.35	106.52	136.62
6	21.42	29.01	44.18	59.35	101.06	139.98
7	26.10	32.19	38.27	56.54	99.15	141.76
8	22.86	28.73	43.41	58.08	102.11	138.81
9	24.88	31.04	38.74	58.74	100.30	140.32
13	23.74		41.51	59.29	98.40	141.06
14	24.82	29.44	38.69	61.81	98.81	140.43
15	21.66	29.10	40.26	58.85	110.91	133.22
16		30.22		58.40	99.39	140.39
N	10	9	9	11	11	11
Mean	24.1	29.7	40.0	59.3	102.	139.
% CV	7.13	4.37	6.42	2.79	3.72	1.75
% Error	0.43	-1.1	-0.11	-1.16	1.74	-0.60

TABLE 17. BACK-CALCULATED CONCENTRATIONS OF PYR BUFFER STANDARDS USING A LINEAR FIT OF PEAK HEIGHT VERSUS CONCENTRATION FOR THE HIGH CONCENTRATIONS

	Calibration Standards (ng/ml)				
Day	140	200	400	600	1000
2	144.05	196.72	387.55	616.54	995.15
3	151.62	221.41	369.71	577.63	1019.63
4	139.60	205.87	396.24	593.94	1003.97
8	138.34	206.87	412.46	571.15	1011.18
10	138.81	200.79	400.51	600.23	999.67
11	132.65		390.95	629.38	987.02
12		196.57	388.49	571.27	1019.09
16	140.39	218.68	383.23	587.80	1010.29
N	7	7	8	8	8
Mean	141.	207.	391.	593.	1010.
% CV	4.16	4.83	3.22	3.57	1.14
% Error	0.56	3.4	-2.22	-1.09	0.58

TABLE 18. BUFFER CONTROLS

Day	40	100	140	280	480	700
1	41.94					
2	43.27					
	37.82					
4			139.98	289.84	476.79	674.48
			139.86	279.09	487.17	716.07
			143.81		462.14	
					502.95	
6	40.39	93.48				
8	39.74				469.03	
10					448.72	
11					500.23	
12					479.88	712.93
					489.02	
13	41.51		133.95			
14		100.04			498.94	
		93.39			485.65	
		100.04			512.24	
		100.04			512.24	
		96.72			532.19	
		96.72				
15			150.80			
16		109.64			481.07	
					485.51	
					485.51	
N	6	8	5	2	17	3
Mean	41.	99.	142.	284.	489.	701.
% CV	4.66	5.25	4.37	2.67	4.10	3.30
% Error	1.95	-1.24	1.20	1.59	1.83	0.17.

Percent CV = (Standard Deviation/Mean) X 100

Table 19. Linear regression on calibration curves for buffer peak height versus PYR concentration

Low Concentrations

Day	Slope	R	Y-intercept
1*	0.249	0.999	-1.46
4	0.127	0.999	0.281
5*	0.332	0.996	-1.38
6	0.132	0.999	-0.325
7*	0.329	0.999	-2.58
8	0.136	0.999	-0.92
9*	0.325	0.999	-1.58
13	0.141	0.999	0.162
14	0.108	0.999	0.817
15	0.135	0.992	1.09
16	0.195	0.999	-0.400

High Concentrations

2*	0.655	0.999	-35.86
3*	0.688	0.998	-33.28
10	0.145	1.000	-0.155
11	0.101	0.999	-1.35
12	0.219	0.998	-12.0
16	0.225	0.999	-12.2

*different reconstitution volume than others

5.3 Vacutainer™ pH as a function of additive and time

There is a rapid and significant increase in plasma pH in unsealed containers as the CO_2 escapes. In contrast, there is almost no change in RBC pH because of their greater buffer capacity.

Sealing the tubes results in a more constant pH as one can see in Tables 20 and 21 by comparing the pH values for the sealed and unsealed tubes.

The results of ANOVA using SAS are in Table 22 below. There is a significant difference in the zero-time pH for heparin tubes compared to Vacutainers™ containing EDTA and citrate anticoagulants. Citrate is the only one of the 3 additives with buffering power in these small quantities. In fact, the tubes are labeled "0.105M buffered sodium citrate."

Graphs of the rapid rise in plasma pH are also shown in Figures 13a and 13b which follow Table 21.

Table 20. Measured pH values at various times

Unsealed Tubes

Time	Additive	Plasma pH	% C.V.	RBCs pH	% C.V.
0	EDTA (n=5)	7.306	0.32	7.33	0.30
	Heparin	7.496	0.58	7.54	0.08
	Buffered Citrate	7.29	0.01	7.28	0.09
15	EDTA (n=4)	7.40	0.46	7.32	0.51
	Heparin	7.572	0.07	7.52	0.41
	Buffered Citrate	7.378	0.07	7.30	0.0
30	EDTA (n=4)	7.465	0.32	7.35	0.28
	Heparin	7.575	0.08	7.52	0.17
	Buffered Citrate	7.428	0.28	7.34	0.08
60	EDTA (n=4)	7.57	0.42	7.35	
	Heparin	7.602	0.00	7.50	0.00
	Buffered Citrate	7.495	0.08	7.35	0.0
120	EDTA (n=4)	7.68	0.55	7.36	0.39
	Heparin	7.705	0.00	7.54	0.00

(continued on next page)

Table 20 continues:

Sealed Tubes N=1		
60 EDTA	7.32	
Buffered Citrate	7.29	7.29
120 EDTA	7.38	7.22
Heparin	7.52	7.22
180 EDTA	7.39	7.40
Heparin	7.51	7.40

N=4 except for zero time when N=5 for each set of unsealed tubes.

Percent CV = (standard deviation/mean) X 100%

Table 21. Change in pH of medium for the first hour

Unsealed	pH units/hr	pH at zero time
Plasma in Vacutainers™ containing:		
0.105 M buffered Na citrate	0.2	7.29
143 USP units Na heparin	0.3	7.55
Whole blood in Vacutainers™ containing 0.105 M buffered Na citrate	0.07	7.28
RBCs in Vacutainers™ containing 143 USP units Na heparin	0.0	7.48
Sealed		
Whole blood in a Vacutainer™ containing 0.105 M buffered Na citrate	0.0	7.29

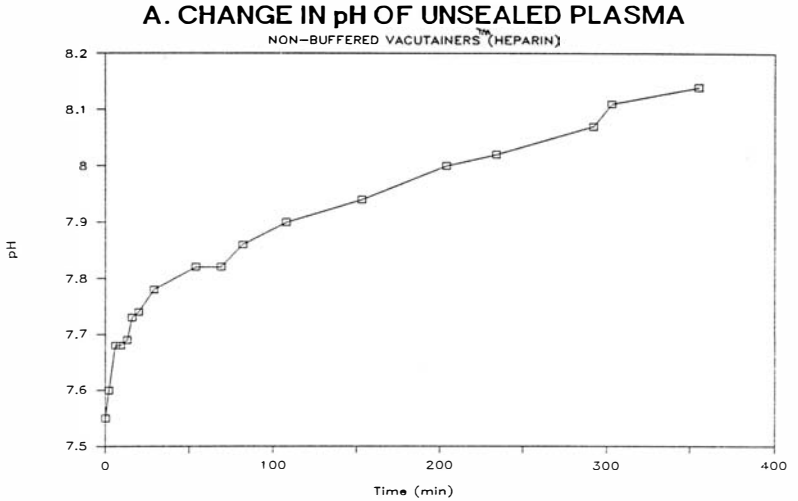

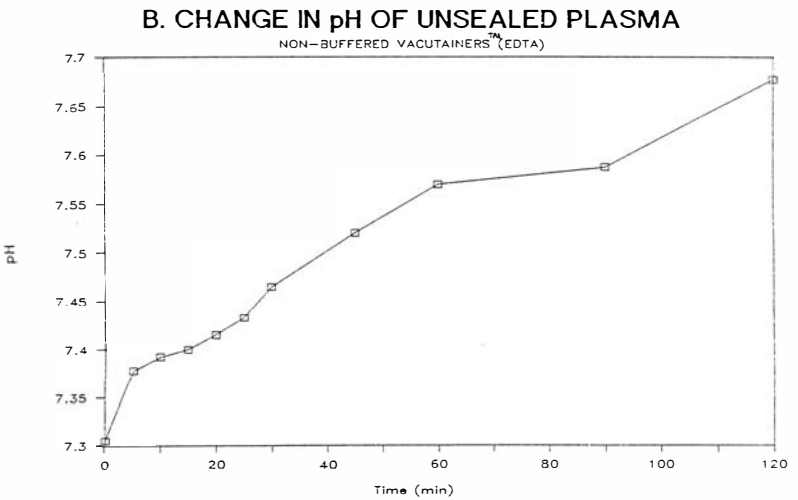

Figures 13a, 13b. Time dependent rise in pH of plasma in 2 Vacutainers™.

5.3.1 Differences in zero time pH in Vacutainers™

Results of ANOVA are in Table 22 below. The fact that F = 80.07 exceeds the F table value by a large margin indicates that there is a significant difference in the zero time pH produced by the anticoagulant additives in the tubes. The Tukey grouping shows that the zero time pH values in tubes containing heparin are significantly different from the pH values in tubes containing EDTA or buffered citrate.

EDTA and citrate produced the same pH at zero time according to the ANOVA.

Table 22. ANOVA for zero time pH in different Vacutainers™.

Analysis of Variance Procedure

Dependent variable: zero time pH

Source	DF	SS	MS	F-value	PR>F
Model	2	0.13132000	0.06566	80.07	0.0001
Error	12	0.00984000	0.00082		
Cor. total	14	0.14116000			

R-square 0.930292 CV 0.3889%

pH mean 7.364000

Tukey's studentized range test for variable: pH

Alpha = 0.001 DF = 12 MSE = 0.00082

Critical value of studentized range = 6.917

Minimum significant difference = 0.08858

Means with the same letter are not significantly different.

Tukey Grouping	Mean	N	Anticoagulant
A	7.49600	5	Heparin
B	7.30600	5	EDTA
B	7.29000	5	Citrate

5.4 Effect of pH on cell/medium ratios

Table 23 contains calculated cell/medium ratios for theoretical pairs of pH values most likely to be encountered in the body and laboratory. These pH values were introduced in Section 2.9.1 in Chapter 2. Muscle tissue cells are pH 7.02. Physiological plasma is 7.4. Unsealed plasma is pH 8.0. In buffer, cell-medium pH pairs are 6.67, 6.7; 7.26, 7.4; and 7.69, 8.0.

Overall, Table 23 shows the effects of medium pH on partitioning of several drugs into cells. In this table, the medium is either plasma or buffer. The purpose of this table is three-fold. First, it shows that the pKa of each weak acid or weak base determines the magnitude of the effect on the cell/medium ratio as changes occur in the medium pH. The weaker the acid or base, the less effect pH has on the ratio. Secondly, in the situation where RBC pH is 7.26 and unsealed plasma pH is 8.0, the ratios do not always reflect the *in vivo* situation of RBC pH 7.26 and plasma pH 7.4. Thirdly, the last column (muscle pH 7.02 and plasma pH 7.4) shows that weak bases have higher cell/medium ratios that weak acids in every case.

The cell/medium ratios for the hydrogen ion are included to show that bases which have a high pKa have the same cell/medium ratio as the hydrogen ion.

Table 23. Cell/medium ratios for weak acids and weak bases

	CELLS pH	6.67	7.26	7.69	7.26	7.02
	MEDIUM pH	6.7	7.4	8.0	8.0	7.4
Drug pKa						
WA 3.49		0.93	0.72	0.49	0.18	0.42
WA 7.13		0.98	0.82	0.55	0.28	0.62
WA 8.31		0.97	0.92	0.65	0.97	0.94
WA 10.0		1.0	1.0	1.0	1.0	1.0
PYR 7.13		1.05	1.13	1.12	1.53	1.49
WB 8.1		1.07	1.32	1.58	3.5	2.17
WB 9.1		1.07	1.37	1.97	5.16	2.37
WB 10.0		1.07	1.38	2.04	5.5	2.4
Hydrogen ion		1.07	1.38	2.04	5.5	2.4

WA = weak acid

WB = weak base

5.5 Equilibrium dialysis

5.5.1 Water content of dialysis membranes

The differences in wet and dry membranes were taken as their water content. The differences in weight (before and after drying) for 2 cut membranes were 0.0399 and 0.0429. Assuming 1 ml of water weighs 1 g, there is about 41.4 μl of water held by each membrane. To make a correction for volume of ED cells to which 1 ml has been added to each cell-half, one could add about 41 μl for a total volume of 2.041 ml. This is not a large dilution of cell contents.

5.5.2 Volume shifts

For each experiment involving albumin, it was measured in each cell at the end of dialysis. To study volume shifts, the albumin concentration at the end of dialysis was compared to the albumin concentration in the original plasma. Disregarding dilution from the water content of the membranes, the results in Table 24 show that there were less than 10% shifts of water volume in the cells.

Table 24. Albumin (g/L) changes during dialysis

Original	Ending	N	Percent change
45.8	43.7	15	-4.56
25.9	23.5	15	-9.19
47.5	45.6	15	-3.98
8.0	8.13	15	+1.62
44.2	43.6	3	-1.34
44.2	40.66	3	-7.97
45.1	42.13	3	-6.50

5.5.3 Binding to ED apparatus

Binding to the Spectrum cells and membrane did not occur. The original solution of PYR in pH 7.4 IPB was assayed to be 85.1 ng/ml. At the end of a 4 h dialysis, the PYR content of each cell-half was assayed and reported below. The mean concentration recovered in each cell-half was 42.7 ng/ml (2.9% CV). Combined recovery in each half was 85.4 ng/ml.

Table 25. PYR (ng/ml) at end of dialysis

Cell	Half 1	Half 2
1	42.8	44.3
2	41.6	43.3
3	42.8	44.3
4	41.6	40.9

5.5.4 Determination of time to equilibrium

Two ED experiments were run at 12 rpm to determine time to equilibrium for PYR binding to plasma proteins. The graphs of the changes in the free and total PYR concentrations, PYR in the two cell-halves, are shown in Figure 14. The results of the moment analysis of the areas under the curves (AUCs) and areas under the moment curves (AUMCs) for only the free PYR (measured in the buffer cell-half) are below. The determination of time to equilibrium as described here is a new application of noncompartmental analysis based on statistical moment theory.

For the first experiment using expired blood bank plasma pH 8.0 with albumin 25.9 g/L, the AUC is 15000 ng ml^{-1} min^{-1}, AUMC is 1070000 ng ml^{-1}, mean residence time (MRT) calculated as AUMC/AUC is 71.5 min, and the half-life is 0.693 X MRT or 49.5 min.

For the second experiment using the same lot of plasma adjusted to pH 7.4 with albumin 30.4 at the end of dialysis, the AUC is 22000 ng $ml^{-1}min^{-1}$, AUMC is 1580000 ng ml^{-1}, MRT is 72.6 min, and halflife is 50.3 min.

These experiments were done at the slowest rpm of any ED experiment, thus it is safe to assume that the time to equilibrium would also be the slowest in comparison with experiments run at higher rpms.

The results for these two experiments were remarkably similar. The half-lives to equilibrium are necessary for the design of the other experiments. It was assumed that in 6 half-lives, equilibrium was reached.

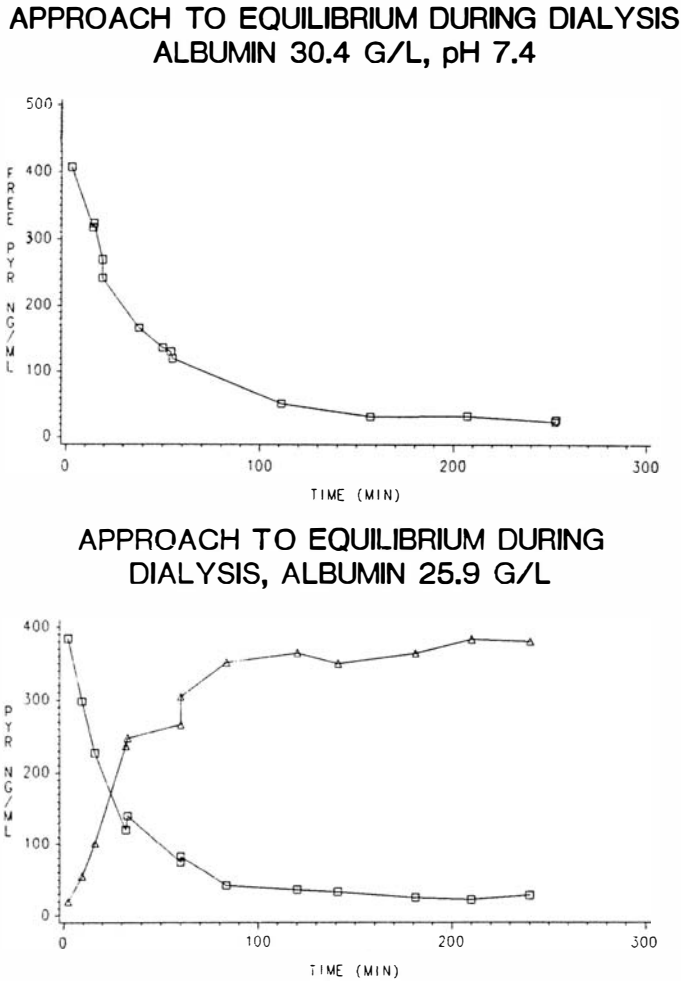

Fig 14. Approaches to equilibrium in dialysis experiments.

5.5.5 Influence of pH on protein binding

5.5.5.1 Binding at pH 7.4 versus pH 8.0

The plasma protein binding at pH 7.4 was not significantly different than at pH 8.0. The results of a Student's t test are in Table 26.

Table 26. Binding at pH 7.4 vs. pH 8.0

T Test Procedure

Variable: Percent free PYR

pH	N	Mean	SD	SE	Min	Max
8	3	14.46667	0.34674679	0.20019435	14.08	14.75
7.4	3	15.16333	0.37753587	0.21797044	14.75	15.49

Variances	T	DF	PR>T
Unequal	-2.3540	4.0	0.0788
Equal	-2.3540	4.0	0.0782

For H_o: VARIANCES ARE EQUAL, F' = 1.19 with 2 and 2 DF

PROB>F' = 0.9151

SE = Standard Error

SD = Standard Deviation

DF = Degrees of Freedom

5.5.5.2 Influence of a range of pH values on binding

Plasma protein binding was definitely influenced by plasma pH even though as described above, the influence did not reach statistical significance in that experiment.

The pH values reported in Figure 15 are for the cells at the end of the dialysis. Albumin concentrations were 43.7 g/L (n=15, 3.9% CV) for the higher pH values and 45.6 g/L (n=15, 6.5% CV) for the lower pH values.

In Figure 15, each point represents the mean of 3.

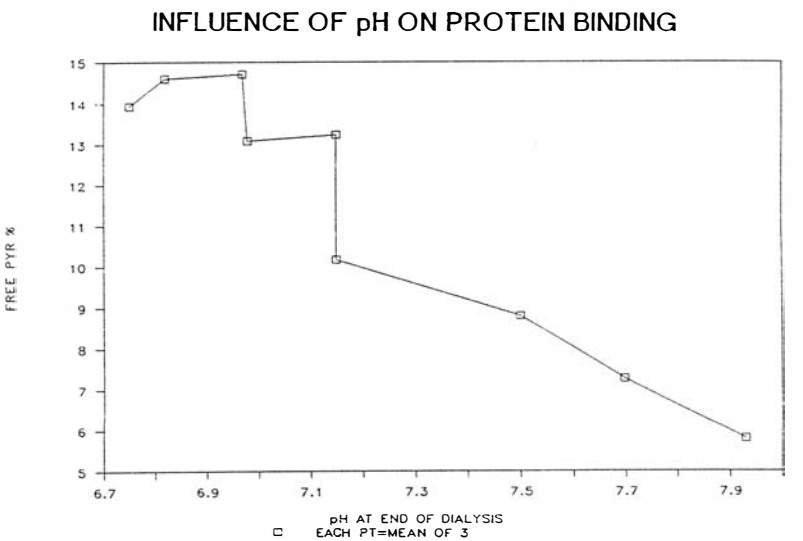

Figure 15. Influence of pH on plasma protein binding.

5.5.6 Concentration dependence of protein binding in the therapeutic range

The binding at two levels of PYR was studied. The *t* test shows that there is a significant difference between percent free at 118 ng/ml versus 363 ng/ml. These 2 levels of PYR were chosen because they are both within the therapeutic range, and due to assay limits, lower concentrations of PYR could not be examined. The albumin concentration was 45.6 g/L (1.52% CV).

Table 27. Binding at 2 PYR concentrations

T TEST PROCEDURE

Variable: Percent free PYR

Conc	N	Mean	SD	SE	MIN	MAX
118	5	3.53200	0.49529789	0.22150395	3.080	4.080
363	5	4.91200	0.98133582	0.43886672	3.550	5.890

Variances	T	DF	P>T
Unequal	-2.8072	5.9	.0315
Equal	-2.8072	8.0	.0229

For H_o: VARIANCES ARE EQUAL, F'= 3.93 with 4 and 4 DF

PROB > F' = 0.2138

5.5.7 Summary of influence of albumin on PYR binding

In Figure 16 below, the relationship between plasma albumin and percent free PYR can be seen. These were the combined data for 7 different days involving experiments where the ending pH was 7.3 to 7.5. The results show that there is a significant correlation (R=0.893) between percent free PYR and albumin yielding the equation % free = -0.467(albumin g/L) + 23.5.

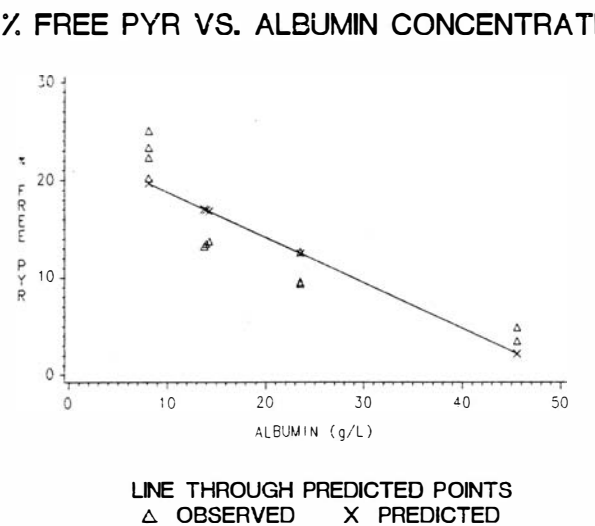

Fig 16. Influence of albumin on percent free PYR.

Table 28. Linear regression of percent free PYR on albumin concentration

Dependent variable: Percent free PYR

SOURCE	DF	SS	MS	F VALUE	P>F
Model	1	439.26190	439.26190	39.305	0.0001
Error	10	111.75829	11.17583		
C Total	11	551.02020			

Root MSE	3.343027	R-Square	0.7972
Dep Mean	14.29058	Adj R-square	0.7769
CV	23.39322	R	0.893

Parameter estimates

Variable	DF	Estimate	SE	T for Ho: Parameter = 0	P > T
Intercept	1	23.487508	1.755937	13.376	0.0001
Albumin	1	-0.467165	0.074516	-6.269	0.0001

Cook's D on observations range 0.003 to 0.400

5.5.8 Percent free PYR in different tubes

There was no difference in percent free PYR (1000 ng/ml) in plasma or serum collected in three different types of Vacutainers™ containing 2 different anticoagulant additives. The results of PROC GLM in SAS are in Table 29 below.

Table 29. Percent free PYR in different tubes

General Linear Models Procedure

Dependent variable: Percent free PYR

Source	DF	SS	MS	F-value	PR>F
Model	2	20.69766786	10.34883393	1.53	0.2804
Error	7	47.24866517	6.74980931		
C total	9	67.94633302			

R-square 0.304618 CV 37.5540%

Free mean 6.91815000

Source	DF	Type I SS or Type III SS	F-value	PR>F
Anticoagulant	2	20.69766786	1.53	0.2804

DF = Degrees of Freedom

SS = Sum of Squares

MS = Mean Square

PR>F = Significance probability for the F value.

C total = Corrected Total

5.5.9 Binding to pure human serum albumin

The binding of 350 ng/ml PYR to pure human serum albumin in IPB (14.2 g/L, 2.06 X 10^{-4} M) resulted in bound PYR values slightly higher than those predicted for whole plasma by the equation in Table 28.

The "Free" column is the buffer cell-half and the "Albumin" column is the albumin-containing cell-half PYR concentration (ng/ml). The average albumin was 14.2 g/L.

Table 30. Binding to purified human albumin

PYR ng/ml

Free	Albumin	% Free	% Bound
38.95	283.58	13.74	86.26
42.39	319.26	13.28	86.72
Mean		13.5	86.5

5.5.10 Binding to AAG

PYR binding at 2 levels of AAG was determined, at stress level AAG 3.7 g/L and at normal level 0.571 g/L. The binding was about 10% at the high level of AAG. Table 31 shows the results.

Table 31. Binding to 3.7 g/L AAG

PYR (ng/ml)

Free	AAG	% Bound	% Free
173.24	199.66	13.23	86.77
173.24	184.08	5.89	94.11
Mean		9.56	90.4

No binding was apparent in the diluted AAG. In fact, there was more drug on the free side in every cell. Possible explanations are that equilibrium had not been established or the AAG was damaged. The AAG had been used in the previous experiment.

5.5.11 Analysis of protein binding data from Studies 1, 2, and 3

Data from Studies 1, 2, and 3 were fit to the Blanchard, Larsen, Scatchard, and double reciprocal equations described in Chapter 2. After fitting the three sets of data to the Scatchard model, it was obvious that all of the assumptions of drug-protein interactions had not been met.

In the plot of percent free PYR versus plasma concentration (Fig. 17), one can see that the drug is not obeying the law of mass action, the most basic assumption of drug-protein binding interactions. This figure more likely shows a concentration dependent distribution between the aqueous phase and plasma proteins (albumin as well as lipoproteins). In other

words, the Figure 17 shows a partitioning that is a function of the solubility of PYR, not the law of mass action. The low water solubility of the PYR makes it avoid the plasma water in favor of adsorption on the proteins. The proteins act as a sink at low drug concentrations.

Table 32 summarizes the PYR and albumin concentrations in Studies 1, 2, and 3. Data from Study 1 were collected in the system with the highest protein level (albumin 3.4 X 10^{-4}M or 23.5 g/L), yielding opportunity for the simple precipitation or adsorption of drug on the proteins. The data from Studies 2 and 3 did not display a trend of increasing binding with increasing plasma concentration, the opposite of what should happen in protein binding.

Table 32. Summary of protein binding Studies 1,2 and 3

Study	PYR Conc. Range (ng/ml)	Albumin Concentration (g/L)
1	140-4100	23.5
2	140-4100	8.13
3	720-45000	0.66

Initial estimates for the first stoichiometric binding constant from the relationship (bound/free)/albumin in molar units (63) as listed below (Table 33) were in excellent agreement with the K_1 values from the

nonlinear fits of data from Studies 1 and 2. However, for data from Study 3, because of its higher PYR concentrations and lower albumin concentration, the initial estimates for K_1 were more variable and less likely to reflect the true K_1 values for the interaction of PYR with albumin at physiologic concentrations.

Table 33. Estimates of the first stoichiometric binding constant K_1

.Study	1	2	3 .
	28895.8	25381.0	81235.7
	20232.4	24196.4	79587.6
	21983.0	30080.3	50711.8
	27748.5	25313.3	30835.5
	28234.1	31261.9	64204.6
	29918.6	33491.4	74517.0
	32714.5	29595.1	47893.5
	29284.1	27884.4	40189.4
	29378.5	30345.2	47739.3
	36540.5	27718.3	46063.9
	34253.4	28267.4	43667.9
	30335.4	29323.8	56980.3
		26714.7	48328.2
		26770.7	37421.9
.		29568.7	26709.5
N	12	15	15
Mean	29000	28000	52000
% CV	15.7	8.78	32.2

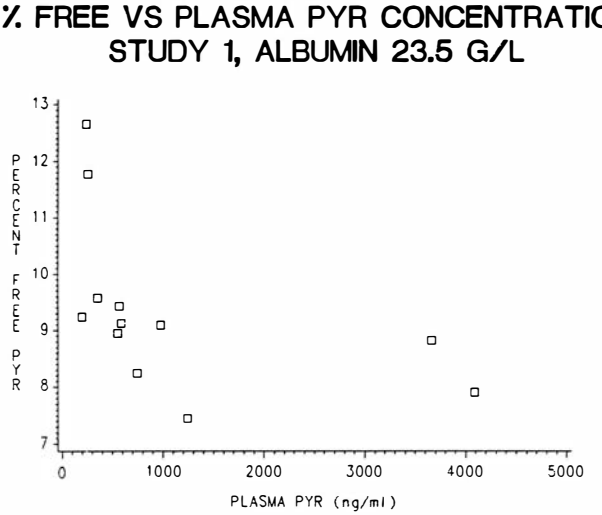

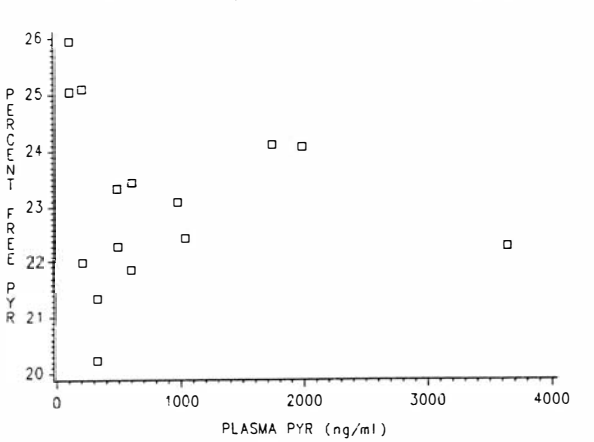

Figure 17a and b. Percent free PYR versus total plasma concentration for data from Studies 1 and 2.

A linear relationship was not obtained after plotting according to the Scatchard equation as one can see in Figures 18-20. The parameter estimates from PROC REG in SAS using the Scatchard Eq. (9) for one or two sites were also nonsensical. Due to the previously described problems associated with the double reciprocal plot, what looked like a straight line was obtained but the parameter estimates were meaningless.

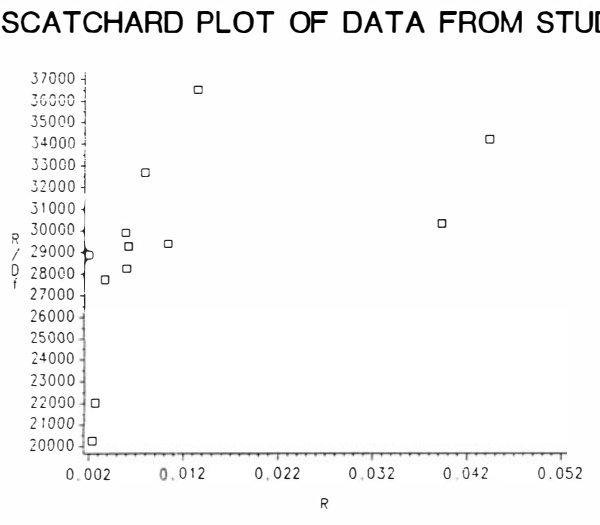

Fig. 18. Scatchard plot of data from Study 1.

SCATCHARD PLOT OF DATA FROM STUDY 2

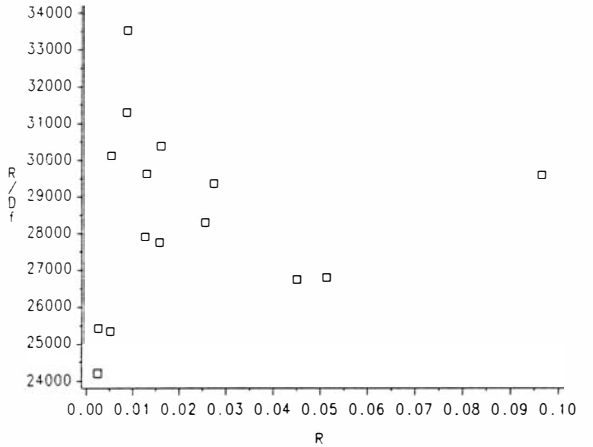

Fig. 19. Scatchard plot of data from Study 2.

SCATCHARD PLOT OF DATA FROM STUDY 3

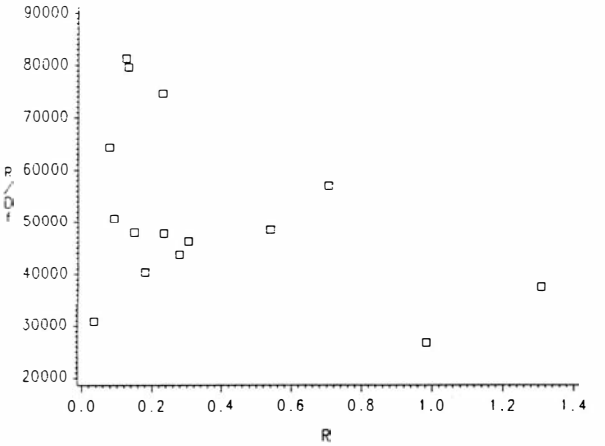

Fig. 20. Scatchard plot of data from Study 3.

The most success was obtained with the stoichiometric approach. Data from Studies 1,2, and 3 were fit using one and two site unweighted models of the Klotz equation (Eq. (10) in Chapter 2). They were compared using an F-ratio test (13) and then weighting functions were added. The reason that the one and two site models were compared using the unweighted fits was that the residuals were too small to have significance using weighted residuals. Thus, a more correct model could not be chosen. Weighting was used for fits of both models, but only the unweighted models were used in calculating F values.

Data from Study 1 had the lowest range of PYR concentrations (summarized in Table 32) and the highest albumin concentration (3.4×10^{-4} M). The highest plasma concentration was 3660 ng/ml or 1.47×10^{-5} M. The two site fit for this set of data did not show significant improvement over the one site model where F was 1.327 ($F_{.01} = 9.65$; 1, 11). The weighting factor of 1/buffer concentration improved the fit only at the high concentrations. The results of the fit to the Klotz equation are in Table 34.

The plots of the observed and predicted values are in Figure 21 and the residuals are in Figure 22. The residuals show that the model may be inappropriate.

Table 34. Nonlinear fit of data from Study 1 using the Klotz equation

SAS NLIN Statistics using method DUD

Dependent variable: r

Source	DF	Weighted SS	Weighted MS
Regression	1	.000018159549	.00001815949
Residual	11	2.515001E-07	2.286364E-08
Uncorr. Total	12	.000010768167	

Parameter	Estimate	Asymptotic SE	Asymptotic 95% Confidence interval
K_1	32018.47028	1166.6638927	29450.651 - 34586.29

Correlation matrix of the parameters

Corr	K_1
K_1	1.0000

Weighted Residual Sums of Squares (WRSS) 2.51500×10^{-7}

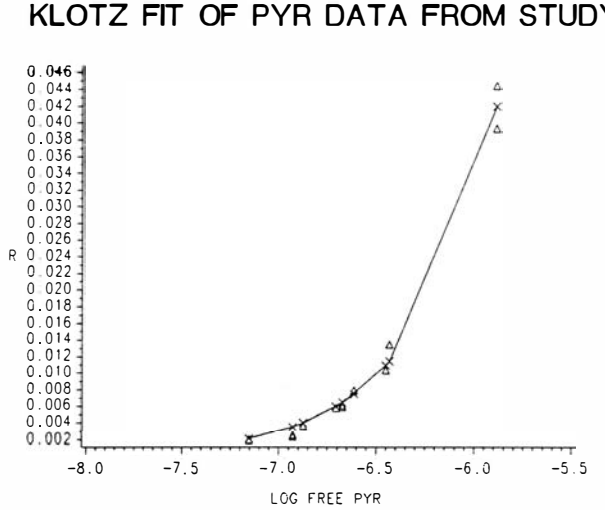

Figure 21. Klotz plot of data from Study 1 showing observations and predicted points from the fit. Line through fitted points.

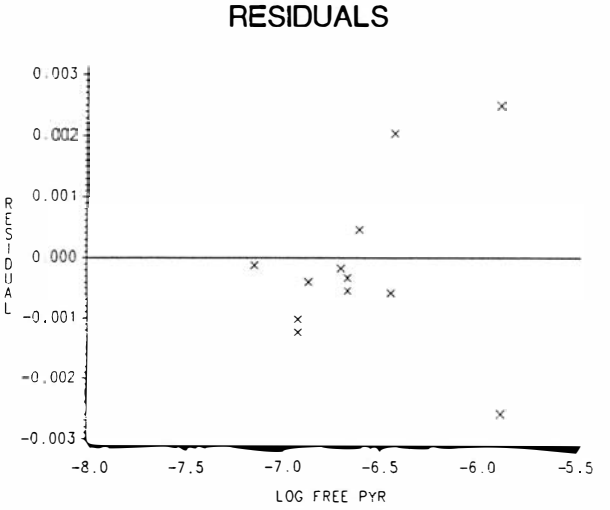

Figure 22. Residuals for Klotz fit of above data.

Data from Study 2 had a low range of concentrations (maximum on plasma side 3650 ng/ml, 1.5 X 10^{-5} M), but had slightly more in the higher range compared to data from Study 1. The albumin concentration was 8.13 g/L (1.179 X 1^{0-4} M). The highest PYR concentration was 3646 ng/ml (1.46 X 10^{-5} M).

The two site model was significantly better than the one site model in the Klotz fit. F = 21.2 exceeds the table $F_{0.01}$ = 9.07 (1, 13). Weighting improved the fit. The parameter estimates for the affinity constants K_1 and K_2 were more likely correct in that K_1 was larger than K_2. The results of the fit to the Klotz equation are in Table 34 and the plots are in Figures 23 and 24. The plot of the residuals shows, even though these were improved by weighting, that this may be an inappropriate model to describe the data. The fit appears to very good, however. The standard error of the estimate for K_1 was only 3% of the estimate. The standard error for the estimate of K_2, however, was 47% of the estimate, indicative of a problem with the model or poor data.

Table 35. Nonlinear fit of data from Study 2 using the Klotz equation

SAS NLIN Statistics using method DUD

Dependent variable: r

Weighting 1/buffer PYR concentration

Source	DF	Weighted SS	Weighted MS
Regression	2	0.00003856191	0.00001928096
Residual	13	1.306542E-07	1.005032E-08
Uncorr. Total	15	0.000038692563	
Corr Total	14	0.000023911245	

Parameter	Estimate	Asymptotic SE	Asymptotic 95% Confidence interval
K_1	28228.08436	873.4580261	26341.094 - 30115.07
K_2	17367.91997	8249.3182413	-453.638 - 35189.48

Correlation matrix of the parameters

Corr	K_1	K_2
K_1	1.0000	-0.8372
K_2	-0.8372	1.0000

Weighted Residual Sums of Squares (WRSS) 1.30654×10^{-7}

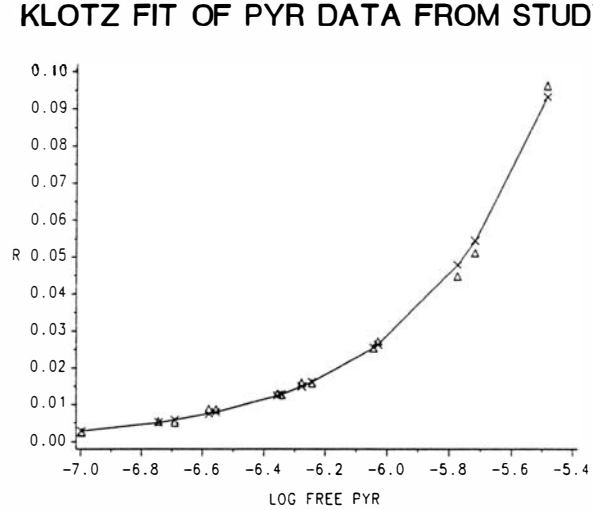

Figure 23. Klotz plot of data from Study 2 showing observations and predicted points from the fit. Line through fitted points.

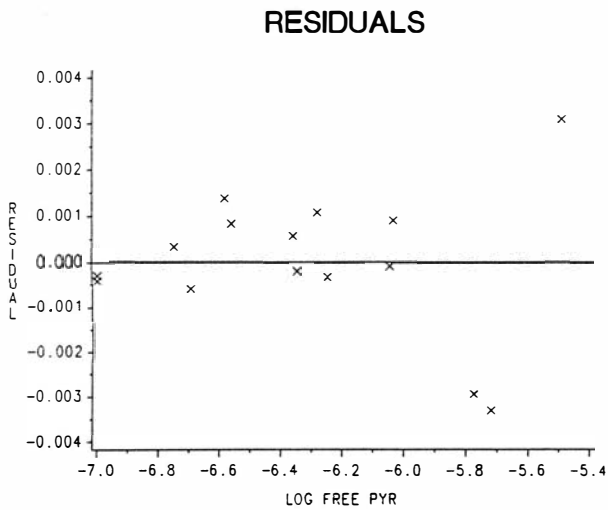

Figure 24. Residuals for Klotz fit of above data.

Study 3 had by far the largest range of plasma PYR concentrations, going up to 33,000 ng/ml (1.33×10^{-4} M) which is ten times the highest concentrations (1.5×10^{-5} M) for the other two sets of data. According to Klotz, it is very important to go past the inflection point in his plot to find accurate parameter estimates. Data from Study 3 also had the lowest albumin concentration (0.66 g/L, 9.56×10^{-6} M). For this reason, it may have the least chance of the three data sets to have the solubility phenomenon be the main interaction between the drug and proteins. In other words, the albumin level and the high PYR levels may allow one to observe a drug-protein interaction as a function of the law of mass action.

On the other hand, such a low protein concentration may have produced unusual binding results.

Fits of data 47 to the Klotz equation were similar whether or not weighting was used and between fits for different weighting functions. The one site model yielded large standard errors for estimates, 24 % of the estimate, and the F value for the comparison with the two site model was 43.234, highly significant at the α 0.01 level ($F_{.01} = 9.07;1,13$). The fit using 1/plasma weighting was a little better than the others. The results for the Klotz fit are in Table 36. The pattern in the residuals (increasing with increasing free PYR)

clearly indicates an ill-conditioned model. The standard errors for the estimates K_1 and K_2 are 13.5 % and 33 % of the estimates, respectively. The plasma and buffer concentrations in this experiment were beyond the range of the assay and had been diluted to within the range. There is evidence of greater variability in the assay in the plot of the observed points. There is greater spread in the duplicate points. The increasing residuals with increasing concentration most likely reflect the assay variability at high concentrations.

Table 36. Nonlinear fit of data from Study 3 using the Klotz equation

SAS NLIN Statistics using method DUD

Dependent variable: r

Weighting 1/plasma PYR concentration

Source	DF	Weighted SS	Weighted MS
Regression	2	0.00017434921	.00008717460
Residual	13	0.00000607148	4.6704E-07
Uncorr. Total	15	0.00010296615	

Parameter	Estimate	Asymptotic SE	Asymptotic 95% Confidence interval
K_1	53234.99852	7211.3897685	37655.747 - 68814.25
K_2	24870.11010	8127.3952066	7311.951 - 42428.27

Correlation matrix of the parameters

Corr	K_1	K_2
K_1	1.0000	-0.7410
K_2	-0.7410	1.0000

Weighted Residual Sums of Squares (WRSS) 6.07148×10^{-6}

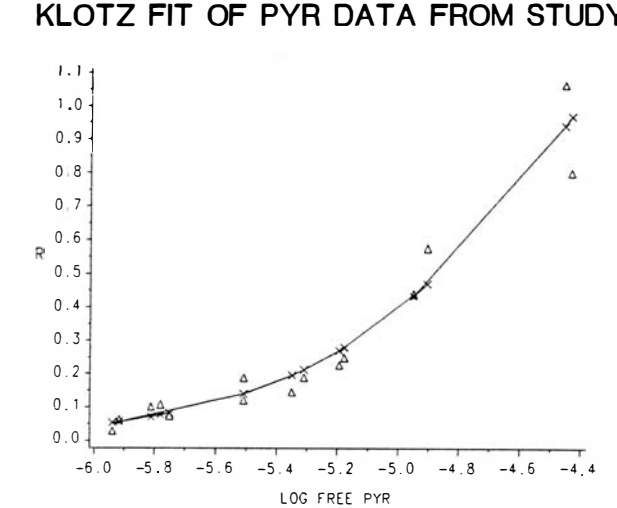

Figure 25. Klotz plot of data from Study 3 showing observations and predicted points from the fit. Line through fitted points.

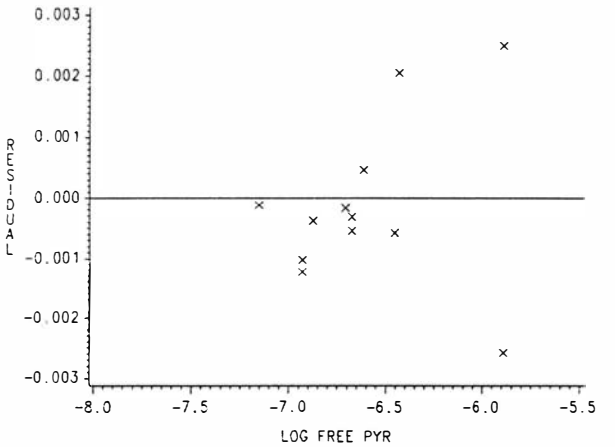

Figure 26. Residuals for Klotz fit of above data.

5.6 RBC partitioning and binding

5.6.1 Binding to hemolysate

There was an unusual amount of variability in the binding of PYR to hemolysate. There was variability in the Hb concentrations at the end of the 5 h dialysis even though each cell-half was filled in the same manner. There was also variability in the percent PYR bound. The results are given below. The free PYR concentration was that PYR in the buffer cell-half, and the total PYR was that in the hemolysate cell-half. The average hemoglobin concentration at the end of dialysis was 1.6×10^{-3} M.

There are at least two sources of this variation. Within 15 min after filling the Spectrum cells, 3 of them appeared to be leaking (cells 5, 6 and 7). Also, the assay variability's role is great when the buffer concentrations have almost no error (direct injection) and the hemolysate levels have error due to the extraction procedure. In the same way, because the percent free and percent bound were similar, the calculation of them has a lot of error from the hemolysate PYR concentration but not from the buffer PYR concentration.

The average percent bound from Table 37 is 42.5% to the hemolysate. The hemolysate in this experiment contains more dilute Hb than that found inside a RBC because in making the hemolysate, the RBC contents were

diluted to about one-half the normal concentration. However, higher binding than about 43% would not be expected because there does not appear to be a trend for greater binding with higher Hb concentration. There is also no apparent PYR concentration dependency in binding. Mean bound PYR was 42.5 (19% CV).

Table 37. Binding to hemolysate

Free PYR (ng/ml)	Total (ng/ml)	Free %	Hb (g/dl)	Bound %
177.77	270.51	65.72	10.998	34.28
129.03	229.59	56.20	10.723	43.8
177.77	247.97	71.69	9.345	28.31
21.66	39.93	54.24	9.436	45.76
21.66	47.10	45.99	9.069	54.01
103.67	189.91	54.59	13.479	45.41
85.38	188.15	45.38	10.539	54.62
114.63	187.81	61.04	9.804	38.96
355.79	597.75	59.52	9.069	40.48
350.40	579.60	60.46	8.885	39.54
N		10	10	10
Mean		57.5	10.1	42.5
% CV		14.1	13.6	19.1

5.6.2 RBC/buffer concentration ratio as a function of pH

The observed RBC/buffer ratio was compared to the theoretical ratio predicted by Equation (15) in Chapter 2. The results are in the figures below and in Tables 38 and 39. Figure 27, the plot of RBC/buffer PYR ratio versus buffer pH, compares the observed data with theoretical points which have been fit to a line. A graph of the residuals from the fits to linear equations has also been included to show that this relationship is not linear, but approximates one because the pKa and pH of the medium are so close.

The figure shows that there is a profound effect of pH on the partitioning of PYR into RBCs. This stresses the importance of the maintenance of physiologic pH or at least the reporting of pH in partitioning studies. This effect would likely be diminished in a system containing albumin.

Note that the slopes of the fitted lines are not equal for the observed versus the theoretical ratios. The overall observed mean ratio was 5.27 (21.3% CV, n=7). At pH 7.4, the mean ratio was 5.16 (11.8% CV, n=2). The mean difference between the observed and theoretical ratios was 4.15 (19.7% CV). There is 4 times as much PYR in the cells as predicted by the theoretical ratio. This indicates binding to the cell membrane or Hb inside the cell.

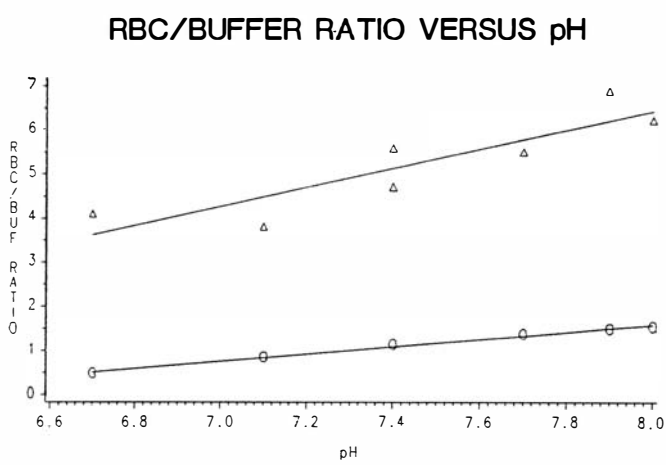

Figure 27. Graph of RBC/buffer ratio vs. buffer pH for observed △ and theoretical O data.

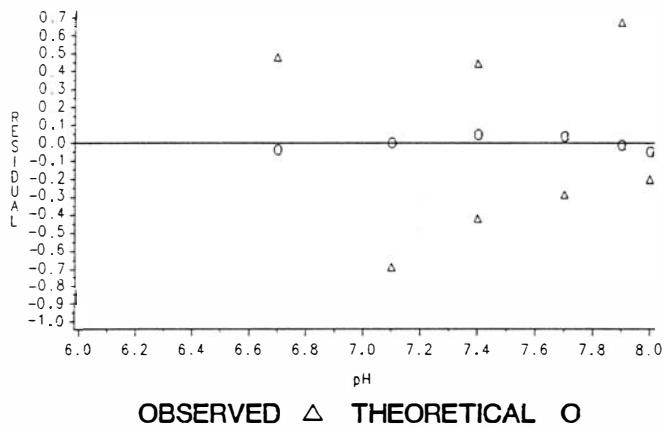

Figure 28. Plot of residuals for fits of observed △ and theoretical O data.

Table 38. RBC/buffer ratio as a function of buffer pH

Analysis of Variance

Dependent Variable: observed ratio

Source	DF	SS	MS	F-value	PR>F
Model	1	5.94534443	5.94534443	18.112	0.0080
Error	5	1.64125599	0.32825120		
C Total	6	7.58660042			

R-square = 0.7837 Adj R-square = 0.7404 CV = 10.8629

Parameter Estimates

Variable	DF	Parameter Estimate	SE	T for H0: Parameter=0	PR>T
Intercept	1	-10.9427	3.81665992	-2.867	0.0351
pH	1	2.174684	0.51098817	4.256	0.0080

Sum of residuals	1.83187E-15
Sum of squared residuals	1.641256
Predicted Resid SS	3.894491

Table 39. Theoretical RBC/buffer ratio as a function of buffer pH

Dependent Variable: Theoretical ratio

Source	DF	SS	MS	F-value	PR>F
Model	1	0.85782696	0.85782696	462.159	0.0001
Error	5	0.00928064	0.001856129		
C Total	6	0.86710761			

R-square 0.9893 Adj R-square 0.9872 CV 3.78256

Parameter Estimates

Variable	DF	Parameter Estimate	SE	T for H0: Parameter=0	PR>T
Intercept	1	-5.021	0.28700164	-17.495	0.0001
pH	1	0.8260523	0.03842481	21.498	0.0001

Sum of residuals	2.08167E-17
Sum of squared residuals	0.009280645
Predicted Resid SS	0.02494775

5.6.3 RBC/plasma PYR ratio

In Study R1, the experiment to determine RBC/plasma ratio as a function of albumin, a high level of PYR was chosen to avoid the solubility phenomenon observed at low levels of PYR. There was a problem with the column failing that day, and the column had been turned around 3 - 4 times by then. Assay of drug in RBCs is difficult because of the tendency of them to form bubbles. Due to the lack of controls, it is difficult to estimate the accuracy of assaying PYR in RBCs.

Attempts to make RBC controls were unsuccessful because of their viscous nature, tendency to form bubbles, and clot formation. To measure volumes of RBCs, syringes were chosen. Packed RBCs cannot be pipetted by air-displacement pipettors because of the viscous nature of RBCs. Controls in pre-measured 0.5 ml volumes in tubes clotted in the refrigerator, and when vortexed, the clots did not completely break up. In addition, the RBCs coat the walls of the tube and the addition of organic extracting solvents cements RBCs to the walls of the tubes. Even adding water to the cells and vortexing does not completely break up the clots enough to get good recovery of drug. Thus, the storage of controls was impossible.

However, even though there is an unknown factor of error in these RBC experiments, trends and relationships

can still be discerned.

There are two plots of the RBC/plasma PYR ratio versus plasma albumin concentration on the following page. Figure 29 shows data from Study R1, the experiment that was designed to show the relationship between the ratio and the albumin concentration. The other plot (Fig. 30) shows the combined data of Study R1 and Study R2, the study to determine the RBC/plasma ratio. The data from Study R2 was not corrected for hematocrit or albumin concentration before plottiong in Fig. 30.

There appears to be a negative relationship between the ratio and the albumin concentration. Partitioning into RBCs decreases as plasma albumin increases. Albumin is changing in Figure 29 for the first experiment. However, albumin is fairly constant in Figure 30 at 45.5 g/L (3.34% CV) and HCT is constant at 0.44 for the points not included in Figure 29, and there is still a negative relationship apparent. Still, there is a large amount of scatter in the data.

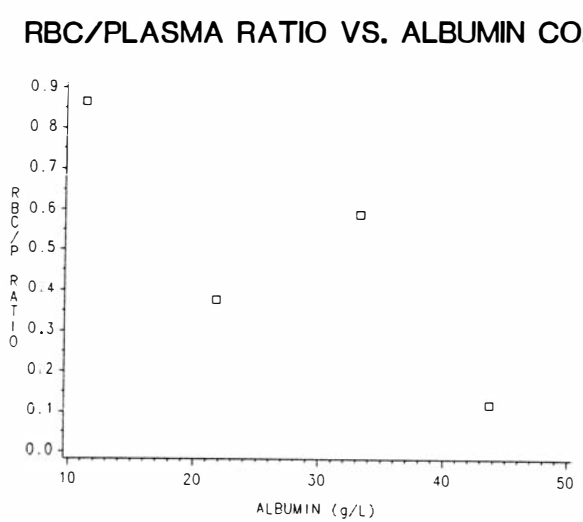

Figure 29. RBC/plasma ratio vs. plasma albumin concentration for data from Study R1.

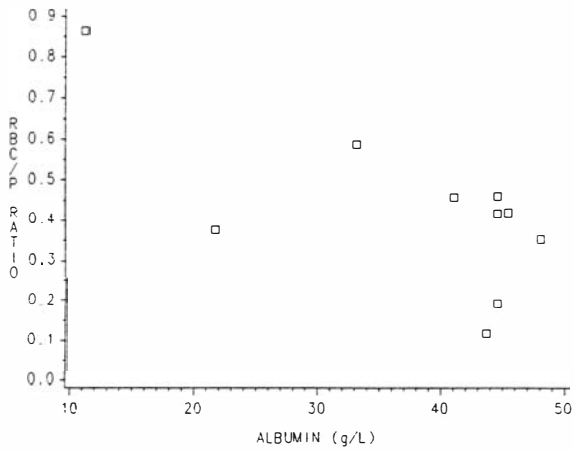

Figure 30. RBC/plasma ratio vs. plasma albumin concentration for data from Studies R1 and R2.

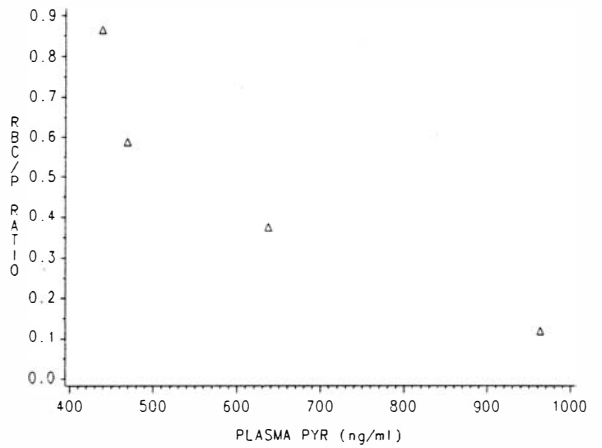

Figure 31. RBC/plasma ratio vs. plasma PYR concentration for data from Study R1.

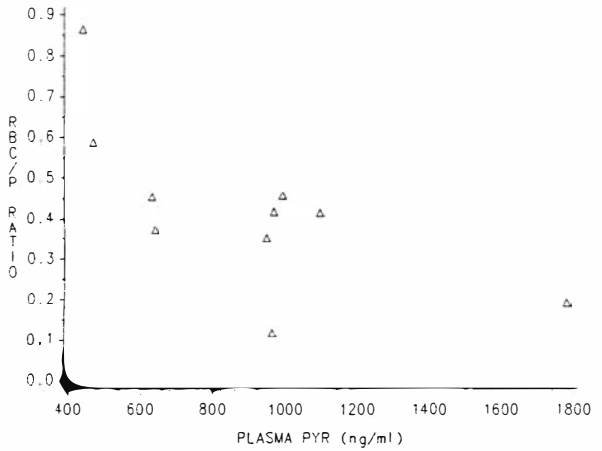

Figure 32. RBC/plasma ratio vs. plasma PYR concentration for data from Studies R1 and R2.

The data showing the relationship between RBC or plasma and whole blood PYR levels are plotted in Figures 33-36. It is obvious that there is a strong positive relationship between plasma and whole blood PYR levels. As plasma levels increase, whole blood levels increase.

This relationship is not as strong for the RBC versus whole blood PYR plots. On the contrary, there appears to be a random distribution between RBC and whole blood PYR levels in Figures 35 and 36. The range of PYR concentrations in RBCs is narrower for data from Study R2 compared to Study R1, but for Study R1 that involved varying albumin levels, there is a negative relationship between RBC and whole blood concentrations of PYR.

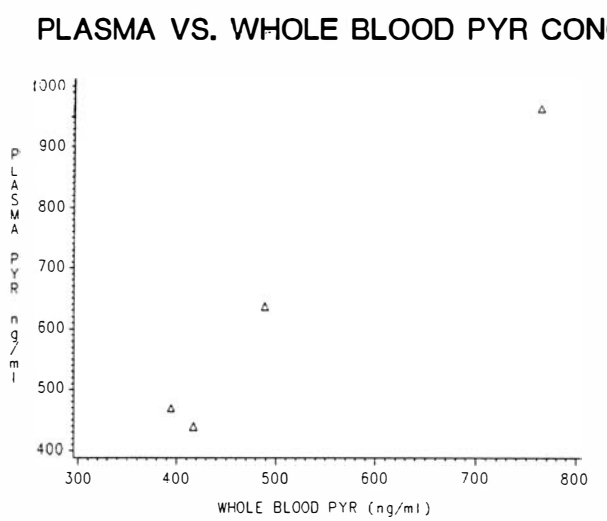

Figure 33. Plasma vs. whole blood PYR concentrations for data from Study R1.

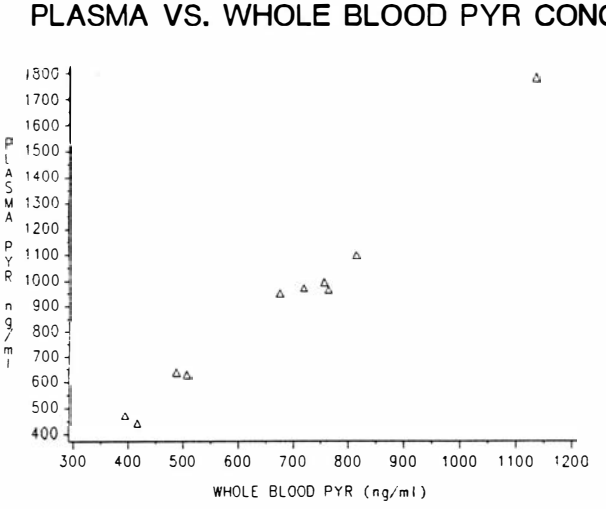

Figure 34. Plasma vs. whole blood PYR concentration for data from Studies R1 and R2.

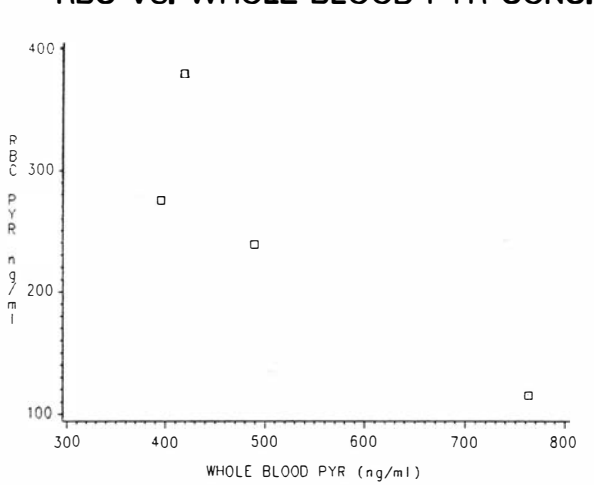

Figure 35. RBC vs. whole blood PYR concentrations for the data from Study R1.

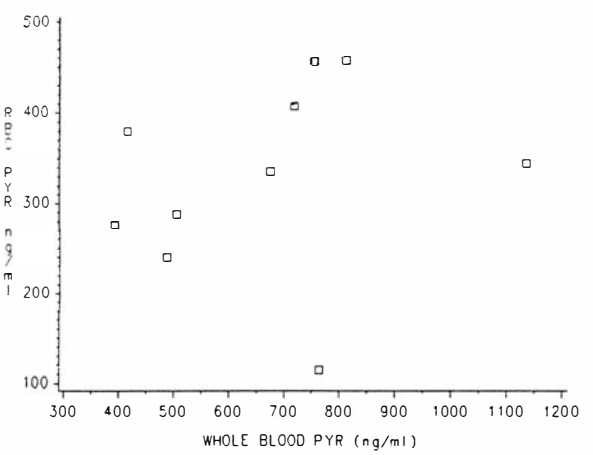

Figure 36. RBC vs. whole blood PYR concentrations for the data from Studies R1 and R2.

Chapter 6

Discussion

6.1 Analytical methodology

Initial studies with Edstein's assay (39) indicated that it was not adequate for the proposed studies. Edstein's assay may have worked if a new μBondapak™ column had been used, but the one used was in poor condition initially with only a maximum of 19,000 plates/meter. Deterioration of this column was rapid. The peaks were broad and tailed (Fig. 4).

Several facts support the idea that decreasing the solubility of PYR in the mobile phase improves the chromatography of PYR. Solubility was decreased by increasing the ionic strength of the reconstituting solvent or the mobile phase.

After evaporation of the organic solvent used to extract PYR from biological fluids, Edstein used mobile phase to reconstitute the residue. Very poor chromatography resulted from using mobile phase to reconstitute the residue. Peaks displayed tailing, fronting and were much shorter. The use of 100% methanol to reconstitute the residue resulted in tailing, fronting, and decreased

peak height also. On the other hand, potassium phosphate buffer like that used in the mobile phase gave excellent narrow peaks and so it was used. The results with 50% methanol in water were identical to the results with phosphate buffer as a reconstitution solvent. This suggests that the solubility of PYR in the reconstitution solvent and its interaction with the mobile phase were factors determining the peak shape and resolution.

The composition of the mobile phase also influenced the chromatography. As discussed in Chapter 5, the use of both monobasic and dibasic potassium salts of phosphate, so that the ionic strength of the mobile phase could be increased, was necessary for better peak height and resolution. The addition of more than 15% of acetonitrile to the mobile phase (while holding the ratio of organic to aqueous components in the mobile phase constant) resulted in peak fronting and tailing. The solubility of PYR in acetonitrile is probably greater than that in water. Improving the solubility of PYR in the mobile phase was advantageous to a limited degree.

This "salting out" effect in the mobile phase resulted in improved efficiency for the interaction of the PYR with the stationary phase.

Previous assays have used other antimalarials as internal standards. However, it was preferred not to use

another compound that binds to glass and antimalarials are bases that often bind to glass. After it was found that NAPA had appropriate chromatographic and extraction characteristics, it was chosen as the internal standard even though it has an unrelated chemical structure and hydrophilic properties.

Spectral data for PYR (90) has shown good absorbance at 254 or 280.

By far the biggest problem with this assay was the rapid deterioration of the Econosphere™ columns. In addition, since 1000 ml batches of mobile phase were made, for 10-15 samples there was a relatively long equilibration time for the system each day. Each new batch of mobile phase had to be run through the system for an hour before consistent responses were observed.

The saturator column helped prolong the lifetime of the columns considerably (Table 6). However, eventually the economy of the columns was revealed in their rapid failure. In the future, it would be prudent to use columns with higher carbon load and not the cartridge type of column. Cartridges cannot be opened for the purpose of filling voids that form. It was the formation of voids that caused the failure of the columns.

These studies used four Econosphere™ columns. The first one was different from the others in that the NAPA

had a longer retention time than the PYR. Confounding this observation was the fact that at that time a lower molarity and the sodium salt of phosphate buffer was used in the mobile phase. It was with the first column that the preliminary work was done, and so the graphs of the effect of pH on retention times are odd. The latter three columns demonstrated consistent results, and a single mobile phase composition was used.

Composition of the mobile phase was determined by trial and error. Using the potassium salt of the phosphate buffer in the mobile phase was very important. The increased solubility of potassium in organics compared to sodium allowed the molarity of the buffer to be increased in order to get better chromatography (better resolution and peak height) and it also lengthened the lifetime of the column. Two piston seals had to be replaced during a week's time when the sodium salt was used due to the salt precipitation on the seals. The column was also damaged by the sodium salt.

The longer the tubes sat while processing other tubes, the lower the recovery of PYR and NAPA. The reduced recovery of NAPA with time indicates that it also binds to glass. The time involved in the extraction of the plasma and RBC samples was critical. This was due to the alkalinization step in the extraction procedures.

The water-soluble silanizing agent AquaSil™ was much easier to work with than SurfaSil™, a hydrocarbon-soluble agent. AquaSil™ was easily removed, however, by neutral or basic pH buffers. Thus, glassware had to be re-silanized with every use, and the removal of the silanes from the glass during any procedures resulted in PYR binding to the glass.

Recovery was consistent and Table 7 showed no concentration dependency. Overall recovery of PYR was 81.9% (8.7% CV) in the low concentration range curve and 85.4% (7.9% CV) in the high curve. NAPA recovery was also consistent with averages of 82.6% (10.2% CV) and 80.9% (7.7% CV) for the plasma curves.

Recovery from RBCs was similar to recovery from plasma with overall recovery 84.45% (4.53% CV) for the low curve and 84.38% (10.39% CV) for the high curve. A quantitative method was used in the RBCs extraction procedure. Thus, the variation was produced when spiking the RBCs with the methanol solutions of PYR.

The problems with recovery due to binding to glass could have been solved by two actions. First, the use of a combination of a nonpolar extraction solvent (for good recovery of the nonpolar PYR) and a small amount of a polar solvent like isopropanol has been used to keep drugs from binding to glass. Second, the use of 50% methanol for reconstitution of the residue from the

organic extraction solvent might have helped. The methanol would not have removed the silanes from glass and thus, would not have contributed to the loss of PYR.

However, the addition of only 5% v/v of polar solvents to the extraction solvents resulted in the extraction of unwanted plasma constituents that interfered with the NAPA and PYR peaks.

Two standard curves were necessary for the entire concentration range 24-1000 ng/ml, although both curves were not always run on each day. The curves went from 24 to 140 ng/ml for the low curve and from 140 to 1000 ng/ml for the high curve. Below 140 ng/ml, errors near 20% were found using the high curve for the 100 ng/ml standard. Because the concentration range was great, it was better to have two curves for more confidence in the lower concentration range.

Linearities of the biphasic curves for PYR in plasma were good with correlation coefficients of 0.995 or better. Replicate analysis of the same plasma control indicated that the variation was less than 10%. Intra-day variation was not reported. Due to the availability of only 15 dialysis cells, a maximum of 15 samples were run each day. On each day, there would be a standard curve of 5 or 6 samples, 1 or 2 controls and 5 to 15 samples. Often, there were more standards and controls than samples.

Calibration curves for PYR in RBCs were excellent with an overall CV less than 9% for standards and overall error less than 5%. Linear regression on the RBC calibration curves produced consistent slopes and R greater than 0.995 although on the last day, the high curve for the RBCs was off due to column failure.

Calibration curves for PYR in buffer were also excellent. Overall CV for standards was less than 7.5%, and error was less than 2.3%. Buffer controls were also consistent from day to day with error less than 2% and CV less than 6%. Peak heights were nearly identical from day to day.

Controls were unacceptable if more than 10% different from the known spiked concentrations. If controls were unacceptable, the samples run with them were also considered unacceptable. Whenever samples were rejected in this manner, experiments were repeated. Controls showed no signs of decompostion for the duration of the study.

No planned attempt was made to check for interferences. However, there was an opportunity to rule out interferences when searching for an internal standard. Trimethoprim, quinine, chlorpheniramine and procainamide do not interfere with the NAPA or PYR peaks.

6.2 Mass balance considerations

Proven procedures for studying protein binding are

prerequisites for accurate results. One assumes, of course, that assay error has been minimized. Error was not concentration dependent for the range 24 to 1000 ng/ml in the assay presented here. Low concentrations have been assayed very accurately as reported in Tables 10 and 18. However, assay error will ultimately play a role in studies. The limit of a study is often the assay limit of detection as it has been in determining the lowest unbound drug range in my work.

It is important to consider mass balance. Losses from binding to glass may prevent accounting for mass which makes accurate measurement of RBC levels, plasma levels, and hematocrit more important, but also more dubious because one can never be sure of the true source of error (i.e. random error, analytical error, or loss from binding to glass). When there is binding to glass, spiked amounts may be greater than the amount recovered, and the source of error will never be realized.

When there is binding to glass, one should never assume that the spiked amount is the total amount at the end or use any form of Equation 17 without measuring at least two of the quantities.

6.3 Vacutainer™ pH and cell/medium ratios

These studies show that one cannot take the pH of plasma for granted, especially when using Vacutainer™ tubes. Anticoagulant additives to tubes not only have

different anticoagulant properties, but different chemical properties that cannot be ignored.

The initial pH of tubes is different depending on the additive. EDTA is the best choice of the anticoagulants tested because it has good anti-clotting properties and because it tends to lower the plasma pH slightly which allows for whatever small rise there might be in further immediate processing. Sodium heparin produced a significantly different zero-time pH in Vacutainers™ compared to EDTA and sodium citrate when analyzed using ANOVA ($p<.001$) and Tukey's studentized range (HSD) test (α 0.001). Heparin also allowed the most rapid rise in pH as plotted in Figure 13 and in Table 20.

Sealing tubes is necessary. Parafilm is not as good as tightly fitting caps or stoppers because parafilm tends to loosen with time. Also, parafilm performs poorly on silanized glassware because the glass becomes slippery, and the contents flow out readily when the tube is tilted. In addition, pH changes so rapidly that it was necessary to continue gassing the vials of plasma while loading the ED cells, a procedure that took about 15-30 seconds per cell. Even in the short time to fill 15 cells, pH changes occur.

There is a difference in the behavior of plasma and RBCs with regards to pH changes when these two

components of blood are open to the atmosphere. CO_2 escapes from plasma and the pH changes rapidly due to its low buffer capacity. In contrast, there is almost no change in RBC pH because of their greater buffering ability.

In general, the pH of plasma rises rapidly while RBCs tend to maintain their physiological pH. The result is a nonphysiological situation. The effect of pH changes on the distribution of drugs in mediums with different pH values and different tissues can be seen in Table 23. That table illustrates the critical nature of measuring and reporting pH values in RBC partitioning studies.

6.4 The theoretical effects of pH on RBC partitioning

The reason for examining the changes in pH and contribution to those changes by different anticoagulants is to be able to comment on the effects of pH change on RBC partitioning. According to calculations using Eq. (15) the following trends can be seen:

(1) For bases, as the pH of the medium increases, cell/medium ratios increase, and as the pKa increases, the effect on the ratio increases. There is little difference in ratios for a drug like PYR, a weak base with a pKa near physiologic pH.

(2) For acids, as the pH of the medium increases, cell/medium ratio decreases, and as the pKa decreases,

the effect on the ratio increases.

(3) Unsealed plasma produces falsely high cell/medium ratios for bases and falsely low ratios for acids.

(4) Bases are more ionized at lower pH values and are therefore ion-trapped in areas of lower pH such as in muscle tissue.

(5) Acids are more ionized at higher pH values and thus are ion-trapped in the plasma.

(6) Trend 4 is responsible for the larger volume of distribution for most basic drugs and is why RBC levels of bases should be examined.

6.5 Protein binding and ED in general

Dilutions from the water content of membranes or volume shifts were small. For very highly bound drugs with concentration dependent protein binding, these small volume shifts might make a difference. Albumin measurement in each cell-half at the end of dialysis is a simple and rapid way of detecting volume shifts and leakage of protein from the cells. With this information for each cell, one can provide a reason for unusual results from any one cell. This is helpful in the designation of outliers and assurance of identical conditions in each cell. The use of isotonic buffer in dialysis did not prevent volume shifts entirely, as reported in Table 24.

The adjusting of pH by gassing with 5% CO_2 in

oxygen resulted in concentrating protein in plasma. This is due to the loss of water through evaporation. This could have been offset by volume shifts from the buffer side (92). However, the data for the original albumin levels in Table 24 are for after gassing the plasma, and so, the author can only state that the phenomenon happens from experience.

There were no losses due to binding to the Spectrum cells or membranes because there was 100% recovery from the amount put in the cells as found in Table 25.

Statistical moment theory can be used to evaluate equilibration time in ED. Virtually identical results were achieved in two experiments. Therefore, the equilibration half-life at 12 rpm is 50 min. It was assumed that in 6 half-lives, or 300 min, that equilibrium was reached, and so dialysis experiments were run for 5 hours.

6.5.1 Influence of pH on protein binding

The results of the Student's t test in Table 26 for binding data collected at pH 7.4 versus pH 8.0 showed no significant difference. However, there is an influence of pH on protein binding as one can see in Figure 15. For this reason, pH should be controlled or at least reported in all protein binding studies.

6.5.2 Influence of PYR concentration on protein binding

A Student's t test showed a significant difference

($p<.03$) in binding at 2 different PYR concentrations in the therapeutic range, 120 and 360 ng/ml, and this has been reported in Table 27. There is more free drug at a higher total plasma concentration.

However, examination of Figure 17 shows the opposite, that there is more percent free drug at lower concentrations, in opposition to the law of mass action. This is probably due to the fact that the experiment done to show a difference between binding at 120 and 360 ng/ml was done at normal albumin levels (45.6 g/L) while the data in Figure 17 was collected in plasma with a lower than normal albumin level (23.5 g/L). Changing the protein concentration, if the interaction between the drug and protein is a partitioning phenomenon, could result in different percent binding of PYR.

The phenomenon seen in Figure 17 and in the other binding experiments shows the importance of using more than one albumin level in binding experiments for the purpose of determining binding affinity constants. The difference in percent free drug is not great enough in the therapeutic range to be significant clinically. Yet, while this difference may not be significant clinically, it makes a great deal of difference in ED experiments involving concentrations beyond the therapeutic range. This is especially true for poorly soluble drugs like PYR that demonstrate a solubility phenomenon in binding

experiments at low albumin levels.

Another conclusion is that binding affinity constants derived from studies using different albumin levels, even in the same laboratory, may not be equal and may not reflect the values *in vivo*.

6.5.3 Influence of albumin on protein binding

Albumin concentration greatly influences the percent free PYR. Even under slightly different conditions and on 7 different days, combined data shows a significant correlation (R^2 = 0.797) between albumin concentration and percent free PYR. The high coefficient of determination, R^2, indicates that a great deal of the total variation is attributed to the fit rather than to residual error. The equation for the relationship is percent free = -0.467(albumin) + 23.5.

6.5.4 Influence of tubes on PYR binding

There was no difference in percent free PYR in plasma collected in Vacutainer™ tubes containing EDTA or heparin or serum collected in tubes with no additive at the PYR concentration 1000 ng/ml (4.02×10^{-6} M). The average percent free was 6.92 (37% CV, n=10) which is equal to 93.8% bound. There was more variation in results in that particular experiment than in other experiments. There was both inter- and intra-tube variation.

6.5.5 Binding to pure human serum albumin and AAG

The average binding to pure human serum albumin at 14.2 g/L (2.06 X 10^{-4} M) at 300 ng/ml PYR (1.2 X 10^{-6} M) was 86.5% bound or 13.6% free. This is slightly more bound than predicted (83.1%) from the equation in Table 28.

At a stress level of AAG, 3.7 g/L (8.4 X 10^{-5} M), PYR (200 ng/ml, 8 X 10^{-7} M) was only 9.56% bound. At a lower level of AAG, there was no binding detected.

The sum of the binding to AAG (0 at normal AAG levels) and pure albumin (86.5%) does not equal the 93.8% bound found in the plasma binding experiment for the comparison of different Vacutainers™. These experiments were done at two very different PYR levels and different albumin levels, however, and so corrections should be considered. If PYR is bound more at higher levels and more at higher levels of albumin, it is possible that the pure albumin binding accounted for all of the plasma protein binding. It does not rule out the presence of more binding proteins in the plasma than these two proteins.

There were two previous reports on the binding of PYR to plasma proteins. Ahmad and Rogers (2) reported the plasma protein binding of PYR as 82.3% *in vitro* and 84.9% *ex vivo*. Cavallito and others (19) reported the plasma protein binding of PYR as 87%. The authors of

those reports did not provide albumin concentrations, but it was assumed normal. The results reported here do not disagree with theirs, but the incompleteness of their method of reporting supports the purpose of this dissertation.

6.5.6 Plasma protein binding

Ahmad (1) has shown that PYR displaces dapsone from dapsone's binding site which implies that both drugs bind to a specific site on albumin.

However, the extremely poor fits to the Scatchard (106) and Blanchard (9) models and the less than perfect fits to the Larsen (82) model show that all of the assumptions of the site approach to drug-protein interactions have not been fulfilled. Moreover, the graph of percent free PYR versus plasma PYR concentration (Fig. 17a) shows that the drug does not obey the law of mass action at low concentrations. This suggests that the more flexible Klotz analysis is more appropriate because it does not assume the presence of sites and it can be applied in nonsaturable binding situations. The differences between the Klotz (stoichiometric) approach and the site approach have been discussed in Sections 2.5, 2.6 and 2.7 of Chapter 2.

More likely, due to the low water solubility of PYR, it is avoiding the plasma water in favor of hydrophobic association with the plasma proteins (albu-

min or lipoproteins). This is a solubility phenomenon rather than a specific binding to albumin and is the most likely reason that PYR does not obey the law of mass action in Study 1.

Although binding data for PYR has been limited in the literature, a thorough examination of the binding of metoprine, a structurally related compound, has been done and is reviewed in Chapter 2 (Table 3). If the binding of PYR is like the binding of metoprine, it is possible that with the conditions of Study 1, binding to lipoproteins disturbed the interaction of PYR with albumin at the low levels of PYR. The affinity of metoprine for β-lipoprotein was much greater than the affinity for albumin when affinities were determined in pure protein fractions. However, binding of metoprine to lipoproteins was not apparent in whole plasma. Metoprine is more lipophilic than PYR (19) and may have a stronger attraction for lipoproteins for that reason.

There are three reasons for attributing the total binding of PYR in whole plasma to binding to albumin: (1) the more lipophilic compound (metoprine) did not bind to lipoproteins in the presence of albumin in whole plasma, (2) PYR did not bind to AAG at normal AAG levels, and (3) PYR binding in a solution of pure albumin was a little greater than binding in whole plasma.

However, binding to albumin, which was assumed to

be the major binding protein after finding no binding to AAG, may be still be confounded by binding to lipoproteins. The lipoprotein interaction may be confounding albumin binding at all drug levels, but is noticable only at low drug levels. The lipoproteins play an indeterminant role in the solubility phenomenon.

The data from Studies 2 and 3 do not show the trend of increased binding with increasing plasma concentration. They were collected in plasma that had been diluted with buffer, so that all the proteins would be more dilute. This could have influenced the binding of PYR to the proteins.

Solubility phenomena in drug-protein interactions have been reported by others (92, 98) and will be discussed shortly.

Data from Studies 1, 2, and 3 were fit with the Blanchard, Larsen, Scatchard, double reciprocal, and Klotz equations. Although the double reciprocal plot produced what looked like a straight line, the parameter estimates from linear regression of the data were meaningless (negative values for numbers of sites), and the problems associated with this plot that have been reviewed in Chapter 2 were revealed. The data were transformed in a way that covered up errors and fluctuations in the data so that the true binding interaction was lost. The double reciprocal plot should not be used

in protein binding except for initial estimates when only limited data is available.

The Blanchard fits were extremely poor. The Larsen equation is robust, but even so, did not show improvements over the fits to the Klotz equation, probably because it had the same number of parameters (82). Data from Studies 1 and 2 were fit well by the Larsen equation, but data from Study 3 were not. The parameter estimates for K_1 and K_2 were similar to the ones from the fit to the Klotz equation. For the Larsen fits, the parameter estimates for fits to data from Study 1 had standard errors (SE) in percent that were 8.3 and 83% of the estimates. For data from Study 2, the SE of the estimates were 3 and 16.5% of the estimated parameters. For fits to the data from Study 3, the estimates were very different compared to the estimates for the other data sets and the SE values were 15.7 and 19.2% of the estimates of K_1 and K_2. These fits are shown in Appendix B.

The Klotz or stoichiometric approach made the most sense for reasons mentioned above. Fits to the Klotz equation seemed more reasonable that the fits to the other equations.

Comparisons of a one site and two site model for each set of data revealed that only the data from Study 1 were fit better by a one site model. As stated

before, this data had the lowest concentrations of PYR (Table 32), demonstrated a solubility phenomenon, and did not obey the law of mass action. Therefore, it is not appropriate to fit data from Study 1 to any equation based on the law of mass action.

Higher concentrations of PYR in the other studies did not show signs of a solubility phenomenon according to the graph in Figure 17b. According to Klotz (76), more accurate parameter estimates require higher concentrations. The results of the fits and the weighting factors that produced the best fits are given in Tables 34-36.

On the other hand, a comparison of the binding isotherms in Figures 21, 23, and 25 reveal that data may not have been collected past the inflection point if there is one (82). In other words, the saturation of albumin binding sites may not have been approached. A differential curve, a plot of the slope versus change in free drug, was not entirely successful because of the irregularity of the data, but did seem to reveal that data from Studies 2 and 3 had gone past inflection points and that saturation had been approached. Study 3 had been designed to include the highest concentrations of PYR that solubility would permit and the lowest albumin concentrations that practical circumstances would allow. Unfortunately, the low albumin concentra-

tions may have disturbed the true binding phenomenon and resulted in the poorer parameter estimates (Tables 33 and 36).

If the parameter estimates for each set of data are compared, it appears that there are two stoichiometric binding constants K_1 at 2.82 X 10^4 M^{-1} and K_2 at 1.74 X 10^4 M^{-1} from the nonlinear fits of the data from Study 2. The estimates from fits to data only from Study 2 have been reported because data from Study 1 did not follow the law of mass action and data from Study 3 had other errors.

The fits agree with the estimates from the equation K_1 = (bound/free)/albumin for small concentrations of PYR. The averages were 2.91 X 10^4 and 2.84 X 10^4 M^{-1} for data from Study 1 and Study 2, respectively.

Similar inconsistencies with the law of mass action have been reported elsewhere (92, 98, 104). The interaction with tetracycline was assumed to be a result of a dissolution of tetracycline in a lipophilic portion of the lipoprotein molecule, rather than an association with specific binding sites. The tetracycline binding to lipoproteins increased as the concentration of tetracycline increased, and it was remarkably similar to the graph of the distribution of tetracycline between chloroform and Krebs phosphate buffer (98).

The quinidine-lipoprotein interaction was not the

same as the drug's distribution between buffer and chloroform, in contrast to the tetracycline work (92). Nilsen (92) found a decreasing binding ratio bound/free with increasing concentration of quinidine in accordance with the law of mass action except for with lipoproteins.

This positive cooperativity seems to dominate in the low concentrations of PYR while the albumin-PYR interaction following the law of mass action probably blurs this effect at higher PYR concentrations (PYR 1.6 X 10^{-4} M) in Study 3.

Sager et al. (104) have shown that propranolol is also not bound, but distributed to lipoproteins (similar to tetracycline) independent of propranolol concentration. The binding to plasma proteins for this data plotted according to Scatchard looks very much like their plot of the binding of propranolol to lipoproteins. Both have a large amount of scatter and a slope not significantly different from zero.

There is an alternative way of portraying the binding of PYR to protein in these studies. If one considers the binding as a partitioning phenomenon between the aqueous plasma water and the hydrophobic protein, it is possible that the partition coefficient, Pyr on protein/PYR in water, changes with the increasing concentration of PYR and results in increased percent

binding with increased PYR concentration (Fig. 17a). It is also possible that the greatest change occurs at the lower levels of PYR and is reflected by changes in the affinity for the protein. Changes in affinity for the protein can be seen in data from Study 3 and Table 33, where the estimates of the affinity constants are much higher than in the other two sets of data (Studies 1 and 2) where the protein levels were lower. Since the affinity is low (K_1 values are low), it is possible that nonspecific binding rather than specific binding is able to predominate at low concentrations. It is possible that nonspecific binding to lipoproteins is enough to alter the binding to albumin at low concentrations.

The pH dependency of the protein binding depicted in Figure 15 suggests that there is ionic binding to protein. This may not be the case, however, because both acids and bases show pH dependency in protein binding in the same direction (16). More likely, there is a change in the conformation of the albumin molecule that is responsible for the pH dependency of binding.

6.6 RBC partitioning and binding

6.6.1 Partitioning from buffer

Washing packed cells was necessary to remove the plasma albumin in my some of my studies, but not all. There have been reports that washing cells may alter the physiologic binding properties of RBCs (52, 40).

Consequently, the binding of PYR to RBCs was determined in whole blood assuming RBCs to be the majority of the cellular fraction of blood. The observed interaction between PYR, proteins, and RBCs should therefore reflect conditions in blood. This procedure allowed plasma proteins, plasma water, and the presence of other cells and lipids to contribute to the distribution between plasma and cells.

The basic lipophilic compound PYR with pKa 7.13 would be expected to penetrate the RBC membrane (108). Accordingly, the pH-gradient across the membrane should influence the distribution between the unbound drug in the plasma water and the interior cellular water.

Assuming a pH of 7.26 inside the RBC (122) and 7.4 in the plasma, a distribution ratio of 1.13 can be calculated from Jacobs' equation. This type of distribution should produce a straight line parallel to and at a distance of 1.13 from the abscissa in an RBC/buffer ratio graph similar to the one in Figure 27 at pH 7.4. The actual ratios in Figure 27 demostrate a 4-6 times higher ratio than expected. This strongly suggests than additional binding takes place that influences the distribution of PYR into cells. Binding to hemoglobin inside the cell and binding to the cell membrane are possible contributors to this increased ratio.

Hemoglobin has a hydrophobic cage around its heme

center (127). It is not surprising that the lipophilic PYR would associate with it. There did not appear to be any concentration dependency of PYR binding to hemoglobin (Table 37). Binding to hemolysate was 42.5% which would not account for all of the uptake by RBCs. The mean difference between the theroretically predicted and the observed ratios was 4.13. On average, there was 4 times as much bound to the cell or bound inside the cell than unbound inside the cell. Therefore, the RBC membranes must bind PYR.

When plasma was removed and RBCs suspended in buffer, there was a profound effect of buffer pH on partitioning of PYR in the RBCs. Using the equation by Jacobs, the theoretical ratios at each pair of pH values were calculated and compared to the observed values. Linear regression on these values revealed different equations for the lines. This analysis assumed that the buffer pH did not affect the theoretical RBC pH. More likely, however, the pH of the RBCs did change slightly and for this reason, the observed data does not match the theoretical data. The main reason the observed does not match the theoretical data is the binding inside and to the cells.

The uptake of PYR by RBCs from buffer in which binding was absent showed a relationship to buffer pH (Fig 27) and did not show any evidence of saturability.

The average RBC/buffer ratio was 5.16 (11.8% CV, n=2) at pH 7.4.

6.6.2 Influence of protein binding on RBC uptake

PYR accumulated rapidly in RBCs which had been washed and resuspended in buffer to yield RBC/buffer ratios greater than 1. However, the presence of plasma markedly reduced RBC uptake. The average RBC/plasma ratio was 0.42 (10% CV, n=5). This indicates that the plasma binding of PYR diminishes the RBC uptake by reducing the concentration of unbound drug. Confirmation of this hypothesis is provided by the experiments in which plasma binding was decreased by dilution of plasma with buffer.

The most common assumption is that RBC distribution to the blood cells is determined solely by the concentration of unbound PYR in the plasma (65). Experiments in this report had shown that albumin was the main binding protein in the plasma, so it should be the main determinant of RBC partitioning in whole blood. The manner in which the plasma was diluted would have diluted the other proteins equally, and thus, it cannot be determined from any one experiment that albumin was the sole determinant of free fraction. The good correlation between albumin level and free PYR from several different experiments using different plasma sources does support the original hypothesis however.

The advantages of determining unbound fraction of drug from the RBC/plasma ratio as outlined by many authors (11, 53, 54, 65, 81) do not provide a great advantage over the "tedious" ED methods of measuring plasma binding in the clinical setting. Fremstad (52) has commented that for the application of this method, if the distribution of drug to RBCs is directly and linearly related to the free concentration in the plasma and if binding properties of the RBCs are constant and predictable in different pathological conditions, each drug would have to be thoroughly investigated before such "simple" methods could be used. To date, there is no drug that has been that thoroughly investigated. Garrett has a point however, in cases where the usual methods of ultrafiltration and ED do not work, his "method of variable plasma concentrations" in RBC suspensions to yield percent protein bound may be necessary (54).

There are more disadvantages than advantages in determining unbound fraction of drug in the plasma from the partitioning of the drug into RBCs. The validation of that technique for any individual drug would be more tedious than using ED to determine the fraction of unbound drug. Working with RBCs and accounting for mass balance are difficult and add to the reasons why the technique using partitioning into RBCs as a protein

binding screening procedure has not been accepted. It has remained obscure in the literature since its introduction in 1973.

While on this topic, it would not be recommended that ED with 1 ml Spectrum cells be used for the study of RBC uptake. The RBCs are too viscous to manipulate and difficult to remove from these type of cells. At least two authors have used ED for the study of RBC uptake (40, 87).

Chapter 7

Conclusions

7.1 Analytical methodology

The assay presented in this work is adequate for pharmacokinetic studies. It has been applied to the study of protein binding and RBC partitioning and binding. The assay is relatively simple and should easily be reproduced in other labs. It requires a 5 micron C_{18} column and a UV detector with a 254 filter. Due to the near-neutral pH of the mobile phase, a silica saturator column is recommended. The mobile phase consisted of methanol-acetonitrile-phosphate buffer (K salts, 0.03 M, pH 6.95) in 45:15:40 v/v proportions. The flow rate was 1.6 ml/min.

Extraction of PYR from plasma required 7 ml of methylene chloride. Extraction from RBCs required 12 ml of a 1:3 combination of methylene chloride and n-butyl chloride. Mean recoveries from plasma and RBCs were between 81.9 and 85.4% and were not concentration dependent. Extraction of PYR from RBCs was quantitative.

NAPA was used as an internal standard for the plasma curves. NAPA recovery from plasma was 82%. No

internal standard was used for the RBC or buffer curves. Solutions of PYR in buffer could be injected directly onto the HPLC system without an extraction step. Using an internal standard for buffer curves introduced more error than necessary because it was a direct injection technique. All solutions of PYR were found to stable for the duration of the study.

Two calibration curves were used for each matrix. The range of the calibration curves were 24-140 ng/ml and 140-1000 ng/ml. They were linear with correlation coefficients greater than 0.995. The limit of detection was 24 ng/ml for each matrix.

Retention times were 4.5 and 5.35 minutes for the internal standard and PYR respectively.

The two biggest problems with this assay were the binding of PYR to glass and the dissolution of the column packing because of the pH of the mobile phase. In the future, using an HPLC column with a higher carbon load would be recommended. Using the cartridge type of column which prevents the re-packing of voids in the column packing would not be recommended.

7.2 Medium pH and theoretical cell/medium ratio

There is a rapid and significant rise in pH of plasma upon exposure to the atmosphere because of the loss of CO_2. The different additives in Vacutainers™ are partly responsible for the different degree to which

pH changes in plasma collected in Vacutainers™. Heparin causes the fastest rise in pH of the additives tested. It also produces a significantly different zero-time pH according to ANOVA ($p<0.0001$) and Tukey's studentized range test (HSD) at $\alpha=0.001$. The average zero-time plasma pH in the three Vacutainers™ tested was 7.36 (0.4% CV, n=15). The tubes containing sodium heparin had an average pH of 7.50 (0.6% CV, n=5).

RBCs tend to maintain their physiologic pH. Thus, when measuring RBC/plasma concentration ratios, it is necessary to prevent the change in pH, to adjust it to normal pH, or to report the pH of the medium. Otherwise, cell/medium ratios will be falsely low for acidic compounds and falsely high for basic compounds with the magnitude of the error depending on the pKa of the compound. For a lipophilic drug like PYR for which the partitioning time is short, significant partitioning is possible while processing blood to yield cell/medium ratios which would be in error. Ratios could become technician dependent if standardized procedures were not followed. The most extreme case would be when one technician who removed the stoppers of Vacutainers™ on rows of tubes before separation of the plasma was paired with another technician who removed the stopper and the plasma from one tube at a time.

Ratios of drugs across the RBC membrane are

affected by the pH of the medium because the distribution of drugs across a semi-permeable membrane is a pH-dependent phenomenon. The large volumes of distribution for basic drugs supports the idea that basic drugs tend to leave the plasma compartment and distribute to regions of the body with lower pH such as the tissues and blood cells.

7.3 Protein binding of PYR

PYR was not bound to the dialysis cells nor membranes that were used in these studies. Volume shifts of fluid occurred, but they were not large (<10%). The use of isotonic buffer did not prevent volume shifts entirely. Statistical moment theory was used to determine that equilibrium between the two sides of the dialysis cells was reached in 300 minutes.

The pH of the plasma influenced the protein binding of PYR as seen in Figure 15, although there was not a statistically significant difference between binding at pH 7.4 and pH 8.0.

There was a statistically significant ($p<.03$) difference in protein binding at two therapeutic levels of PYR, 118 and 363 ng/ml. There was more percent free PYR at the higher total PYR concentration. In one protein binding experiment in which higher PYR concentrations and lower albumin concentrations were used, there was a concentration dependent protein binding occurring in

opposition to the law of mass action (Figure 17a) where there was less free drug at higher total drug levels. This artifact was due to the solubility phenomenon seen in data from Study 1 and was not seen in the two other binding studies.

There was a significant effect of albumin concentration on the plasma protein binding of PYR ($p<0.0001$, $R^2 = 0.797$, $R = 0.893$). For whole plasma, linear regression yielded the equation percent free PYR = -0.467(albumin in g/L) + 23.5. The high y-intercept suggests binding to other constituents of the plasma besides albumin. However, the R^2 value shows that most of the data is explained by albumin binding.

There was no difference in the percent free PYR in plasma collected in three different types of Vacutainers™ at 1000 ng/ml. The average unbound concentration was 6.9% (37% CV, n=10) at albumin 41.8 g/L. This is the same as 93.1% bound.

Binding to pure human albumin in isotonic phosphate buffer was 86.5%. This was slightly more bound that predicted by the equation above (83.1%). This means that the equation for binding in plasma predicts well for pure albumin binding in buffer. This supports the conclusion that binding to proteins other than albumin is negligible.

Binding to 8.4×10^{-5} M AAG was 9.56% and to 1.3 X

10^{-5} M AAG was zero. Binding to AAG would not be expected in normal plasma or serum according to these results.

At low concentrations, PYR does not follow the law of mass action in its interaction with plasma proteins. For this reason, it is not possible to analyze all of these data using standard protein binding equations.

At higher concentrations, PYR follows the law of mass action. Binding to albumin is presumed to be most prevalent and binding to other proteins is assumed negligible. Data analysis revealed better fits to two binding sites; however, in both cases large standard errors were found for parameter estimates for the second stoichiometric binding constant. The residuals revealed patterns that indicate an ill-conditioned model. Saturation of the albumin binding capacity was not reached.

Honore and Brodersen's (63) simplification of the stoichiometric equation where (bound/free)/albumin concentrations in molar units = K_1 at low concentrations gave as good estimation of K_1 as did the nonlinear fits of data sets 38 and 41. From this approximation, the average estimates for K_1 are 2.91 X 10^4 M^{-1} (15% CV) for data from Study 1 and 2.84 X 10^4 M^{-1} (8.8% CV) for data from Study 2.

From the nonlinear fits of data 41, the first and second classical stoichiometric binding constants for

PYR are 2.83 X 10^4 M^{-1} and 1.74 X 10^4 M^{-1}.

The double-reciprocal plot should not be used to find parameter estimates for drug-protein binding interactions. The Blanchard and Larsen equations do not offer any advantage over the established stoichiometric approach of Klotz. The Scatchard equation and plot would be satisfactory only for ideal data without cooperativity, except that it incorrectly assumes no error in the "independent" variable axis and this results in under-estimation of the slope of the regresson line and erroneous parameter estimates. The gross manipulation of the data makes the Scatchard plot a poor choice since methods for nonlinear fitting of the data exist. Except in ideal cases, the parameter estimates from the Scatchard analysis do not reflect actual binding site affinity constants (77).

The reason that the Scatchard equation and plot are still popular in the literature is that this linear equation had been firmly established as "the method of analysis" before the arrival of the computers on which nonlinear regression can easily be done. Unfortunately, departure from the use of the Scatchard equation has been slow. Klotz's stoichiometric approach is clearly superior in that it (1) requires less data manipulation and hence covers up fewer poorly collected data, (2) has fewer restrictive assumptions, and (3) does not ignore

the basic rules of statistical analysis. The main advantage of the Klotz plot is that it shows immediately whether or not sufficient data has been collected (by the presence of an inflection point). Whereas, from data on linearized plots, one cannot tell if enough data has been collected and many errors are covered up.

In summary, linear expressions for protein binding suffer from the problems discussed in Section 2.6. Two important problems discussed were poor parameter estimates arising from ignoring error in the x-axis and inability to tell if enough data has been collected. In the nonlinear Klotz plot, one can assume that little error exists in the variable on the x-axis compared to the variable on the y-axis and one can tell that enough data has been collected. Thus, Klotz's approach is recommended with the assumption of integer values for n.

7.4 RBC partitioning and binding

The present in vitro study shows that upon incubation with human blood, PYR was preferentially bound to plasma proteins. However, when plasma (and proteins) were replaced with buffer, the PYR concentration was increased four times over the normal concentration in RBCs at normal hematocrit.

The average percent bound to hemolysate (Hb 1.57 X 10^{-3} M) was 42.5% (19% CV, n=10) at several levels of PYR. There was no concentration dependency in PYR bind-

ing to hemolysate. At about half the normal Hb concentration inside the cells, Hb binding does not account for all the PYR inside the cells. This would be true for the normal Hb concentration also.

When washed RBCs were suspended in buffer of varying pH values from 6.7 to 8.0, there was a pronounced effect of buffer pH on the partitioning of PYR into the cells (Figure 27). The RBC/buffer concentration ratio at pH 7.4 was 5.16 (12% CV, n=2). The average difference between the observed and theoretical RBC/buffer ratios was 4.14 (20% CV, n=7) for all the data. Four times as much PYR was found inside the cells or bound to the cells as was predicted to be unbound inside the cells. Binding to hemoglobin did not entirely account for this high ratio. Therefore, PYR binds to the RBC membrane. Alteration of the plasma binding by dilution with isotonic phosphate buffer showed that uptake into RBCs was proportional to the free drug concentration. The average RBC/plasma ratio was 0.42 (10.2% CV, n=5).

7.5 Final comments

These studies confirm that final drug concentration, albumin concentration, and pH make a difference in protein binding and RBC partitioning. However, albumin concentrations, pH, and final drug concentration are rarely reported in the literature. Many other researchers have stated that protein binding as a per-

centage does not stand alone. A full description of the conditions of the study is as important as the percent bound and a mention of the technique (e.g. ED or ultrafiltration) used to find the value. The mimicking of physiologic conditions cannot be assumed when all that is reported is percent bound. Albumin concentration and pH are two of the most important experimental conditions in protein binding studies, yet they are missing from most reports.

Data analysis from studies of drug-protein binding and measuring RBC levels of drugs have something in common. In both cases, sources of errors are compounded by data manipulation. For instance, the axes in the Scatchard plot are (bound drug concentration/protein concentration)/unbound drug concentration versus bound drug concentration/protein concentration. Each concentration was measured by an assay that has a small amount of error. Then the concentrations are converted to molar concentrations. The latter calculation results in rounding error.

Many of the analytical artifacts reviewed in Chapter 2 introduce error in measuring drug concentrations in RBCs. Experience has shown that hemolysis is the most common problem in determining RBC levels of drugs. If the RBCs in the original whole blood sample hemolyze, both the plasma and the RBC levels cannot be determined

accurately.

Errors result when RBC drug levels are measured in the way presented here. Error is introduced by measuring the hematocrit of the whole blood and the hematocrit of the packed cells to account for trapped plasma. The difficulty in measuring the volume of viscous RBCs results in error in assaying for drug concentration in RBCs. Error from assaying drug in the plasma is also introduced when correcting the RBC drug level for drug in the trapped plasma in the packed RBCs. The fact that there are many more sources of error when measuring RBC drug levels compared to plasma drug levels is evident when comparing Figures 33-36. The relationship between plasma and whole blood PYR levels shows much less error than the relationship between RBC and whole blood PYR levels.

Therefore, it is recommended that when determining the RBC levels of drugs, it is better to measure the plasma and whole blood drug levels, take one hematocrit measurement and subtract the plasma drug level from the whole blood drug level to find the RBC drug level. This procedure will establish mass balance. In addition, it is necessary to validate that the extraction of drug from the whole blood represents equal extraction from the components of blood (cells as well as plasma).

Chapter 8

Prospectus

To extend this work, the author would like to examine the binding of PYR to purified defatted albumin, to several purified plasma lipoproteins, and several concentrations of hemoglobin for the purposes of stoichiometric data analysis.

In addition, the author would like to apply the RBC partitioning techniques to examination of the blood from patients receiving PYR for malaria and toxoplasmosis.

Bibliography

Bibliography

1. Ahmad RA, Rogers HJ. Pharmacokinetics and protein binding interaction of dapsone and pyrimethamine. Br J Clin Pharmacol 1980;10:519-524.

2. Ahmad RA, Rogers HJ. Salivary elimination of pyrimethamine. Br J Clin Pharmacol 1981;11:101-102.

3. Ahtee L, Paasonen MK. Distribution of some phenothiazines in red blood cells and platelets. J Pharm Pharmac 1966;18:126-128.

4. Altmayer P, Garrett ER. Plasmolysis, red blood cell partitioning and plasma protein binding of etofibrate, clofibrate, and their degradation products. J Pharm Sci 1983;72:1309-1318.

5. Atwood JG, Schmidt GJ, Slavin W. Improvements in liquid chromatography column life and method flexible by saturating the mobile phase with silica. J Chromatogr 1979;171:109-115.

6. Beermann B, Hellstrom K, Lindstrom B, Rosen A. Binding-site interaction of chlorthalidone and acetazolamide - two drugs transported by red blood cells. Clin Pharmacol Ther 1975;14:424-432.

7. Bergqvist Y, Domeij-Nyberg B. Distribution of chloroquine and its metabolite desethyl-chloroquine in human blood cells and its implication for the quantitative determination of these compounds in serum and plasma. J Chromatogr 1983;272:137-148.

8. Bickel MH. Binding of chlorpromazine and imipramine to red cells, albumin, lipoproteins and other blood components. J Pharm Pharmacol 1975;27:733-738.

9. Blanchard J, Fink WT, Duffy JP. Effect of sorbitol on interaction of phenolic preservatives with polysorbate 80. J Pharm Sci 1977;66:1470-1473.

10. Borga O, Piafsky KM, Nilsen OG. Plasma protein

binding of basic drugs I. Selective displacement from α_1-acid glycoprotein by tris(2-butoxyethyl)phosphate. Clin Pharmacol Ther 1977;22:539-544.

11. Borondy P, Dill WA, Chang T, Buchanan RA, Glazko AJ. Effect of protein binding on the distribution of 5,5-diphenylhydantoin between plasma and red cells. Ann NY Acad Sci 1973;226:82-87.

12. Bower S. The uptake of fentanyl by erythrocytes. J Pharm Pharmacol 1982;34:181-185.

13. Boxenbaum HG, Riegelman S, Elashoff RM. Statistical estimations in pharmacokinetics. J Pharmacokin Biopharm 1974;2:123-148.

14. Briggs CJ, Hubbard JW, Savage C, Smith D. Improved procedure for the determination of protein binding by conventional equilibrium dialysis. J Pharm Sci 1983;72:918-921.

15. Brodersen R, Honore B, Larsen FG. Serum albumin - a non-saturable carrier. Acta Pharmacol et Toxicol 1984;54:129-133.

16. Brørs O, Nilsen OG, Sager G, Sandnes D, Jacobsen S. Influence of pH and buffer type on drug binding in human serum. Clin Pharmacokin 1984;9:85-86.

17. Brørs O, Jacobsen S. pH lability in serum during equilibrium dialysis. Br J Clin Pharmacol 1985;20:85-88.

18. Brown JE, Kitchell BB, Bjornsson TD, Shand DG. The artifactual nature of heparin-induced drug protein-binding alterations. Clin Pharmacol Ther 1981;30:636-643.

19. Cavallito JC, Nichol CA, Brenckman WD, DeAngelis RL, Stickney DR, Simmons, Sigel CW. Lipid-soluble inhibitors of dihydrofolate reductase I. Kinetics, tissue distribution, and extent of metabolism of pyrimethamine, metoprine, and etoprine in the rat, dog, and man. Drug Met Disp 1978;6:329-337.

20. Chaplin H, Mollison, PL. Correction for plasma trapped in the red cell column of the hematocrit. Blood 1952;7:1227-1238.

21. Coleman MD, Edwards G, Mihaly GW, Howells RE, Breckenridge AM. High performance liquid chromatography

method for the determination of pyrimethamine and its 3-N-oxide metabolite in biological fluids. J Chromatogr 1984;308:363-369.

22. Coleman MD, Mihaly GW, Edwards G, Howells RE, Breckenridge AM. The disposition of pyrimethamine base and pyrimethamine pamoate in the mouse: effect of route of administration. Biopharm Drug Disp 1986;7:173-182.

23. Coleman MD, Mihaly GW, Edwards G, Ward SA, Howells RE, Breckenridge AM. Pyrimethamine pharmacokinetics and its tissue localization in mice: effect of dose size. J Pharm Pharmacol 1985;37:170-174.

24. Coleman MD, Mihaly GW, Ward SA, Edwards G, Howells RE, Breckenridge AM. The sustained release of pyrimethamine base or pyrimethamine pamoate from a biodegradable injectable depot preparation in mice. J Pharm Pharmacol 1985;37:878-883.

25. Cotham RH, Shand D. Spuriously low plasma propranolol concentrations resulting from blood collection methods. Clin Pharmac Ther 1975;18:535-538.

26. Cruze CA, Meyer MC. Binding of salicylate and sulfathiazole by whole blood constituents. J Pharm Sci 1976;65:33-37.

27. Currie DJ. Estimating Michaelis-Menten parameters: bias, variance, and experimental design. Biometrics 1982;38:907-910.

28. Davison C. Protein binding. In: LaDu BN, Mandel HG, Way GL, eds. Fundamentals of Drug Metabolism and Drug Disposition. Baltimore: Williams and Wilkins Co., 1971:63-75.

29. Daylily SO, Poznanski WJ, Smith FM. Effects of contact with Vacutainer tube stoppers on the estimation of quinidine in serum and plasma. Clin Biochem 1980;13:297-300.

30. DeAngelis RL, Simmons WS, Nichol CA. Quantitative thin-layer chromatography of pyrimethamine and related diaminopyrimidines in body fluids and tissues. J Cromatogr 1975;106:41-49.

31. Derendorf H, El-Koussi AEA, Garrett ER. Electrochemical chromatographic determinations of morphine antagonists in biological fluids, with applications. J Pharm Sci 1984;73:621-624.

32. Derendorf H, Garrett ER. High-performance liquid chromatographic assay of methadone, phencyclidine, and metabolites by postcolumn ion-pair extraction and on-line fluorescent detection of the counterion with applications. J Pharm Sci 1983;72:630-635.

33. Diem K, Lentner C, eds. Scientific Tables, 7th ed. Basle: Ciba-Geigy Ltd., 1970:562-563.

34. Dieterle W, Wagner J, Faigle JW. Binding of chlorthalidone (Hygroton^{R}) to blood components in man. Eur J Clin Pharmacol 1976;10:37-42.

35. Dowd JE, Riggs DS. A comparison of estimates of Michaelis-Menten kinetic constants from various linear transformations. J Biol Chem 1965;240:863-869.

36. Draper NR, Smith H. Applied Regression Analysis, 2nd ed. New York: John Wiley and Sons, 1981:122-124.

37. Drayer DE, Strong JM, Jones B, Sandler A, Reidenberg MM. In vitro acetylation of drugs by human blood cells. Drug Met Disp 1974;2:499-505.

38. Edstein M. Quantification of antimalarial drugs I: Simultaneous measurements of sulphadoxine, N_4-acetylcuphadoxine, and pyrimethamine in human plasma. J Chromatogr 1984;305:502-507.

39. Edstein M. Quantification of antimalarial drugs II: Simultaneous measurement of dapsone, monoacetyldapsone, and pyrimethamine in human plasma. J Chromatogr 1984;307:426-431.

40. Ehrnebo M, Agurell S, Boreus LO, Gordon E, Lonroth U. Pentazocine binding to blood cells and plasma proteins. Clin Pharmacol Ther 1974;16:424-429.

41. Ehrnebo M, Odar-Cederlof I. Binding of amobarbital, pentobarbital, and diphenylhydantoin to blood cells and plasma proteins in healthy volunteers and uraemic patients. Eur J Clin Pharmacol 1975;8:445-453.

42. Ellison G, Straumfjord JV, Hummel JP. Buffer capacities of human blood and plasma. Blood 1958;4:452-461.

43. Evans GH, Nies AS, Shand DG. The disposition of

propranolol III. Decreased half-life and volume of distribution as a result of plasma binding in man, dog and rat. J Pharmacol Exp Ther 1973;186:114-222.

44. Evans GH, Shand DG. Dispositon of propranolol VI: Independent variation in steady-state circulating drug concentrations and half-life as a result in plasma drug binding in man. Clin Pharmacol Ther 1973;14:494-500.

45. Falco EA, Goodwin LG, Hitchings GH, Rollo IM, Russell PB. 2,4-diaminopyrimidines - a new series of antimalarials. Br J Pharmacol Chemother 1951;6:185-200.

46. Fletcher JE, Ashbrook JD, Spector AA. Computer analysis of drug-protein binding data. Ann NY Acad Sci 1973;226:69-81.

47. Fletcher JE, Spector AA, Ashbrook JD. Analysis of macromolecule-ligand binding by determination of stepwise equilibrium constants. Biochemistry 1970;9:4580-4587.

48. Fleuren HLJ, van Rossum JM. Nonlinear relationship between plasma and red blood cell pharmacokinetics of chlorthalidone in man. J Pharmacokin Biopharm 1977;5:359-375.

49. Fraser JRE, Lovell RRH, Nestel PJ. The production of lipolytic activity in the human forearm in response to heparin. Clin Sci 1961;20:351-356.

50. Frazer A, Secunda SK, Mendels J. A method for the determination of sodium, potassium, magnesium, and lithium concentrations in erythrocytes. Clin Chim Acta 1972;36:499-509.

51. Fremstad D. Reduced binding of quinidine in plasma from Vacuatiners. Clin Pharmacol Ther 1977;20:120.

52. Fremstad D. Increased plasma binding and decreased blood cell binding of quinidine in blood from anuric rats. Acta Pharmacol Toxicol 1977;41:148-160.

53. Garrett ER, Hunt CA. Physicochemical properties, solubility, and protein binding of Δ^9-tetrahydrocannabinol. J Pharm Sci 1974;63:1056-1064.

54. Garrett ER, Lambert HJ. Pharmacokinetics of trichloroethanol and metabolites and interconversions among variously referenced pharmacokinetic

parameters. J Pharm Sci 1973;62:550-572.

55. Gerson B, Anhalt JP. High-pressure liquid chromatography and therapeutic drug monitoring. Chicago: Am Soc Clinical Pathologists, 1980.

56. Giacomini KM, Wong FM, Tozer TN. Correction for volume shift during equilibrium dialysis by measurement of protein concentration. Pharmaceu Res 1984;1:179-181.

57. Gibaldi M, Perrier D. Pharmacokinetics. In: Swarbrick J ed., Drugs and the Pharmaceutical Sciences, vol. 15, 2nd ed. New York: Dekker, 1982.

58. Gloor R, Johnson EL. Practical aspects of reversed phase ion pair chromatography. J Chromatogr Sci 1977;15:413-423.

59. Gram HC. Composition and physical properties of normal human blood: compilation of values from literature. Am J Med Sci 1924;168:511-526.

60. Guentert TW, Oie S. Factors influencing the apparent protein binding of quinidine. J Pharm Sci 1982;71:325-328.

61. Ha HR, Vozeh S, Follath F. Evaluation of a rapid ultrafiltration technique for determination of quinidine protein binding and comparison with equilibrium dialysis. Ther Drug Monit 1986;8:331-335.

62. Hinderling PH, Bres J, Garrett ER. Protein binding and erythrocyte partitioning of disopyramide and its monodealkylated metabolite. J Pharm Sci 1974;63:1684-1690.

63. Honore B, Brodersen R. Albumin binding of anti-inflammatory drugs: utility of a site-oriented vs. a stoichiometric analysis. Mol Pharmacol 1984;25:137-150.

64. Hu OY-P, Curry SH. Calculation of fraction bound in equilibrium dialysis with specila reference to drug losses by decomposition and adsorption. Biopharm Drug Disp 1986;7:211-214.

65. Hughes IE, Ilett KF, Jellett LB. The distribution of quinidine in human blood. Br J Clin Pharmacol 1975;2:521-525.

66. Hughes IE, Jellett LB, Ilett KF. The influence of various factors on the in vitro distribution of haloperidol in human blood. Br J Clin Pharmacol 1976;3:285-288.

67. Isaacs VE, Schoenwald RD. Binding of quinidine to a RBC hemolysate preparation. J Pharm Sci 1974;63:1267-1271.

68. Jacobs MH. Some aspects of cell permeability to weak electrolytes. Cold Spring Harbor Symp Quant Biol 1940;:30-39.

69. Jellett LB, Shand DG. Uptake of propranolol by washed human red blood cells. Pharmacologist 1973;15:245.

70. Jones CR and Ovenell SM. Determination of plasma concentrations of dapsone, monoacetyl dapsone and pyrimethamine in human subjects dosed with maloprim. J Chromatogr 1979;163:179-185.

71. Jones CR, Ryle PR, Weatherly BC. Measurement of pyrimethamine in human plasma by gas-liquid chromatography. J Chromatogr 1981;224:492-496.

72. Keen P. Effect of binding to plasma proteins on the distribution, activity, and elimination of drugs. In: Brodie, BB ed., Handbook of Experimental Pharmacology, Berlin: Springer-Verlag, 1971;28:213-233.

73. Kessler KM, Leech RC, Spann JF. Blood collection techniques, heparin and quinidine protein binding. Clin Pharmacol Ther 1979;25:204-210.

74. Klotz IM. The application of the law of mass action to binding by proteins - interactions with calcium. Archiv Biochem 1946;9:109-117.

75. Klotz IM. Numbers of receptor sites from Scatchard Graphs: facts and fantasies. Science 1982;217:1247-1249.

76. Klotz IM. Introduction to Biomolecular Energetics Including Ligand-Receptor Interactions. Orlando:Academic Press Inc., 1986:113-118.

77. Klotz IM and Hunston DL. Protein affinities for small molecules: conceptions and misconceptions. Arch Biochem Biophys 1979;193:314-328.

78. Klotz IM, Walker FM, Pivan RB. The binding of organic ions by proteins. J Am Chem Soc 1946;68:1486-1490.

79. Kornguth ML, Kunin CM. Uptake of antibiotics by human erythrocytes. J Inf Dis 1976;133:175-184.

80. Korten K, Miller KW. Erythrocyte-buffer partition coefficients of phenobarbital, pentobarbital, and thiopental support the pH-partition hypothesis. Can J Physiol Pharmacol 1979;57:325-328.

81. Kurata D, Wilkinson GR. Erythrocyte uptake and plasma binding of diphenylhydantoin. Clin Pharmacol Ther 1974;16:355-362.

82. Larsen CG, Larsen FG, Brodersen R. A two-constant equation for multiple albumin binding isotherms. J Pharm Sci 1986;75:669-671.

83. Levy G, Yacobi A. Effect of plasma protein binding on elimination of warfarin. J Pharm Sci 1974;63:805-806.

84. Luecke RH, Wosilait WD. Estimation of drug binding parameters. J Pharmacokin Biopharm 1986;14:65-78.

85. Maren TH, Robinson B, Palmer RF, Griffith ME. The binding of aromatic sulfonamides to erythrocytes. Biochem Pharmacol 1960;6:21-46.

86. Martin A, Swarbrick, J, Cammarata A. Physical Pharmacy - Physical Chemical Principles in the Pharmaceutical Sciences, 3rd ed. Philadelphia: Lea and Febiger 1983:335-337.

87. McArthur JN, Dawkins PD, Smith MJH. The binding of indomethacin, salicylate, and phenobarbitone to human whole blood in vitro. J Pharm Pharmacol 1971;23:32-36.

88. McGuire KP, Burrows GD, Norman TR, Scoggins BA. Blood/plasma distribution ratios of psychotropic drugs. Clin Chem 1980;26:1624-25.

89. Midskov C. High-performance liquid chromatographic assay of pyrimethamine, sulfadoxine, and its N_4-acetyl metabolite in serum and urine after ingestion of Suldox. J Chromatogr 1984;308:217-27.

90. Moffat AC, ed. Clarke's Isolation and Identification

of Drugs, 2nd ed. London:The Pharmaceutical Press, 1986.

91. Munson PJ, Rodbard D. LIGAND: A versitile computerized approach for characterization of ligand binding systems. Anal Biochem 1980;107:220-239.

92. Nilsen OG. Serum albumin and lipoproteins as the quinidine binding molecules in normal human sera. Biochem Pharmacol 1976;25:1007-1012.

93. Nyberg G, Martenssen E. Preparation of serum and plasma samples for determination of tricyclic antidepressants: effects of blood collection tubes and storage. Ther Drug Monit 1986;8:478-482.

94. Overton E. Uber die osmotischen eigenschaften der zelle in ihrer bedeutung fur die toxicologie und pharmacolgie. Z Phys Chem 1897;22:189-209.

95. Parsons DL, Vallner JJ. Scatchard plot analysis of ligand-erythrocyte interactions. J Pharm Sci 1978;67:1344-1345.

96. Pearson RD, Hewlett EL. Use of pyrimethamine-sulfadoxine (Fansidar) in prophylaxis against chloroquine-resistent Plasmodium falciparum and Pneumocystis carinii. Ann Intern Med 1987;106:714-718.

97. Potter JM, Self H. Cyclosporin A: Variation in whole blood levels related to in vitro anticoagulant usage. Ther Drug Monit 1986;8:122-125.

98. Powis G. A study of the interaction of tetracycline with human serum lipoproteins and albumin. J Pharm Pharmacol 1974;26:113-118.

99. Riggs DS, Guarnieri JA, Addelman S. Fitting straight lines when both varialbes are subject to error. Life Sci 1978;22:1305-1360.

100. Rochester CL, Gammon DE, Shane E, Bilezikian JP. A radioreceptor assay for propranolol and 4-OH-propranolol. Clin Pharmacol Ther 1980;28:32-39.

101. Roos A, Boron WF. Intracellular pH. Physiol Rev 1981;61:296-421.

102. Roos A, Hinderling PH. Protein binding and erythrocyte partitioning of the antirheumatic proquazone. J Pharm Sci 1981;70:252-257.

103. Rustad H. Correction for trapped plasma in microhematocrit determinations. Scand J Clin Lab Invest 1964;16:677.

104. Sager, Nilsen OG, Jacobsen S. Variable binding of propranolol in human serum. Biochem Pharmacol 1979;28:905-911.

105. SAS User's Guide: Statistics Version 5. Cary NC: SAS Institute, Inc., 1985.

106. Scatchard G. The attraction of proteins for small molecules and ions. Ann NY Acad Sci 1949;51:660-692.

107. Schanker LS, Johnson JM, Jeffrey JJ. Rapid passage of organic anions into human red cells. Am J Physiol 1964;207:503-508.

108. Schanker LS, Nafpliotis PA, Johnson JM. Passage of organic bases into human red cells. J Pharmacol Exp Ther 1961;133:325-331.

109. Schwartz DE, Weidekamm E, Mimica I, Heizmann P, Portmann R. Multiple-dose pharmacokinetics of the antimalarial drug fansimef^{R} (pyrimethamine + sulfadoxine + mefloquine) in healthy subjects. Chemother 1987;33:1-8.

110. Shah VP, Walker MA, Hunt JP, Schuirmann D, Prasad VK, Cabana BE. Thiazides XI: Partitioning of chlorothiazide in red blood cells after oral administration. Biopharm Drug Disp 1984;5:55-62.

111. Silber B, Lo M, Riegelman S. The influence of heparin administraton on the plasma protein binding and disposition of propranolol. Acta Pharmaceutica Suecica 1980;17:94.

112. Smith CC, Ihrig J. Persistent excretion of pyrimethamine following oral administration. Am J Trop Med Hyg 1959;8:6-62.

113. Smith CC, Schmidt LH. Observations of the absorption of pyrimethamine from the gastrointestinal tract. Exp Parasitol 1963;13:178-185.

114. Sorrells SC, Lopez, LM, Curry SH, Pieper JA. Effect of Vacutainer tubes on lidocaine protein binding. DICP 1987;21:464-465.

115. Stargel WW, Roe CR, Routledge, Shand DG. Importance of blood-collectin tubes in plasma lidocaine determinations. Clin Chem 1979;25:617-619.

116. Taylor EA, Turner P. The distribution of propranolol, pindolol, and atenolol between human erythrocytes and plasma. Br J Clin Pharmacol 1981;12:543-548.

117. Terasaki T, Iga T, Sugiyama Y, Hanono M. Pharmacokinetic study of the mechanism of tissue distribution of doxorubicin: interorgan and interspecies variation of tissue-to-plasma partition coeffeicients in rats, rabbits, and guinea pigs. J Pharm Sci 1984;73:1359-63.

118. Timm U, Weidekamm E. Determination of pyrimethamine in human plasma after administration of fansidar or fansidar-mefloquine by means of high-performance liquid chromatography with fluorescence detection. J Chromatogr 1982;230:107-114.

119. Tozer TN, Gambertoglio JG, Furst DE, Avery DS, Holford NHG. Volume shifts and protein binding estimates using equilibrium dialysis: applications to prednisolone binding in humans. J Pharm Sci 1983;72:1442-1446.

120. Trung AHN-T, Sirois G, Dube LM, McGilveray IJ. Comparison of the erythrocyte partitioning method with two classical methods for estimating free drug fraction in plasma. Biopharm Drug Disp 1984;5:281-290.

121. Tserng K-Y, Wagner JG. Fluorometric determination of erythromycin and erythromycin propionate in whole blood or plasma and correlation of results with microbiological assay. Anal Chem 1976;48:348-353.

122. Waddell WJ, Bates RG. Intracellular pH. Physio Rev 1969;49:285-329.

123. Wang LH, Lee CS, Majeske BL, Marbury TC. Clearance and recovery calculations in hemodialysis: application to plasma, red blood cell, and dialysate measurements for cyclophosphamide. Clin Phamacol Ther 1981;29:365-372.

124. Wehrli A, Hildenbrand JC, Keller HP, Stampfli R, and Frei RW. Influence of organic bases on the stability and separation properties of reversed-

phase chemically bonded silica gels. J Chromatogr 1978;149:199-210.

125. Weidekamm E, Plozza-Nottebrock H, Forgo I, Dubach UC. Plasma concentrations of pyrimethamine and sulfadoxine and evaluation of pharmacokinetic data by computerized curve fitting. Bull WHO 1982;60:115-122.

126. Williams AR. The effect of bovine and human serum albumins on the mechanical properties of human erythrocyte membranes. Biochim Biophys Acta 1973;307:58-64.

127. Williams WJ, Beutler E, Erslev AJ, Lichtman MA. Hematology, 3rd ed. New York: McGraw Hill, 1983.

128. Wong B, Gold JWM, Brown AE, Lane M, Fried R, Grieco M, Mildran D, Giron J, Tapper ML, Lerner CW, Armstrong D. Central-nervous-system toxoplasmosis in homosexual men and parenteral drug abusers. Ann Intern Med 1984;100:36-42.

129. Woo E, Greenblatt DJ. Pharmacokinetic and clinical implications of quinidine protein binding. J Pharm Sci 1979;68:466-469.

130. Wood M, Shand DG, Wood AJJ. Altered drug binding due to the use of indwelling heparinized cannulas (heparin lock) for sampling. Clin Pharmacol Ther 1979;25:103-107.

Appendix A

Computer Programs

```
COMMENT:  PROGRAM FOR RBC/BUFFER RATIO VERSUS PH

GOPTIONS HSIZE=6.5 VSIZE=5 NODISPLAY DEVICE=TEK4014
 GSFMODE=replace GSFNAME=TEK4014 NOPROMPT;
data phratio;
INPUT BUFFER RBC corrbc ph rtheo;
CARDS;
137.82  505.93  565.85  6.7  .4717
140.39  503.59  535.17  7.1  .8406
198.67  836.09  939.86  7.4  1.1329
119.89  587.89  670.48  7.4  1.1329
109.64  550.42  604.90  7.7  1.372
101.96  665.16  704.31  7.9  1.4885
114.77  681.55  717.73  8.0  1.5343
;
DATA CALC;
SET phratio;
ratio = corrbc/buffer;
PROC PRINT DATA = CALC;
TITLE "RBC/BUFFER RATIO VERSUS pH";
PROC REG data=calc;
  MODEL ratio=ph/R CLI CLM;
  OUTPUT OUT=rat PREDICTED=PRD RESIDUAL=RES;
PROC REG data=calc;
  MODEL rtheo=ph/R CLI CLM;
  OUTPUT OUT=rat2 PREDICTED=PRD2 RESIDUAL=RES2;
data sum;set rat rat2 calc;
TITLE H=2 F=XSWISS C=WHITE "RBC/BUFFER RATIO VERSUS pH";
PROC GPLOT;
LABEL RATIO="RBC/BUF RATIO";
LABEL RTHEO="THEORETICAL RATIO";
LABEL PRD2="PREDICTED";
LABEL PRD="PREDICTED";
LABEL PH="pH";
LABEL RES="RESIDUAL";LABEL RES2="RESIDUAL"
 PLOT  ratio*ph=1 PRD*ph=2 rtheo*pH=3 prd2*pH=4 / OVERLAY,
 PLOT RES*PH=5 RES2*PH=6/ OVERLAY VREF=0;
SYMBOL1 C=WHITE V=TRIANGLE I=NONE;
SYMBOL2 C=WHITE V=X I=JOIN;
SYMBOL3 C=WHITE V=CIRCLE I=NONE;
SYMBOL4 C=WHITE V=X I=JOIN;
SYMBOL5 C=WHITE V=TRIANGLE I=NONE;
SYMBOL6 C=WHITE V=CIRCLE I=NONE;
FOOTNOTE H=2 F=XSWISS C=
  WHITE "OBSERVED      THEORETICAL  O    PREDICTED  X";
```

```
COMMENT: PROGRAM FOR ANOVA OF EFFECT OF DIFFERENT
         ANTICOAGULANTS ON pH OF PLASMA AT ZERO TIME.....

Data coag;
  input coag ph @@;
  CARDS;
1 7.29 1 7.28 1 7.3  1 7.29 1 7.29
2 7.27 2 7.3  2 7.32 2 7.33 2 7.31
3 7.42 3 7.50 3 7.52 3 7.52 3 7.52
;
PROC ANOVA;
  CLASSES coag;
  MODEL pH = COAG;
  MEANS COAG/tukey alpha=.01;
TITLE "Zero Time pH in Vacutainers";

COMMENT: PROGRAM TO TEST FOR SIG DIFFERENCE
         BETWEEN BINDING AT PH 7.4 VS PH 8.....

Data phpb;

  input pH FREE @@;
  CARDS;
7.4  15.49  7.4  14.75  7.4  15.25
8.0  14.75  8.0  14.57  8.0  14.08
;
PROC TTEST;
  CLASS pH;
  VAR FREE;
TITLE "Binding pH 7.4 vs 8.0";

COMMENT: PROGRAM TO REGRESS FREE FRACTION OF PYR
         ON ALBUMIN CONCENTRATION.....

data sum45;
INPUT albumin free cptot;
CARDS;
45.56  4.91  363.316
45.56 3.53 118.426
14 13.51 301
14.3 13.74 283.6
13.8 13.28 319.3
8.13 25.05 75
8 13 20.21 258
8.13 23.32 372
8.13 22.3 382
23.5 9.561 314.5
23.5  12.664  202
23.5 9.412  509
;
TITLE "PERCENT FREE VS  ALBUMIN CONCENTRATION";
PROC REG;
  MODEL FREE=ALBUMIN/P R CLI CLM;
  OUTPUT OUT=ALB PREDICTED=PRD RESIDUAL=RES;
 PROC PLOT;
PLOT FREE*ALBUMIN='0' PRD*ALBUMIN='*' / OVERLAY;
PLOT RES*ALBUMIN / VREF=0;
```

```
COMMENT: PROGRAM TO DO ANOVA ON EFFECT OF ANTICOAGULANTS
ON PERCENT FREE PYR

Data frecoag;
  input coag FREE @@;
  CARDS;
1 4.854 1 5.885 1 4.4665
2 7.934 2 4.641 2 7.341
3 13.974 3 7.105 3 6.604 3 6.377
;
PROC GLM;
  CLASSES coag;
  MODEL FREE = COAG;
  LSMEANS COAG;
TITLE "Percent Free PYR in Different Tubes";

COMMENT: PROGRAM TO DO T TEST ON PERCENT FREE
  AT 100 VS 400 NG PYR/ML.....................

Data frether;
  input CONC FREE @@;
  CARDS;
400 3.55 400 5.67  400  5.17  400  5.89  400  4.28
100 4.06  100  4.08 100 3.26 100 3.08 100 3.18
;
PROC TTEST;
  CLASS CONC;
  VAR FREE;
TITLE "Binding at 100 vs. 400 ng/ml";
```

```
COMMENT: PROGRAM TO DO T-TEST ON BINDING AT TWO pHs
.......  .........  ..

Data frether;
  input ph FREE @@;
  CARDS;
8. 14.75 8. 14.57 8. 14.08
7.4 15.49 7.4 14.75 7.4 15.25
;
PROC TTEST;
  CLASS PH;
  VAR FREE;
TITLE "Binding at pH 7.4 vs. pH 8.0";
```

```
COMMENT: PROGRAM TO TEST FOR SIG DIFFERENCE
         BETWEEN BINDING AT PH 7.4 VS PH 8

Data phpb;
  input pH FREE @@;
  CARDS;
7.4  15.49  7.4  14.75  7.4  15.25
8.0  14.75  8.0  14.57  8.0  14.08
;
PROC TTEST;
  CLASS pH;
  VAR FREE;
TITLE "Binding pH 7.4 vs 8.0";

COMMENT: PROGRAM TO REGRESS FREE FRACTION OF PYR
         ON ALBUMIN CONCENTRATION

data sum45;
INPUT albumin free cptot;
CARDS;
45.56  4.91  363.316
45.56 3.53 118.426
14 13.51 301
14.3 13.74 283.6
13.8 13.28 319.3
8.13 25.05 75
8.13 20.21 258
8.13 23.32 372
8.13 22.3 382
23.5 9.561 314.5
23.5  12.664  202
23.5 9.412  509
;
TITLE "PERCENT FREE VS. ALBUMIN CONCENTRATION";
PROC REG;
  MODEL FREE=ALBUMIN/P R CLI CLM;
  OUTPUT OUT=ALB PREDICTED=PRD RESIDUAL=RES;
 PROC PLOT.
PLOT FREE*ALBUMIN='0  PRD*ALBUMIN='*' / OVERLAY;
PLOT RES*ALBUMIN / VREF=0;
```

```
COMMENT: FILE WHONOR38.SAS,1 FOR KLOTZ FIT OF DATA 38

GOPTIONS HSIZE=6.5 VSIZE=5 NODISPLAY DEVICE=TEK4014
 GSFMODE=replace GSFNAME=TEK4014 NOPROMPT;
data ed38;
INPUT BUFFER PLASMA CELL;
CARDS;
17.5 189.87 3
29.31 231.45 4
29.31 248.94 5
33.25 347.75 6
52.95 562.55 7
49  548.72 8
60.83 739.17 9
52.95 581.5 10
88.41 973.77 11
92.35  1242.62 12
323.03 4094.71 13
323.03 3663.3 14
;
DATA CALC;
SET ED38;
BOUND = PLASMA - BUFFER;
DATA CALC2;
SET CALC;
Db = BOUND*.000001/248.71;
Df = buffer*.000001/248.71;
DATA CALC3;
SET CALC2;
R = Db/3.4086957E-04;
Data Calc4;set calc3;
rbalb = r/Df;
lfree = log10(Df);
pfree = buffer/p'asma
pbd = 1.0 - pfree;
RR=1/R,RD=1/DF,
WT=1/BUFFER;
PROC NLIN BEST=20 ITER=:00 METHOD=DUD
PARAMETERS HK1=30000  HK2=10000;
BOUNDS HK1>1000;
_WEIGHT_=WT;
 MODEL R = (Df*HK1 + (2*(Df**2)*HK1*HK2))/(1+DF*HK1 + (DF**2)*HK1*HK2);
OUTPUT OUT=LARS PREDICTED=PRED RESIDUAL=RESID
 ESS=WRSS PARMS=HK1 HK2;
PROC PRINT;
TITLE H=2 F=XSWISS C=WHITE "KLOTZ FIT OF PYR DATA 38";
PROC GPLOT;
LABEL RBALB="R/ALBUMIN";
LABEL R="R";
LABEL LFREE="LOG FREE PYR";
LABEL PRED="PREDICTED";
LABEL RESID="RESIDUAL";
 PLOT R*LFREE=1 PRED*LFREE=2 / OVERLAY;
 PLOT RESID*LFREE=3 / VREF=0;
SYMBOL1 C=WHITE V=TRIANGLE I=NONE;
SYMBOL2 C=WHITE V=X I=JOIN;
SYMBOL3 C=WHITE V=X I=NONE;

**********************
COMMENT:  FILE WHONOR41.SAS;2 FOR KLOTZ FIT OF DATA 41

GOPTIONS HSIZE=6.5 VSIZE=5 NODISPLAY DEVICE=TEK4014
 GSFMODE=replace GSFNAME=TEK4014 NOPROMPT;
data ed41;
INPUT BUFFER PLASMA CELL;
CARDS;
```

```
25.06 100.05 1
25.06 96.55 2
44.87 204.00 3
50.75 202.21 4
69 09 323.74 5
65.42 323.74 6
109.45 491.35 7
113.12 485.01 8
131.47 601.83 9
141.95 605.84 10
224.9 974.43 11
232.16 1034.8 12
419.67 1741.49 13
477.38 1984.12 14
812.81 3646.39 15
;
DATA CALC;
SET ED41;
BOUND = PLASMA - BUFFER;
DATA CALC2;
SET CALC;
Db = BOUND*.000001/248.71;
Df = buffer*.000001/248.71;
DATA CALC3;
SET CALC2;
R = Db/1.178261E-04;
Data Calc4;Set calc3;
rbalb = r/Df;
lfree = log10(Df);
pfree = buffer/plasma;
pbd = 1.0 - pfree
RR=1/R;RD=1/DF.
WT=1/BUFFER;
PROC NLIN BEST=20 ITER=100 METHOD=DUD;
PARAMETERS HK1=30000  HK2=10000
BOUNDS HK1>1000.
_WEIGHT_=WT;
 MODEL R = (Df*HK1 + (2*(Df**2)*HK1*HK2))/(1+DF*HK1 + (DF**2)*HK1*HK2).
OUTPUT OUT=LARS PREDICTED=PRED RESIDUAL=RESID
 ESS=WRSS PARMS=HK1 HK2.
PROC PRINT;
TITLE H=2 F=XSWISS C=WHITE "KLOTZ FIT OF PYR DATA 41";
PROC GPLOT;
LABEL RBALB="R/ALBUMIN";
LABEL R="R";
LABEL PRED="PREDICTED";
LABEL LFREE="LOG FREE PYR";
LABEL RESID="RESIDUAL";
 PLOT R*LFREE=1 PRED*LFREE=2 / OVERLAY;
 PLOT RESID*LFREE=3 / VREF=0;
SYMBOL1 C=WHITE V=TRIANGLE I=NONE;
SYMBOL2 C=WHITE V=X I=JOIN;
SYMBOL3 C=WHITE V=X I=NONE;

*************************
COMMENT:  FILE WHONOR47.SAS;2 FOR KLOTZ FIT OF DATA 47

GOPTIONS HSIZE=6.5 VSIZE=5 NODISPLAY DEVICE=TEK4014
 GSFMODE=replace GSFNAME=TEK4014 NOPROMPT;
data ed47;
INPUT BUFFER PLASMA CELL;
CARDS;
9179.2 32691.22 1
8699.5 39919.93 12
2786.3 15699.89 13
3088.3 19964.04 14
```

```
1588.6 8241.26 15
1650.8 8943.25 6
1215.5 6780.3 7
1108.9 5382.78  8
771.3 4313.87  9
771.3 6283.15 10
301.3 2156.47 1
285.7 1130.55 2
441.2 2586.87 3
412.3 3559.16 4
383.4 3370.28 5
;
DATA CALC;
SET ED47;
BOUND = PLASMA - BUFFER;
DATA CALC2;
SET CALC;
Db = BOUND*.000001/248.71;
Df = buffer*.000001/248.71;
DATA CALC3;
SET CALC2;
R = Db/9.59157E-05;
Data Calc4;set calc3;
rbalb = r/Df;
lfree = log10(Df);
pfree = buffer/plasma;
pbd = 1.0 - pfree;
rr = 1/r;
rd = 1/Df;
 WT=1/BUFFER;
PROC NLIN BEST=20 ITER=100 METHOD=DUD;
PARAMETERS HK1=30000  HK2=10000;
BOUNDS HK1>1000;
_WEIGHT_=WT;
 MODEL R = (Df*HK1 + (2*(Df**2)*HK1*HK2))/(1+DF*HK1 + (DF**2)*HK1*HK2);
OUTPUT OUT=LARS PREDICTED=PRED RESIDUAL=RESID
 ESS=WRSS PARMS=HK1 HK2;
PROC PRINT;
TITLE H=2 F=XSWISS C=WHITE "KLOTZ FIT OF PYR DATA 47";
PROC GPLOT;
LABEL RBALB="R/ALBUMIN",
LABEL R="R",
LABEL LFREE="LOG FREE PYR";
LABEL PRED="PREDICTED";
LABEL RESID="RESIDUAL";
 PLOT R*LFREE=1 PRED*LFREE=2 / OVERLAY;
 PLOT RESID*LFREE=3 / VREF=0;
SYMBOL1 C=WHITE V=TRIANGLE I=NONE;
SYMBOL2 C=WHITE V=X I=JOIN;
SYMBOL3 C=WHITE V=X I=NONE;
```

```
COMMENT: BLANCHARD FIT OF FIRST ED DATA USING NLIN.....

data ed38;
INPUT BUFFER PLASMA CELL;
CARDS;
17.5 189.87 3
29.31 231.45 4
29.31 248.94 5
33.25 347.75 6
52.95 562.55 7
49  548.72 8
60.83 739.17 9
52.95 581.5 10
88.41 973.77 11
92.35  1242.62 12
323.03 4094.71 13
323.03 3663.3 14
;
DATA CALC;
SET ED38;
BOUND = PLASMA - BUFFER;
DATA CALC2;
SET CALC;
Db = BOUND*.000001/248.71;
Df = buffer*.000001/248.71;
DATA CALC3;
SET CALC2;
R = Db/3.4086957E-04;
Data Calc4;set calc3;
rbalb = r/Df;
lfree = log10(Df)
pfree = buffer/plasma
pbd = 1.0 - pfree;
RR=1/R;RD=1/DF;
PROC NLIN BEST=20 ITER=100 METHOD=DUD;
PARAMETERS HK1=30000. HN1=1. C=30000.;
BOUNDS HN1>0.001;
 MODEL RBALB = ((HN1*HK1)/(1+HK1*DF)) + C;
OUTPUT OUT=LARS PREDICTED=PRED RESIDUAL=RESID
 ESS=WRSS PARMS=HK1 HN1 C
PROC PRINT;
TITLE "BLANCHARD FIT OF PYR DATA 38";
PROC PLOT;
 PLOT RBALB*R='0' PRED*R='*' / OVERLAY;
 PLOT RESID*R / VREF=0;
 PLOT RESID*R / VREF=0;

COMMENT: BLANCHARD FIT OF SECOND ED DATA USING NLIN.....

data ed41;
INPUT BUFFER PLASMA CELL;
CARDS;
25.06 100.05 1
25.06 96.55 2
44.87 204.00 3
50.75 202.21 4
69.09 323.74 5
65.42 323.74 6
109.45 491.35 7
113.12 485.01 8
131.47 601.83 9
141.95 605.84 10
224.9 974.43 11
232.16 1034.8 12
419.67 1741.49 13
477.38 1984.12 14
```

```
812.81 3646.39 15
;
DATA CALC;
SET ED41;
BOUND = PLASMA - BUFFER;
DATA CALC2;
SET CALC;
Db = BOUND*.000001/248.71;
Df = buffer*.000001/248.71;
DATA CALC3;
SET CALC2;
R = Db/1.178261E-04;
Data Calc4;Set calc3;
rbalb = r/Df;
lfree = log10(Df);
pfree = buffer/plasma;
pbd = 1.0 - pfree;
RR=1/R;RD=1/DF;
PROC NLIN BEST=20 ITER=100 METHOD=DUD;
PARAMETERS HK1=30000. HN1=1. C=30000.;
BOUNDS HN1>0.001;
 MODEL RBALB = ((HN1*HK1)/(1+HK1*DF)) + C;
OUTPUT OUT=LARS PREDICTED=PRED RESIDUAL=RESID
 ESS=WRSS PARMS=HK1 HN1 C;
PROC PRINT;
TITLE "BLANCHARD FIT OF PYR DATA 41";
PROC PLOT;
 PLOT RBALB*R='0' PRED*R='*' / OVERLAY;
 PLOT RESID*R / VREF=0;

COMMENT: BLANCHARD FIT OF THIRD ED DATA USING NLIN.....

data ed47;
INPUT BUFFER PLASMA CELL;
CARDS;
9179 2 32691 22 11
8699 5 39919 93 12
2786.3 15699.89 13
3088.3 19964.04 14
1588.6 8241.26 15
1650.8 8943 25 6
1215.5 6780.3 7
1108.9 5382.78  8
771 3 4313.87  9
771 3 6283.15 10
301.3 2156.47 1
285.7 1130.55 2
441.2 2586.87 3
412.3 3559.16 4
383.4 3370.28 5
;
DATA CALC;
SET ED47;
BOUND = PLASMA - BUFFER;
DATA CALC2;
SET CALC;
Db = BOUND*.000001/248.71;
Df = buffer*.000001/248.71;
DATA CALC3;
SET CALC2;
R = Db/9.59157E-05;
Data Calc4;set calc3;
*rbalb = r/Df;
 lfree = log10(Df);
 pfree = buffer/plasma;
 pbd = 1.0 - pfree;
```

```
rr = 1/r;
rd = 1/Df;
PROC NLIN BEST=20 ITER=100 METHOD=DUD;
PARAMETERS HK1=30000. HN1=1. C=30000.;
BOUNDS HN1>0.001;
 MODEL RBALB = ((HN1*HK1)/(1+HK1*DF)) + C;
OUTPUT OUT=LARS PREDICTED=PRED RESIDUAL=RESID
 ESS=WRSS PARMS=HK1 HN1 C;
PROC PRINT;
TITLE "BLANCHARD FIT OF PYR DATA 47";
PROC PLOT;
 PLOT RBALB*R='0' PRED*R='*' / OVERLAY;
```

```
COMMENT: DATA FROM FIRST ATTEMPT TO GENERATE SCATCHARD PLOT DATA.....
         PROGRAMS FOR FITS TO LARSEN AND DOUBLE RECIPROCAL EQUATIONS...

data ed38;
INPUT BUFFER PLASMA CELL;
CARDS;
17.5 189.87 3
29.31 231.45 4
29.31 248.94 5
33.25 347.75 6
52.95 562.55 7
49  548.72 8
60.83 739.17 9
52.95 581.5 10
88.41 973.77 11
92.35  1242.62 12
323.03 4094.71 13
323.03 3663.3 14
;
DATA CALC;
SET ED38;
BOUND = PLASMA - BUFFER;
DATA CALC2;
SET CALC;
Db = BOUND*.000001/248.71;
Df = buffer*.000001/248.71;
DATA CALC3;
SET CALC2;
R = Db/3.4086957E-04.
Data Calc4;set calc3;
rbalb = r/Df;
lfree = log10(Df).
pfree = buffer/plasma
pbd = 1.0 - pfree;
RR=1/R;RD=1/DF
TITLE "LARSEN FIT OF PYR DATA 38";
PROC NLIN BEST=20 ITER=100 METHOD=DUD;
PARAMETERS HK1=200000. HK2=30000;
MODEL R=(HK1/(2*(HK1-2*HK2)))*LOG(2*(HK1-2*HK2)*Df+1);
OUTPUT OUT=LARS PREDICTED=PRED RESIDUAL=RES
 ESS=WRSS PARMS=HK1 HK2;
PROC PRINT.
TITLE "LARSEN FIT OF PYR DATA 38";
PROC PLOT;
 PLOT R*lfree= 0' PRED*LFREE='*' / OVERLAY;
 PLOT RES*LFREE / VREF=0;
PROC REG;
TITLE "DOUBLE RECIPROCAL FIT OF DATA 38";
  MODEL rr=rd/P R CLI CLM;
  OUTPUT OUT=LARS2 PREDICTED=PRD RESIDUAL=RES;
 PROC PLOT;
PLOT RR*RD='0' PRD*RD='*' / OVERLAY;
PLOT RES*RD /VREF=0;

COMMENT: DATA GENERATED IN SECOND ATTEMPT TO GENERATE SCATCHARD PLOT ...
         FITS TO LARSEN EQUATION AND DOUBLE RECIPROCAL EQUATION.........

data ed41;
INPUT BUFFER PLASMA CELL;
CARDS;
25.06 100.05 1
25.06 96.55 2
44.87 204.00 3
50.75 202.21 4
50.09 323.74 5
```

```
65.42 323.74 6
109 45 491.35 7
113 12 485.01 8
131.47 601.83 9
141.95 605.84 10
224 9 974.43 11
232 16 1034.8 12
419.67 1741.49 13
477.38 1984.12 14
812.81 3646.39 15
;
DATA CALC;
SET ED41;
BOUND = PLASMA - BUFFER;
DATA CALC2;
SET CALC;
Db = BOUND*.000001/248.71;
Df = buffer*.000001/248.71;
DATA CALC3;
SET CALC2;
R = Db/1.178261E-04;
Data Calc4;Set calc3;
rbalb = r/Df;
lfree = log10(Df);
pfree = buffer/plasma;
pbd = 1.0 - pfree;
RR=1/R;RD=1/DF;
TITLE "LARSEN FIT OF PYR DATA 41";
PROC NLIN BEST=20 ITER=100 METHOD=DUD;
PARAMETERS HK1=200000. HK2=30000;
MODEL R=(HK1/(2*(HK1-2*HK2)))*LOG(2*(HK1-2*HK2)*Df+1);
OUTPUT OUT=LARS PREDICTED=PRED RESIDUAL=RES
 ESS=WRSS PARMS=HK1 HK2;
PROC PRINT;
TITLE "LARSEN FIT OF PYR DATA 41";
PROC PLOT;
 PLOT R*lfree='0' PRED*LFREE='*' / OVERLAY;
 PLOT RES*LFREE / VREF=0;
PROC REG;
TITLE "DOUBLE RECIPROCAL FIT OF DATA 41";
  MODEL rr=rd/P R CLI CLM;
  OUTPUT OUT=LARS2 PREDICTED=PRD RESIDUAL=RES;
 PROC PLOT;
PLOT RR*RD='0' PRD*RD='*' / OVERLAY;
PLOT RES*RD /VREF=0;

COMMENT: DATA GENERATED FOR THIRD ATTEMPT TO MAKE A SCATCHARD PLOT.....
         FITS TO LARSEN AND DOUBLE RECIPROCAL EQUATIONS.................

data ed47;
INPUT BUFFER PLASMA CELL;
CARDS;
9179.2 32691.22 11
8699.5 39919.93 12
2786.3 15699.89 13
3088.3 19964.04 14
1588.6 8241.26 15
1650.8 8943.25 6
1215.5 6780.3 7
1108.9 5382.78  8
771.3 4313.87  9
771.3 6283.15 10
301.3 2156.47 1
285.7 1130.55 2
441.2 2586.87 3
412.3 3559.16 4
```

```
383.4 3370.28 5
;
DATA CALC;
SET ED47;
BOUND = PLASMA - BUFFER;
DATA CALC2;
SET CALC;
Db = BOUND*.000001/248.71;
Df = buffer*.000001/248.71;
DATA CALC3;
SET CALC2;
R = Db/9.59157E-05;
Data Calc4;set calc3;
rbalb = r/Df;
lfree = log10(Df);
pfree = buffer/plasma;
pbd = 1.0 - pfree;
rr = 1/r;
rd = 1/Df;
TITLE "LARSEN FIT OF PYR DATA 47";
PROC NLIN BEST=20 ITER=100 METHOD=DUD;
PARAMETERS HK1=200000. HK2=30000;
MODEL R=(HK1/(2*(HK1-2*HK2)))*LOG(2*(HK1-2*HK2)*Df+1);
OUTPUT OUT=LARS PREDICTED=PRED RESIDUAL=RES
 ESS=WRSS PARMS=HK1 HK2;
PROC PRINT;
TITLE "LARSEN FIT OF PYR DATA 47";
PROC PLOT;
 PLOT R*lfree='0' PRED*LFREE='*' / OVERLAY;
 PLOT RES*LFREE / VREF=0;
PROC REG;
TITLE "DOUBLE RECIPROCAL FIT OF DATA 47";
  MODEL rr=rd/P R CLI CLM;
  OUTPUT OUT=LARS2 PREDICTED=PRD RESIDUAL=RES;
 PROC PLOT;
TITLE "DOUBLE RECIPROCAL FIT OF DATA 47";
PLOT RR*RD='0' PRD*RD='*' / OVERLAY;
PLOT RES*RD / VREF=0;
```

Appendix B

Results of Fits to Additional Models

BLANCHARD FIT OF STUDY 1 DATA

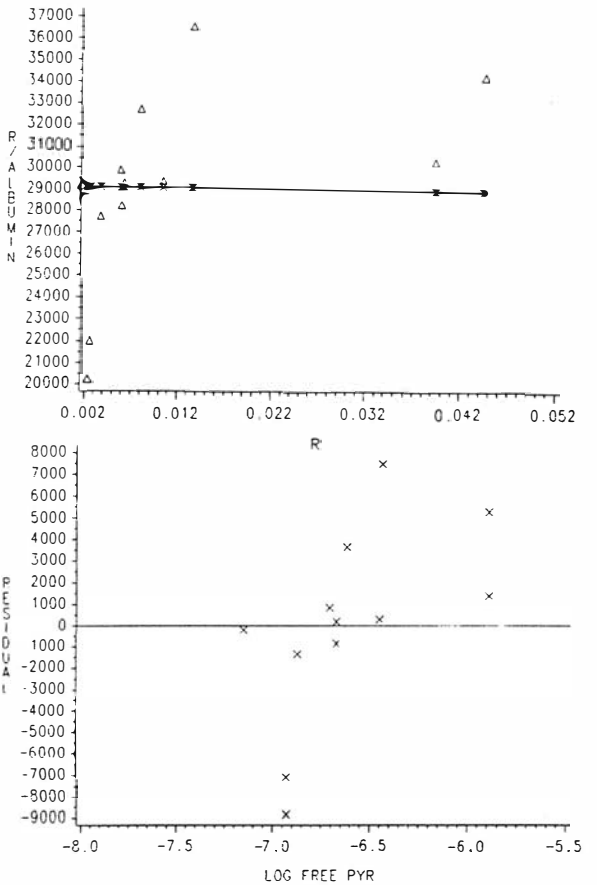

BLANCHARD FIT OF STUDY 2 DATA

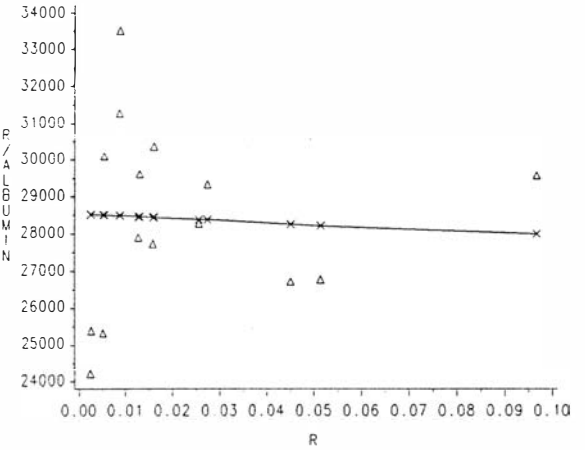

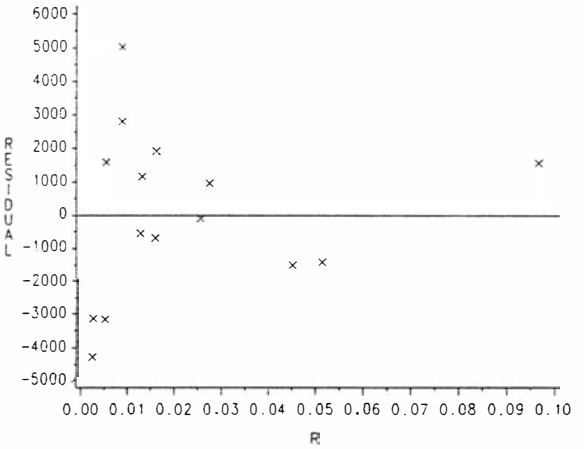

BLANCHARD FIT OF STUDY 3 DATA

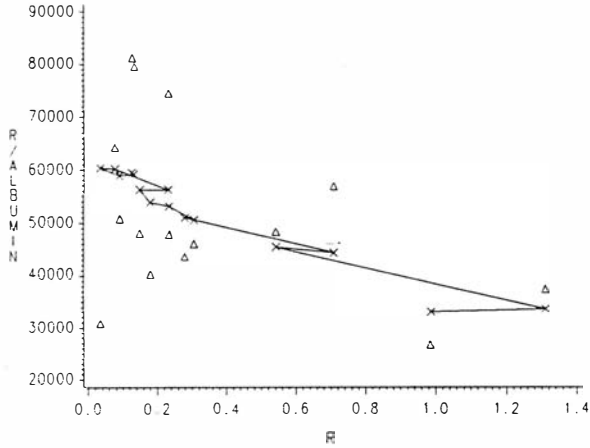

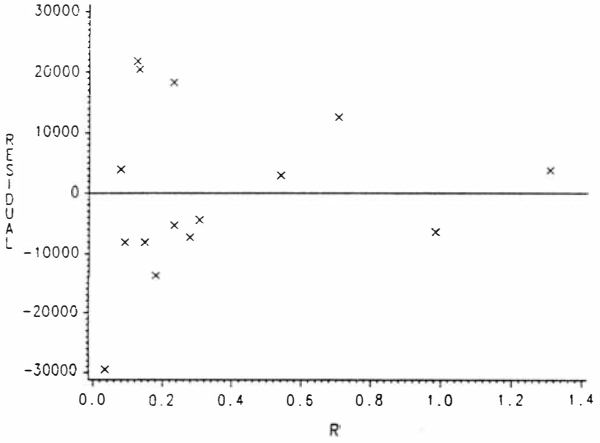

LARSEN FIT OF PYR DATA 38

NON-LINEAR LEAST SQUARES SUMMARY STATISTICS DEPENDENT VARIABLE R

SOURCE	DF	SUM OF SQUARES	MEAN SQUARE
REGRESSION	2	0.00400801357	0.00200400679
RESIDUAL	10	0.00002086886	0.00000208689
UNCORRECTED TOTAL	12	0.00402888243	
(CORRECTED TOTAL)	11	0.00228259020	

PARAMETER	ESTIMATE	ASYMPTOTIC STD. ERROR	ASYMPTOTIC 95 % CONFIDENCE INTERVAL LOWER	UPPER
HK1	30580.55941	2527.207668	24949.554399	36211.56441
HK2	35682.57711	29594.980663	-30259.563874	101624.71809

ASYMPTOTIC CORRELATION MATRIX OF THE PARAMETERS

CORR	HK1	HK2
HK1	1.0000	-0.9578
HK2	-0.9578	1.0000

Data 38 = Study 1

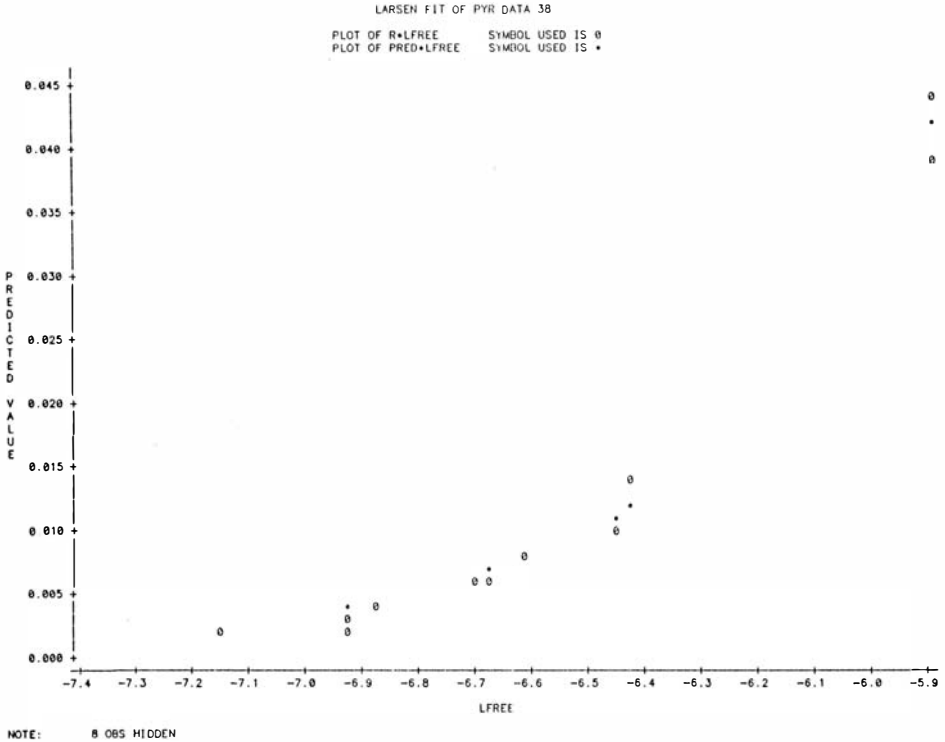
LARSEN FIT OF PYR DATA 38
PLOT OF R*LFREE SYMBOL USED IS 0
PLOT OF PRED*LFREE SYMBOL USED IS *
PREDICTED VALUE
0.045
0.040
0.035
0.030
0.025
0.020
0.015
0 010
0.005
0.000
-7.4 -7.3 -7.2 -7.1 -7.0 -6.9 -6.8 -6.7 -6.6 -6.5 -6.4 -6.3 -6.2 -6.1 -6.0 -5.9
LFREE
NOTE: 8 OBS HIDDEN

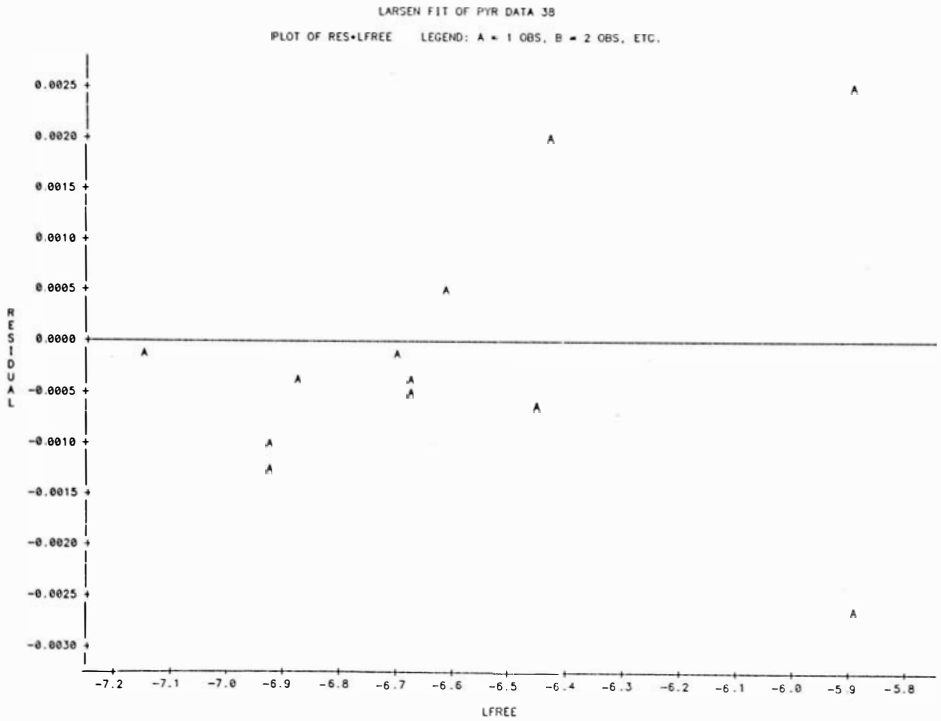
LARSEN FIT OF PYR DATA 38
PLOT OF RES*LFREE LEGEND: A = 1 OBS, B = 2 OBS, ETC.
RESIDUAL
0.0025
0.0020
0.0015
0.0010
0.0005
0.0000
-0.0005
-0.0010
-0.0015
-0.0020
-0.0025
-0.0030
-7.2
-7.1
-7.0
-6.9
-6.8
-6.7
-6.6
-6.5
-6.4
-6.3
-6.2
-6.1
-6.0
-5.9
-5.8
LFREE

LARSEN FIT OF PYR DATA 41

NON-LINEAR LEAST SQUARES SUMMARY STATISTICS DEPENDENT VARIABLE R

SOURCE	DF	SUM OF SQUARES	MEAN SQUARE
REGRESSION	2	0.01646771715	0.00823385858
RESIDUAL	13	0.00002572160	0.00000197858
UNCORRECTED TOTAL	15	0.01649343876	
(CORRECTED TOTAL)	14	0.00892713370	

PARAMETER	ESTIMATE	ASYMPTOTIC STD. ERROR	ASYMPTOTIC 95 % CONFIDENCE INTERVAL LOWER	UPPER
HK1	26693.56354	771.4474509	25026.953647	28360.173438
HK2	26433.62616	4353.9111641	17027.578581	35839.673741

ASYMPTOTIC CORRELATION MATRIX OF THE PARAMETERS

CORR	HK1	HK2
HK1	1.0000	-0.9120
HK2	-0.9120	1.0000

Study 2 = Data 41

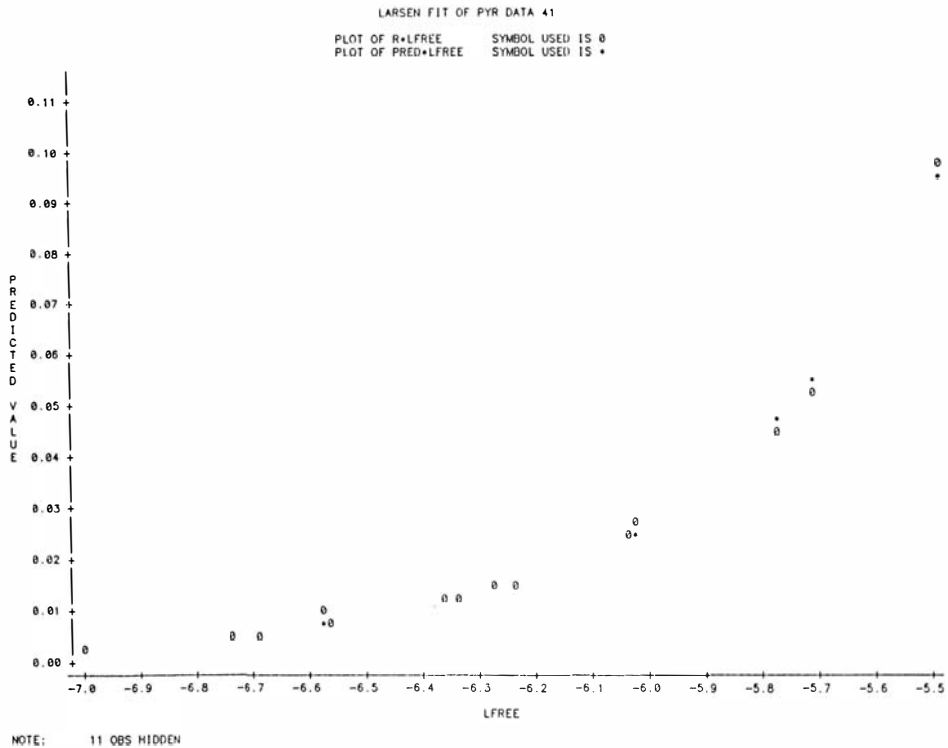

NOTE: 11 OBS HIDDEN

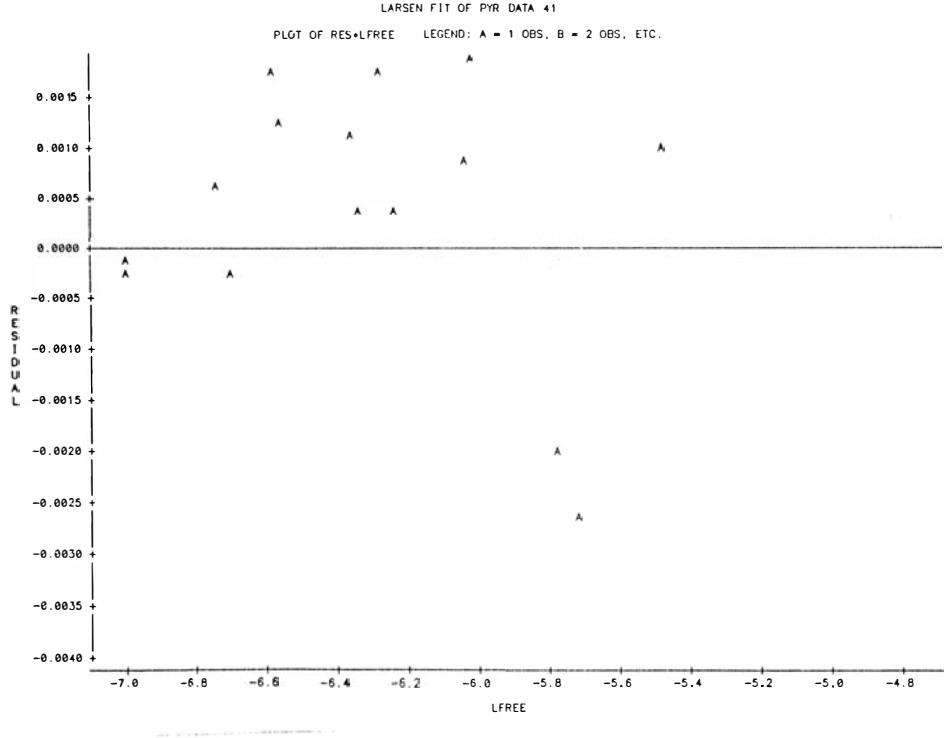
LARSEN FIT OF PYR DATA 41
PLOT OF RES*LFREE LEGEND: A = 1 OBS, B = 2 OBS, ETC.
RESIDUAL
0.0015
0.0010
0.0005
0.0000
-0.0005
-0.0010
-0.0015
-0.0020
-0.0025
-0.0030
-0.0035
-0.0040
-7.0
-6.8
-6.6
-6.4
-6.2
-6.0
-5.8
-5.6
-5.4
-5.2
-5.0
-4.8
LFREE

LARSEN FIT OF PYR DATA 47

NON-LINEAR LEAST SQUARES SUMMARY STATISTICS DEPENDENT VARIABLE R

SOURCE	DF	SUM OF SQUARES	MEAN SQUARE
REGRESSION	2	3.7582120042	1.8791060021
RESIDUAL	13	0.1011818578	0.0077832198
UNCORRECTED TOTAL	15	3.8593938620	
(CORRECTED TOTAL)	14	1.9298129729	

PARAMETER	ESTIMATE	ASYMPTOTIC STD. ERROR	ASYMPTOTIC 95 % CONFIDENCE INTERVAL LOWER	UPPER
HK1	64279.90832	10080.632793	42502.038233	86057.778403
HK2	14641.33400	2808.926120	8573.021681	20709.646310

ASYMPTOTIC CORRELATION MATRIX OF THE PARAMETERS

CORR	HK1	HK2
HK1	1.0000	-0.6659
HK2	-0.6659	1.0000

Data 47 = Study 3

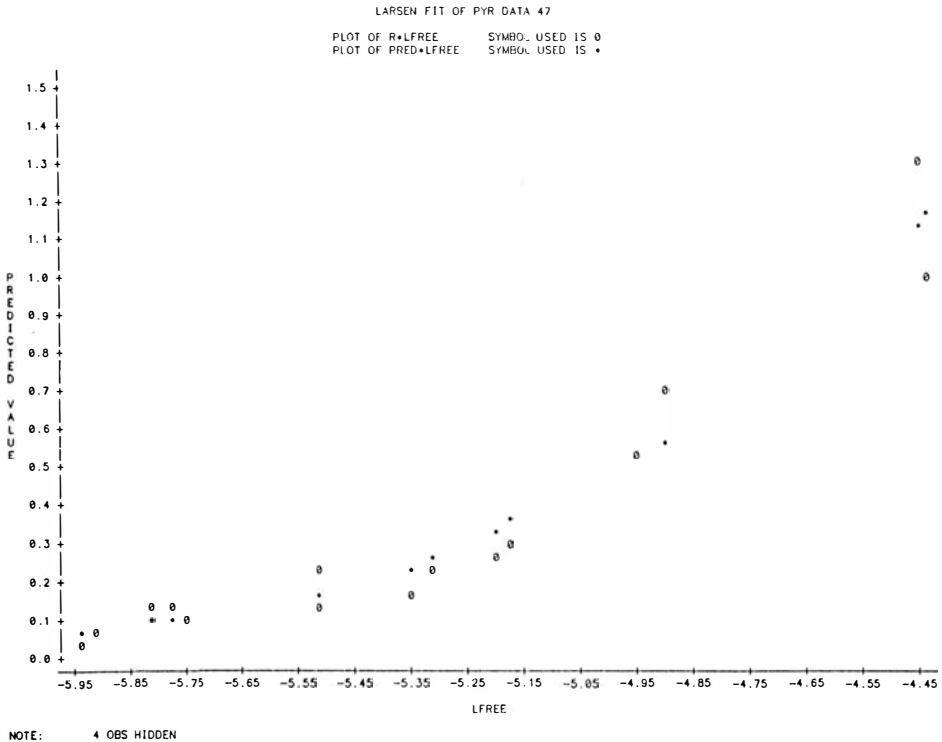

NOTE: 4 OBS HIDDEN

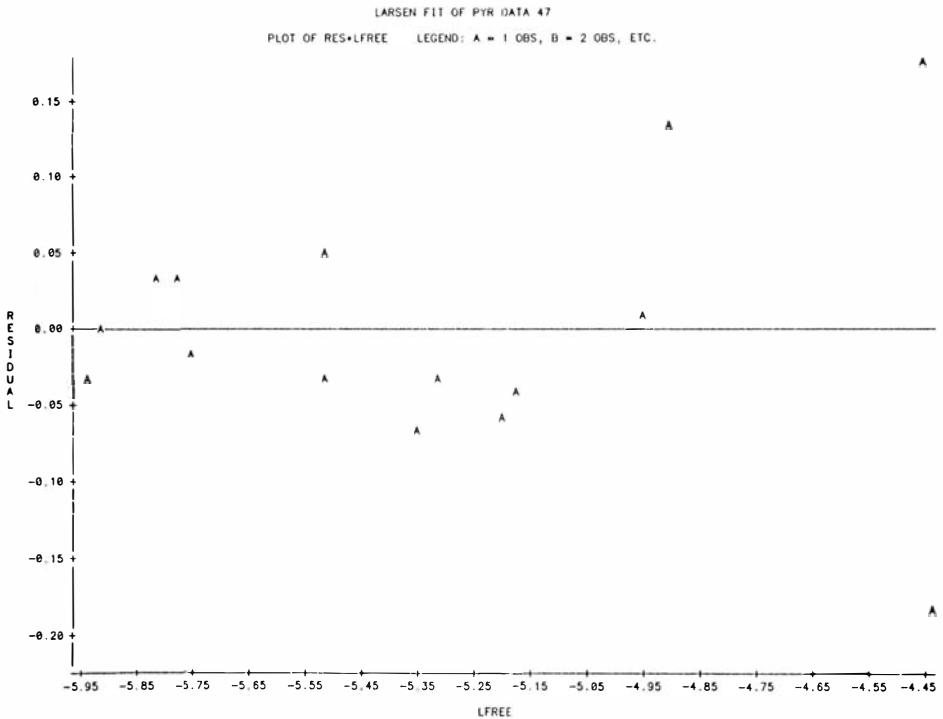
LARSEN FIT OF PYR DATA 47
PLOT OF RES*LFREE LEGEND: A = 1 OBS, B = 2 OBS, ETC.
RESIDUAL
0.15
0.10
0.05
0.00
-0.05
-0.10
-0.15
-0.20
-5.95 -5.85 -5.75 -5.65 -5.55 -5.45 -5.35 -5.25 -5.15 -5.05 -4.95 -4.85 -4.75 -4.65 -4.55 -4.45
LFREE

DOUBLE RECIPROCAL FIT OF DATA 38

DEP VARIABLE: RR

ANALYSIS OF VARIANCE

SOURCE	DF	SUM OF SQUARES	MEAN SQUARE	F VALUE	PROB>F
MODEL	1	252430.5	252430.5	137.331	0.0001
ERROR	10	18381.17	1838.117		
C TOTAL	11	270811.7			

ROOT MSE	42.87326	R-SQUARE	0.9321
DEP MEAN	200.4586	ADJ R-SQ	0.9253
C.V.	21.38759		

PARAMETER ESTIMATES

VARIABLE	DF	PARAMETER ESTIMATE	STANDARD ERROR	T FOR H0: PARAMETER=0	PROB > |T|
INTERCEP	1	-11.8028	21.93745	-0.538	0.6023
RD	1	.00003963331	.00000338202	11.719	0.0001

OBS	ACTUAL	PREDICT VALUE	STD ERR PREDICT	LOWER95% MEAN	UPPER95% MEAN	LOWER95% PREDICT	UPPER95% PREDICT	RESIDUAL	STD ERR RESIDUAL	STUDENT RESIDUAL	-2-1-0 1 2
1	491.835	551.466	32.4087	479.254	623.677	431.715	671.216	-59.63	28.0677	-2.1245	**** |
2	419.401	324.506	16.2857	288.219	360.793	222.318	426.694	94.8952	39.6597	2.39273	| ****
3	386.002	324.506	16.2857	288.219	360.793	222.318	426.694	61.4966	39.6597	1.55061	| ***
4	269.563	284.654	14.3107	252.768	316.541	183.945	385.364	-15.091	40.4144	-.373406	| |
5	166.361	174.358	12.5753	146.338	202.377	74.8051	273.91	-7.9965	40.9876	-.195096	| |
6	169.65	189.365	12.4126	161.707	217.022	89.9133	288.816	-19.714	41.0371	-.480399	| |
7	124.978	150.242	13.0973	121.06	179.425	50.356	250.128	-25.264	40.8237	-.618858	| * |
8	160.397	174.358	12.5753	146.338	202.377	74.8051	273.91	-13.961	40.9876	-.340616	| |
9	95.755	99.6914	15.0703	66.1124	133.27	-1.5666	200.949	-3.9363	40.1373	-.098072	| |
10	73.7024	94.9346	15.3056	60.8315	129.038	-6.4984	196.368	-21.232	40.0482	-.530166	| * |
11	22.4774	18.712	19.842	-25.499	62.9229	-86.551	123.975	3.76542	38.0054	.0990757	| |
12	25.3805	18.712	19.842	-25.499	62.9229	-86.551	123.975	6.66847	38.0054	0.175461	| |

OBS	COOK'S D
1	3.009
2	0.483
3	0.203
4	0.009
5	0.002
6	0.011
7	0.020
8	0.005
9	0.001
10	0.021
11	0.001
12	0.004

SUM OF RESIDUALS	-1.46994E-13
SUM OF SQUARED RESIDUALS	18381.17
PREDICTED RESID SS (PRESS)	39365.57

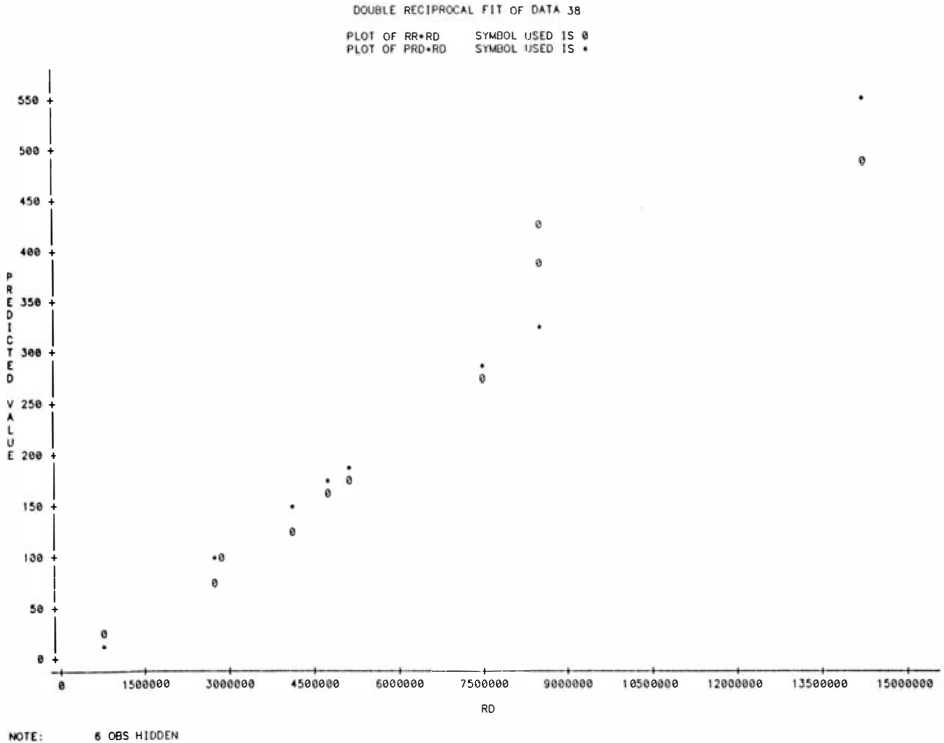

NOTE: 6 OBS HIDDEN

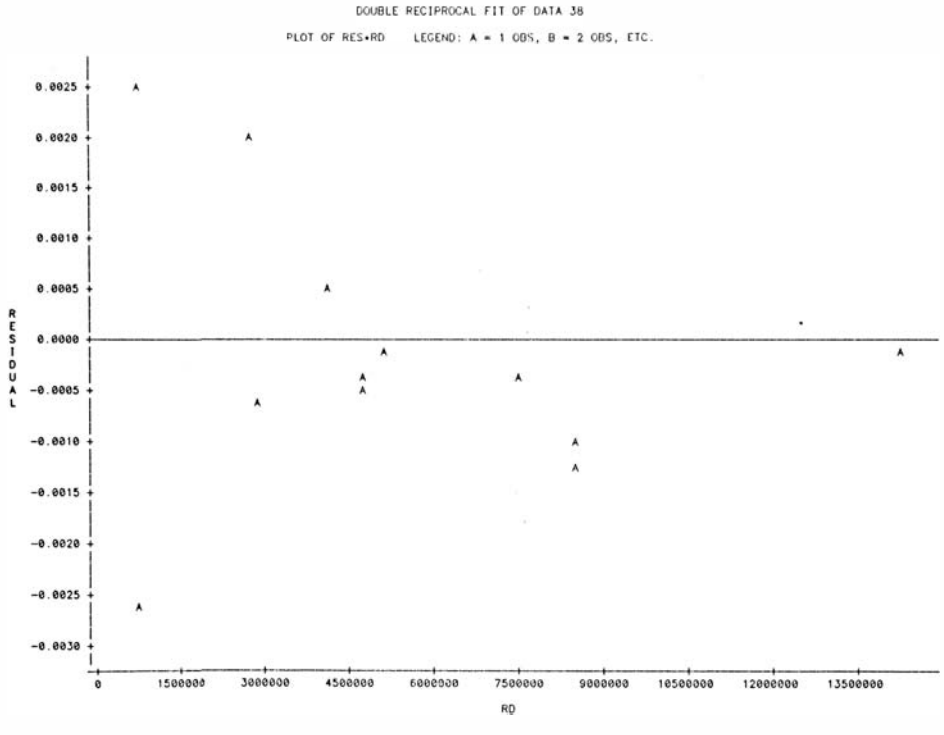
DOUBLE RECIPROCAL FIT OF DATA 38
PLOT OF RES*RD LEGEND: A = 1 OBS, B = 2 OBS, ETC.
RESIDUAL
0.0025
0.0020
0.0015
0.0010
0.0005
0.0000
-0.0005
-0.0010
-0.0015
-0.0020
-0.0025
-0.0030
0
1500000
3000000
4500000
6000000
7500000
9000000
10500000
12000000
13500000
RD

DOUBLE RECIPROCAL FIT OF DATA 41

DEP VARIABLE: RR

ANALYSIS OF VARIANCE

SOURCE	DF	SUM OF SQUARES	MEAN SQUARE	F VALUE	PROB>F
MODEL	1	219477.2	219477.2	1015.731	0.0001
ERROR	13	2809.015	216.0781		
C TOTAL	14	222286.2			

ROOT MSE	14.69959	R-SQUARE	0.9874
DEP MEAN	121.028	ADJ R-SQ	0.9864
C.V.	12.14562		

PARAMETER ESTIMATES

VARIABLE	DF	PARAMETER ESTIMATE	STANDARD ERROR	T FOR H0: PARAMETER=0	PROB > |T|
INTERCEP	1	-11.2151	5.623397	-1.994	0.0675
RD	1	.00004014998	.00000125978	31.871	0.0001

OBS	ACTUAL	PREDICT VALUE	STD ERR PREDICT	LOWER95% MEAN	UPPER95% MEAN	LOWER95% PREDICT	UPPER95% PREDICT	RESIDUAL	STD ERR RESIDUAL	STUDENT RESIDUAL	-2-1-0 1 2
1	390.779	387.257	9.17525	367.435	407.078	349.821	424.692	3.5226	11.4845	0.306728	
2	409.911	387.257	9.17525	367.435	407.078	349.821	424.692	22.6543	11.4845	1.97261	***
3	184.155	211.332	4.73643	201.1	221.565	177.968	244.697	-27.178	13.9156	-1.953	***
4	193.48	185.547	4.30157	176.254	194.84	152.459	218.636	7.93287	14.0561	0.564371	*
5	115.078	133.317	3.81495	125.075	141.558	100.503	166.125	-18.239	14.1959	-1.2848	**
6	113.443	141.425	3.849	133.109	149.74	108.593	174.252	-27.982	14.1867	-1.9724	***
7	76.7335	80.0201	4.00759	71.3623	88.678	47.1046	112.936	-3.2866	14.1427	-0.23239	
8	78.7989	77.0602	4.03837	68.3358	85.7845	44.127	109.993	1.73875	14.134	0.123019	
9	62.3023	64.7391	4.18624	55.6953	73.7829	31.7199	97.7583	-2.4367	14.0909	-.172931	
10	63.1713	59.1315	4.26345	49.9209	68.3421	26.0662	92.1968	4.03981	14.0677	0.287168	
11	39.0972	33.1855	4.69063	23.052	43.319	-.148627	66.5196	5.9117	13.9311	0.424352	
12	36.5102	31.797	4.71636	21.608	41.9861	-1.554	65.1481	4.71315	13.9224	0.338529	
13	22.1698	12.5791	5.09747	1.56664	23.5915	-21.033	46.1908	9.59078	13.7875	0.695617	*
14	19.449	9.7026	5.15816	-1.4409	20.8461	-23.952	43.3575	9.74637	13.7649	0.708061	*
15	10.3419	1.07028	5.3453	-10.478	12.6181	-32.721	34.8612	9.27159	13.6933	0.677091	*

DOUBLE RECIPROCAL FIT OF DATA 41

OBS	COOK'S D
1	0.030
2	1.242
3	0.221
4	0.015
5	0.060
6	0.143
7	0.002
8	0.001
9	0.001
10	0.004
11	0.010
12	0.007
13	0.033
14	0.035
15	0.035

SUM OF RESIDUALS	2.02061E-14
SUM OF SQUARED RESIDUALS	2809.015
PREDICTED RESID SS (PRESS)	4160.77

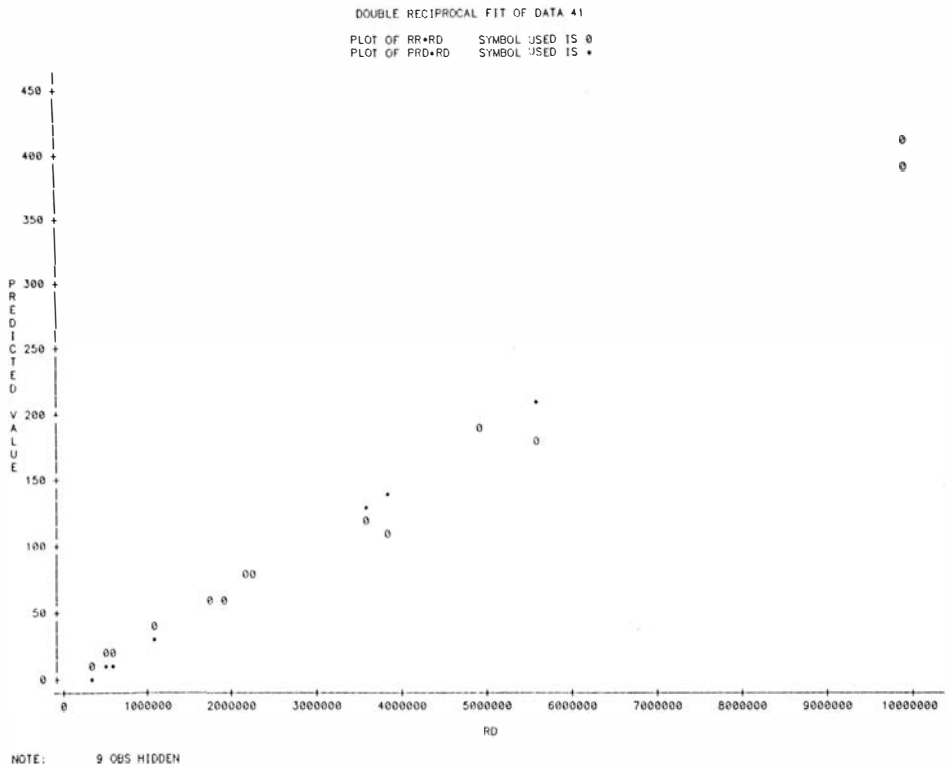
DOUBLE RECIPROCAL FIT OF DATA 41
PLOT OF RR*RD SYMBOL USED IS 0
PLOT OF PRD*RD SYMBOL USED IS *
PREDICTED VALUE
RD
0
1000000
2000000
3000000
4000000
5000000
6000000
7000000
8000000
9000000
10000000
NOTE: 9 OBS HIDDEN

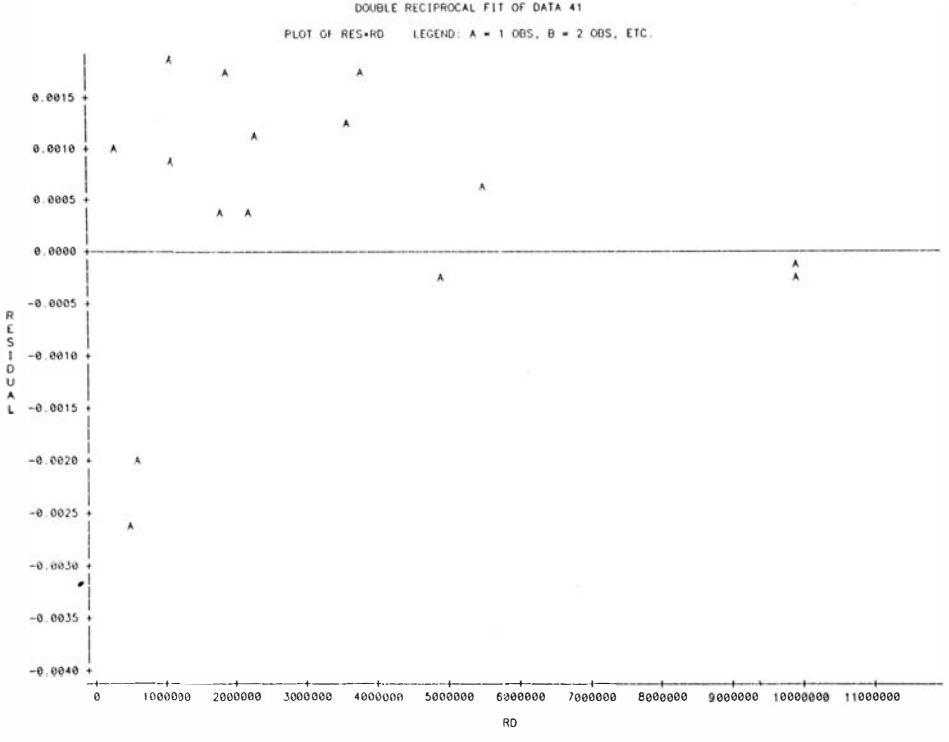
DOUBLE RECIPROCAL FIT OF DATA 41
PLOT OF RES*RD LEGEND: A = 1 OBS, B = 2 OBS, ETC.
RESIDUAL
0.0015
0.0010
0.0005
0.0000
-0.0005
-0.0010
-0.0015
-0.0020
-0.0025
-0.0030
-0.0035
-0.0040
0
1000000
2000000
3000000
4000000
5000000
6000000
7000000
8000000
9000000
10000000
11000000
RD

DOUBLE RECIFROCAL FIT OF DATA 47

DEP VARIABLE: RR

ANALYSIS OF VARIANCE

SOURCE	DF	SUM OF SQUARES	MEAN SQUARE	F VALUE	PROB>F
MODEL	1	495.7232	495.7232	35.572	0.0001
ERROR	13	181.1649	13.93576		
C TOTAL	14	676.8881			

ROOT MSE	3.733064	R-SQUARE	0.7324
DEP MEAN	6.707118	ADJ R-SQ	0.7118
C.V.	55.65824		

PARAMETER ESTIMATES

VARIABLE	DF	PARAMETER ESTIMATE	STANDARD ERROR	T FOR H0: PARAMETER=0	PROB > |T|
INTERCEP	1	-0.350591	1.526219	-0.230	0.8219
RD	1	.00002068444	.00000346808	5.964	0.0001

OBS	ACTUAL	PREDICT VALUE	STD ERR PREDICT	LOWER95% MEAN	UPPER95% MEAN	LOWER95% PREDICT	UPPER95% PREDICT	RESIDUAL	STD ERR RESIDUAL	STUDENT RESIDUAL	-2-1-0 1 2
1	1.0146	0.209853	1.45457	-2.9326	3.35226	-8.4455	8.86523	0.804743	3.43802	0.234072	| |
2	0.764089	0.240756	1.4507	-2.8933	3.37479	-8.4116	8.8931	0.523333	3.43966	0.152147	| |
3	1.84729	1.49574	1.30097	-1.3148	4.30632	-7.0448	10.0362	0.351556	3.49903	0.100472	| |
4	1.41358	1.31519	1.32149	-1.5397	4.1701	-7.24	9.87038	.098391	3.49133	.0281815	| |
5	3.58581	2.88775	1.15721	0.387748	5.38775	-5.5556	11.3311	0.698064	3.54917	0.196684	| |
6	3.27122	2.76573	1.16866	0.241006	5.29046	-5.685	11.2165	0.505486	3.54542	0.142574	| |
7	4.2868	3.88176	1.07399	1.56155	6.20198	-4.5102	12.2737	0.405039	3.57523	0.11329	| |
8	5.58162	4.28862	1.0457	2.02954	6.54771	-4.0866	12.6638	1.293	3.58361	0.360809	| |
9	6.73387	6.31922	0.966065	4.23217	8.40628	-2.0112	14.6497	0.414645	3.6059	0.114991	| |
10	4.32798	6.31922	0.966065	4.23217	8.40628	-2.0112	14.6497	-1.9912	3.6059	-.552218	| * |
11	12.8588	16.7235	1.93636	12.5403	20.9068	7.63834	25.8087	-3.8647	3.1916	-1.2109	| ** |
12	28.236	17.6558	2.07339	13.1765	22.1351	8.43058	26.881	10.5802	3.10432	3.40822	| |******
13	11.1178	11.3095	1.23471	8.64206	13.9769	2.81502	19.804	-.191658	3.52296	-.054403	| |
14	7.58063	12.1268	1.32468	9.265	14.9886	3.5693	20.6843	-4.5462	3.49013	-1.3026	| ** |
15	7.98666	13.0673	1.43744	9.96191	16.1727	4.42531	21.7093	-5.0807	3.44522	-1.4747	| ** |

OBS	COOK'S D
6	0.001
7	0.001
8	0.006
9	0.000
10	0.011
11	0.270
12	2.591
13	0.000
14	0.122
15	0.189

SUM OF RESIDUALS	2.33147E-15
SUM OF SQUARED RESIDUALS	181.1649
PREDICTED RESID SS (PRESS)	334.0045

DOUBLE RECIPROCAL FIT OF DATA 47

OBS	COOK'S D
1	0.005
2	0.002
3	0.001
4	0.000
5	0.002

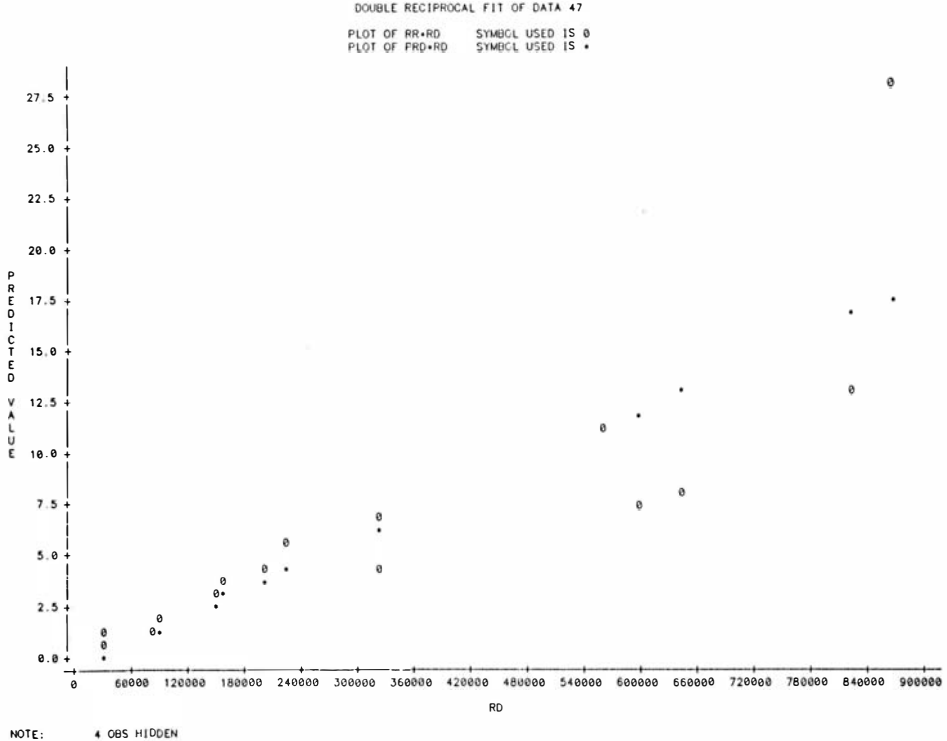

NOTE: 4 OBS HIDDEN

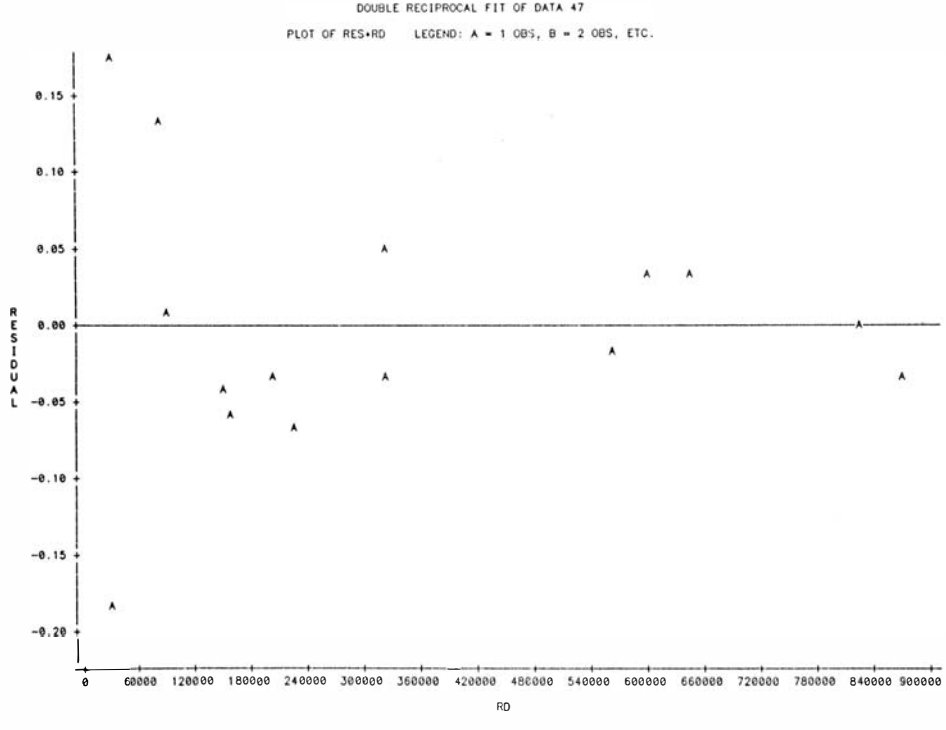
DOUBLE RECIPROCAL FIT OF DATA 47
PLOT OF RES*RD LEGEND: A = 1 OBS, B = 2 OBS, ETC.
RESIDUAL
0.15
0.10
0.05
0.00
-0.05
-0.10
-0.15
-0.20
0
60000
120000
180000
240000
300000
360000
420000
480000
540000
600000
660000
720000
780000
840000
900000
RD

Vita